AUBURN UNIVERSITY

SAMUEL GINN
COLLEGE OF ENGINEERING

Final Report for ALDOT Project 930-945

USE OF GEOPHYSICAL METHODS FOR SINKHOLE EXPLORATION

Submitted to

The Alabama Department of Transportation

Prepared by

Jack Montgomery

Dan Jackson

Michael Kiernan

J. Brian Anderson

OCTOBER 2020

Highway Research Center
Harbert Engineering Center
Auburn, Alabama 36849

www.eng.auburn.edu/research/centers/hrc.html

1. Report No. 930-945	**2. Government Accession No.**	**3. Recipient Catalog No.**
4. Title and Subtitle Use of Geophysical Methods for Sinkhole Exploration		**5. Report Date** October 2020
		6. Performing Organization Code
7. Author(s) Jack Montgomery, Dan Jackson, Michael Kiernan, J. Brian Anderson		**8. Performing Organization Report No.** 930-945
9. Performing Organization Name and Address Highway Research Center Department of Civil Engineering 238 Harbert Engineering Center Auburn, AL 36849		**10. Work Unit No. (TRAIS)**
		11. Contract or Grant No.
12. Sponsoring Agency Name and Address Alabama Department of Transportation 1409 Coliseum Boulevard Montgomery, AL 36130-3050		**13. Type of Report and Period Covered** Technical Report
		14. Sponsoring Agency Code

15. Supplementary Notes
Project performed in cooperation with the Alabama Department of Transportation.

16. Abstract

Karst geology is characterized by the presence of sinkholes and voids, which may pose significant risk to existing infrastructure. Sinkhole formation is often observed near active quarries, where dewatering operations can alter regional groundwater flow patterns leading to subsidence and increased void formation. In these areas, identifying locations which may be susceptible to sinkhole formation requires an ability to map the rock surface and any dissolution features within the rock. Traditional geotechnical explorations alone are not well-suited to this effort as they only provide subsurface information at discrete points and therefore may miss voids within the rock or may provide incomplete information in areas of highly variable rock surfaces. Geophysical methods offer a means to produce continuous profiles of the rock surface and possible locations for voids but interpreting the results of these tests in karstic geology can be challenging. This study uses 2D electrical resistivity and seismic surveys at sites with active sinkholes, repaired sinkholes and pinnacled rock in Alabama. Resistivity data is collected using 2D dipole-dipole and strong-gradient arrays. The seismic data is processed using a full waveform inversion (FWI) technique. Subsurface profiles interpreted from the geophysical surveys are compared to geologic information and borehole data from previous site investigations, where available. Results from the geophysical surveys are found to be consistent with borehole data regarding variation of bedrock depth and identification of possible sinkhole features. Potential limitations and sources of error pertaining to each survey type are considered. The results of the geophysical surveys are used to create a sinkhole investigation plan, which seeks to integrate the various sources of information in order to provide a comprehensive and cost-efficient characterization of sinkhole sites. Recommendations for implementation of the findings from this study and areas for future research are discussed.

17. Key Words Geophysical investigations, site characterization, sinkholes, karst, electrical resistivity, seismic full waveform inversion		**18. Distribution Statement** No restrictions.	
19. Security Classification (of this report) Unclassified	**20. Security Classification (of this page)** Unclassified	**21. No. of Pages** 93	**22. Price** None.

Research Report

USE OF GEOPHYSICAL METHODS FOR SINKHOLE EXPLORATION

Submitted to

The Alabama Department of Transportation

Prepared by

Jack Montgomery

Dan Jackson

Michael Kiernan

J. Brian Anderson

October 2020

DISCLAIMERS

The contents of this report reflect the views of the authors who are responsible for the facts and accuracy of the data presented herein. The contents do not necessarily reflect the official views or policies of the Alabama Department of Transportation, Auburn University, or the Highway Research Center. This report does not constitute a standard, specification, or regulation. Comments contained in this report related to specific testing equipment and materials should not be considered an endorsement of any commercial product or service; no such endorsement is intended or implied.

NOT INTENDED FOR CONSTRUCTION, BIDDING, OR PERMIT PURPOSES

Jack Montgomery, Ph.D.

Research Supervisor

ACKNOWLEDGEMENTS

Material contained herein was obtained in connection with a research project, "Use of Geophysical Methods for Sinkhole Exploration," ALDOT Project 930-945, conducted by the Auburn University Highway Research Center. Funding for the project was provided by the Alabama Department of Transportation (ALDOT). This work was completed in part with resources provided by the Auburn University Hopper Cluster. The funding, cooperation, and assistance of many individuals from each of these organizations are gratefully acknowledged. The authors particularly acknowledge the contributions of the following individuals for serving on the project advisory committee and assisting with the data collection and processing:

Scott George	ALDOT, Materials and Test Engineer, Montgomery
Kaye Chancellor Davis	ALDOT, Deputy State Materials and Tests Engineer, Montgomery
Stacey Glass	ALDOT, State Maintenance Engineer, Montgomery
Skip Powe	ALDOT, State Construction Engineer, Montgomery
Virgil Clifton	ALDOT, Research and Development Bureau, Montgomery
Calvin Smith	ALDOT, Research and Development Bureau, Montgomery
Kristy Harris	FHWA
Brannon McDonald	ALDOT, Materials and Tests Bureau, Montgomery
Renardo Dorsey	ALDOT, Materials and Tests Bureau, Montgomery
Allen Mann	ALDOT, Materials and Tests Bureau, Montgomery
Ashton Babb	Auburn University
Devdeep Basu	Auburn University
Jared Spivey	Auburn University (former student)

ABSTRACT

Karst geology is characterized by the presence of sinkholes and voids, which may pose significant risk to existing infrastructure. Sinkhole formation is often observed near active quarries, where dewatering operations can alter regional groundwater flow patterns leading to subsidence and increased void formation. In these areas, identifying locations which may be susceptible to sinkhole formation requires an ability to map the rock surface and any dissolution features within the rock. Traditional geotechnical explorations alone are not well-suited to this effort as they only provide subsurface information at discrete points and therefore may miss voids within the rock or may provide incomplete information in areas of highly variable rock surfaces. Geophysical methods offer a means to produce continuous profiles of the rock surface and possible locations for voids but interpreting the results of these tests in karstic geology can be challenging. This study uses 2D electrical resistivity and seismic surveys at sites with active sinkholes, repaired sinkholes and pinnacled rock in Alabama. Resistivity data is collected using 2D dipole-dipole and strong-gradient arrays. The seismic data is processed using a full waveform inversion (FWI) technique. Subsurface profiles interpreted from the geophysical surveys are compared to geologic information and borehole data from previous site investigations, where available. Results from the geophysical surveys are found to be consistent with borehole data regarding variation of bedrock depth and identification of possible sinkhole features. Potential limitations and sources of error pertaining to each survey type are considered. The results of the geophysical surveys are used to create a sinkhole investigation plan, which seeks to integrate the various sources of information in order to provide a comprehensive and cost-efficient characterization of sinkhole sites. Recommendations for implementation of the findings from this study and areas for future research are discussed.

TABLE OF CONTENTS

List of Tables

List of Figures

CHAPTER 1: INTRODUCTION

1.1 Background

A significant portion of Alabama is underlain by soil and rock formations that are susceptible to sinkhole development. In northern Alabama, sinkholes often occur in areas with karstic geology comprised primarily of limestone and dolostone. The rock types are susceptible to dissolution and over time the movement of water may lead to development of cavities within the rock and sinkholes.

Sinkholes near highways in Alabama have led to significant traffic disruption and large repair costs. In 2012, a sinkhole closed the westbound lanes of I-20 near Heflin. In 2013, ALDOT repaired three sinkholes along AL-21 in Talladega County (Figure 1-1) by excavating to competent rock and backfilling with rip rap and flowable fill. The repairs cost approximately $10 million and traffic was disrupted for over a month (Orange and Smith 2014). In some areas, persistent sinkhole development has led to the construction of at-grade bridges to span the problem areas. Along the I-59/20 corridor just west of the I-65 interchange in Birmingham, seven bridges were constructed in three phases from the early 1970s into the early 1990s to span an area of active sinkholes. Recent subsidence along the shoulders of these bridges (Figure 1-2) has led to renewed interest in the extent and possible activity of sinkholes in this area.

The two projects discussed above demonstrate the need in Alabama for techniques to evaluate the extent of and monitor the activity of sinkholes along highways. Currently these investigations are performed by using a dense grid of borings to evaluate the variability in depth to competent rock, but this method is time-consuming and expensive. More recent research has demonstrated the ability of surface-based geophysical measurements to map the irregular bedrock surface and give an indication of the size and location of any voids (e.g., Ismail and Anderson 2012). These techniques can offer more detailed information than aerial photographs and topographic maps and can be performed more quickly and at a significantly lower cost than an extensive drilling program. Once a sinkhole has been identified, geophysical measurements can be repeated over time to monitor any changes that may indicate enlargement of the cavity. This type of information can help engineers to better design and prioritize remediation measures.

This report reviews the development of a geophysical investigation program for sinkholes along highways in Alabama. The report discusses geophysical methods that have previously been

Figure 1-1: Sinkhole remediation along AL-21 in 2013 (Orange and Smith 2014).

Figure 1-2: Erosion of the shoulder underneath an at-grade bridge in an area of extensive sinkhole activity along eastbound I-59/20 near Mile Marker 122.

used to investigate sinkholes in karst regions and reviews some of the advantages and disadvantages of each method. Based on this review, electrical resistivity and seismic testing were selected for use in this study. The procedures for performing both electrical resistivity and seismic tests are described including the data collection, processing and inversion requirements. The use of each of these methods is then demonstrated through the discussion of case histories at sites with varying levels of sinkhole activity, including active sinkholes, repaired sinkholes and areas of deep pinnacled rock. The ability of each geophysical method to detect and map the karst features at each of these sites is discussed.

The experience developed through the surveys performed as part of this study was then used to develop a sinkhole investigation plan for future sinkhole sites. This includes a general set of steps that can be used to develop an efficient and effective investigation program, including the use of geophysics. The potential cost-savings associated with integrating geophysics into a site characterization program are examined by analyzing different investigation plans for three example sites. Recommendations for implementing this research into current ALDOT practice are discussed. Topics related to this study that could benefit from future research are discussed.

1.2 Project Objectives

The overall purpose of this research was to provide ALDOT engineers with guidance on surface-based geophysical methods that can be used to investigate the extent of sinkholes and assess changes over time. This was accomplished through several field trials of selected geophysical test methods to determine their ease of use, data processing requirements and ability to map the features of interest. Specific objectives for this project include:

1. Collect detailed information on available geophysical test methods that have been used for mapping sinkholes in karstic geology. Specific information included equipment costs, strengths and weaknesses of each method, types of problems to which they are applicable, restrictions based on site conditions (e.g., soil type, buried utilities, power lines) and training requirements.
2. Determine the ease of use, data processing requirements and limitations of the selected test methods under field conditions. Several sites were selected for these field trials with a focus on areas of known sinkhole activity and any sites where geophysical data can be compared with borings.

3. Evaluate the effectiveness of the selected geophysical methods at mapping the location and size of any subsurface cavities and their ability to detect the potential for continued sinkhole development. Each method was compared to the others and to any available subsurface information.
4. Develop a sinkhole investigation plan and training program for ALDOT engineers based on the results of this study.

1.3 Research Approach

The following tasks were performed to accomplish the research objectives of this project:

- Task 1: Review previous studies focused on using geophysical measurements to evaluate sinkholes and bedrock profiles in karstic geologic settings.
- Task 2: Design field testing program and develop testing procedures.
- Task 3: Implement field testing program at selected sites.
- Task 4: Develop sinkhole investigation plan for ALDOT

CHAPTER 2: LITERATURE REVIEW

2.1 Introduction

Sinkholes along highways are a significant problem for transportation officials. This chapter reviews important literature concerning sinkholes along highways in Alabama and geophysical methods that can be used to investigate them. The causes of sinkholes in karst environments are briefly discussed in Section 2.2. Section 2.3 summarizes some of the challenges associated with site investigation in karst. Section 2.4 reviews geophysical methods that are commonly used to investigate sinkholes and discusses some advantages and disadvantages of each for use along highways in Alabama.

2.2 Karst in Alabama

The formation of karstic features occurs due to dissolution of soluble rocks such as evaporites and carbonate rocks. Karstification most commonly occurs in carbonate dolostones, limestones, and marbles that are weathered by flowing groundwater (De Waele et al. 2009). Surface subsidence associated with sinkholes typically occurs due to transport of loose sediments through fissures and voids with collapse of the underlying rock being less common (Newton 1987). Sinkhole formation is often observed near active quarries, where dewatering operations can alter regional groundwater flow patterns leading to subsidence and increased void formation (e.g., Foose and Humphreville 1979, Lamoreaux and Newton 1986, Newton 1987, Kaufmann and Quinif 1999). Dewatering activities associated with quarries accelerate sinkhole formation by increasing hydraulic gradients and flow velocities, which increases the rate at which unconsolidated sediments are eroded (Langer 2001).

A significant portion of Alabama is underlain by soil and rock formations that are susceptible to sinkhole development. In northern Alabama, sinkholes often occur in areas with karstic geology which are comprised primarily of limestone and dolostone. The rock types are susceptible to dissolution and over time the movement of water may lead to development of cavities within the rock and sinkholes. Figure 2-1 shows locations of sinkholes across the state of Alabama which have been mapped using topographic maps published between 1958 and 1986.

2.3 Site Characterization in Karst

Geotechnical characterization of karstic sites can be challenging due to irregular distribution of rock surface and potential for voids (Roth and Nyquist 2003). Identifying locations that may be susceptible to sinkhole formation requires an ability to map dissolution features within

the rock. In the past, sinkholes have commonly been identified when significant subsidence or an open void is observed at the ground surface. These observations may be made through examining aerial photographs, topographic maps or visual evidence at a site. Once a sinkhole has been

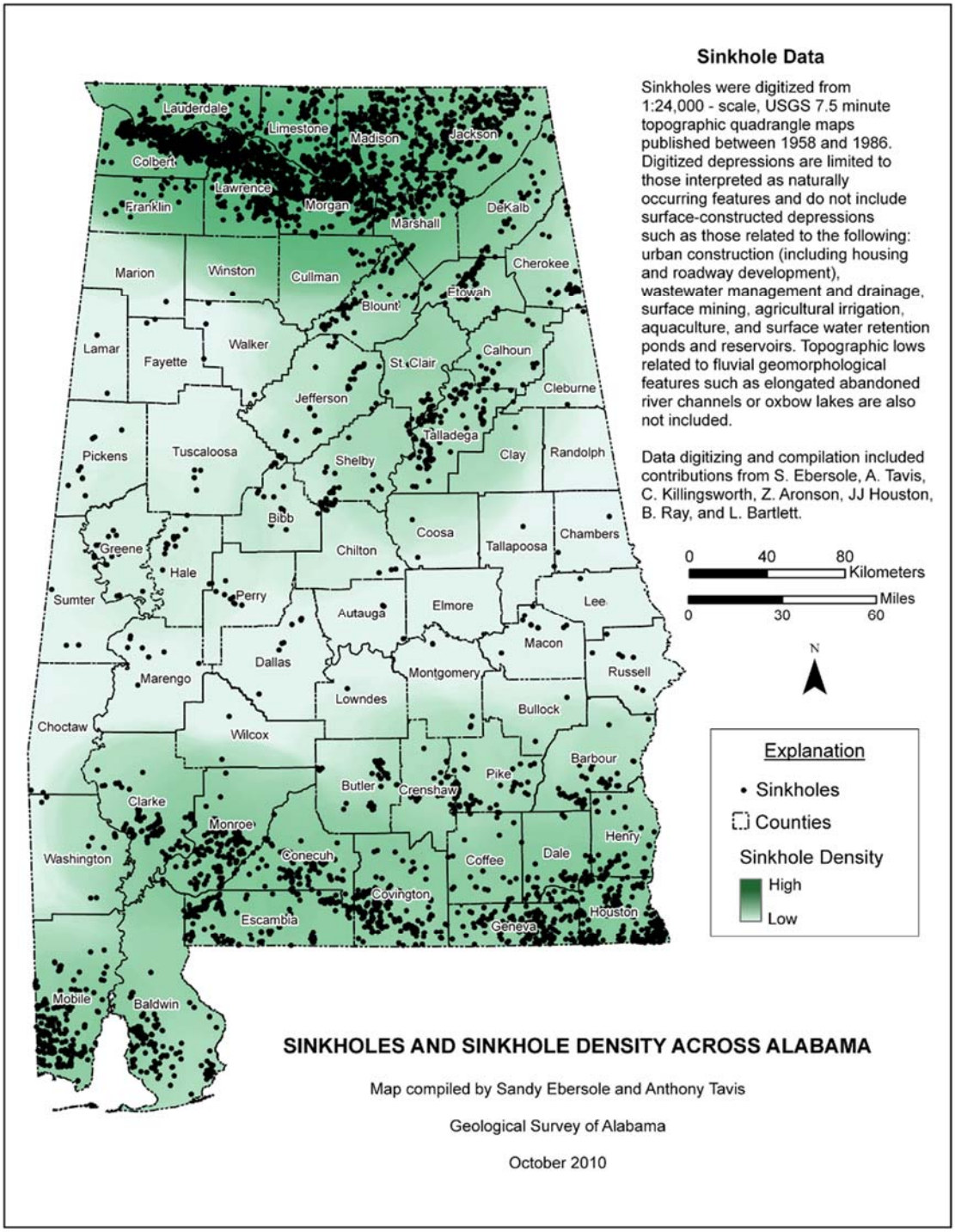

Figure 2-1: Sinkhole Density across Alabama (GSA 2010)

identified, the depth to competent rock in the surrounding area is often determined through an extensive drilling program in which borings are performed on a dense grid. Traditional geotechnical explorations (i.e., borings) alone are not well-suited to this effort as they only provide subsurface information at discrete points and therefore may miss voids within the rock (Thomas and Roth 1999). Drilling operations may take several days leading to traffic delays and significant investigation costs when these features occur near highways.

A feature common in karst environments is blocked or pinnacled rock adjacent to solution-enlarged joints. Joints in the parent rock provide a preferential flow path that causes increased dissolution. However, because more solutional denudation occurs near the surface, these joints are widest at the top and decrease in size and frequency with depth (Ford and Williams 2007). These solution-enlarged joints can be nearly vertical, and thus with a traditional geotechnical exploration, a very dense grid of borings would be required to detect these features. However, geophysical methods may provide a more continuous representation of the rock surface allowing such features to be more easily identified.

2.4 Geophysical Methods

Geophysical tools have a wide variety of application in assessing transportation infrastructure (Sirles 2006). Several geophysical testing methods are available, which can be used for mapping sinkholes and irregular bedrock profiles in areas with karst geology. These include electrical resistivity (Ismail and Anderson 2012), seismic methods (Tran et al. 2013) and ground penetrating radar (Bullock and Dillman 2003).

2.4.1 Ground Penetrating Radar

Ground penetrating radar (GPR) measures the reflection of high frequency electromagnetic waves to detect layer contacts and anomalies in the subsurface (e.g., voids, utilities, boulders). Pulses of radar waves are transmitted into the ground. The characteristics of these waves are altered as changes in the subsurface are encountered (Dojack 2012). The traces of the reflected waves are collected and analyzed to identify where changes in the subsurface occur. GPR provides high resolution detection of shallow anomalies such as utilities or shallow bedrock, but may need to be to be combined with other investigation methods if deeper objects of interest are expected. Conductive environments, such as clay rich overburden or salt-water intrusion sites, can further limit the effective depth of GPR (Jol 2009). Carriere et al. (2013) combined GPR with electrical resistivity to investigate a karst site. The effective depth of the GPR was generally limited to about

40 feet and was effective to only 6 feet when clay rich overburden existed, as is common in Alabama.

2.4.2 Gravity Measurements

Gravity-based geophysical methods can be used to estimate the density of the underlying soil and rock. Reductions in local gravity can indicate missing mass, as would be expected in areas with voids. Because this directly corresponds to the property of interest, gravity methods are often seen as useful for detecting karst features (ASTM D6429). However, there are a number of downsides to gravity based methods.

Gravity methods are very sensitive to noise in the environment. Additionally, numerous corrections are required for gravity data including for local and regional topography, latitude and longitude, positions of the sun and moon, and instrument drift (Hoover 2003). Furthermore, the density contrast between soil and rock is quite small compared to other properties. When coupled with the many corrections required for gravity data, this can make interpretations of gravity data quite difficult as scales smaller than the regional scale.

2.4.3 Electrical Resistivity

Electrical resistivity methods, referred to as electrical resistivity tomography (ERT), are used to map the resistivity distribution of the subsurface. Electrodes may be placed in boreholes or in 2D or 3D arrangements on the ground surface. All surveys presented in this report utilize electrodes placed at the ground surface; primarily in 2D arrangements (Figure 2-2). A direct current (DC) electrical signal of known amperage is injected into the ground using two ‘current’ electrodes. The resulting potential difference is then measured between different pairs of ‘potential’ electrodes. The SuperSting R8, which was used for all surveys conducted in this report, has eight channels with which potential measurements can be taken simultaneously (AGI 2018). An ‘apparent resistivity’ value is calculated for each measurement using the known amperage, measured potential difference and electrode geometry. The apparent resistivity is the resistivity that would be measured for homogenous subsurface using a given electrode arrangement (Loke 2004). An apparent resistivity distribution is created by taking multiple series of measurements. An estimate of the true subsurface resistivity distribution is finally obtained through the process of numerical inversion. More detailed information regarding data collection and inversion specific to the surveys conducted as part of this report is presented in section 3.2.

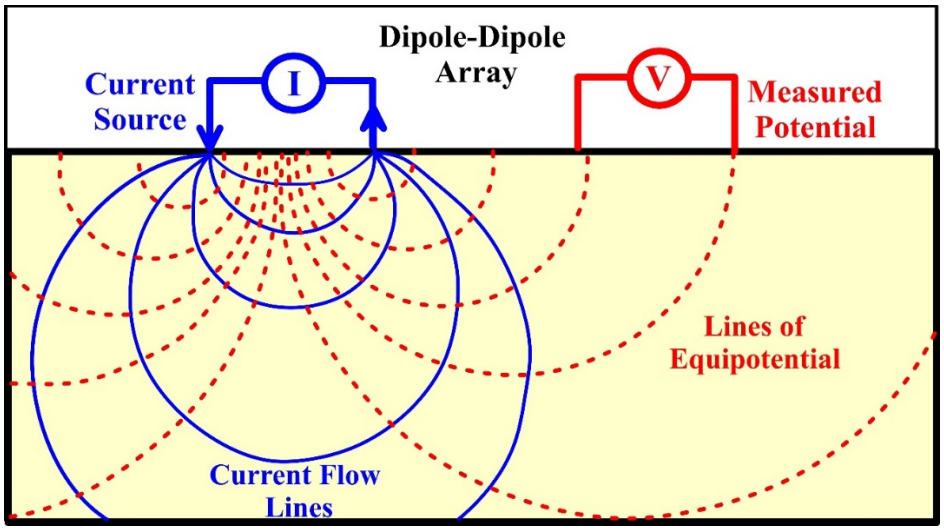

Figure 2-2: Electrode arrangement for a dipole-dipole array.

The term 'array' in ERI refers to the relative positions of the current and potential electrodes used for measurements. Some commonly used arrays in practice include the Wenner, Wenner-Schlumberger, strong-gradient, dipole-dipole, pole-pole, and pole-dipole arrays. Each array type presents unique advantages and disadvantages (Loke 2004). The Wenner array, for example, is good at resolving horizontal structures but poor at resolving vertical structures. The dipole-dipole array is better at resolving vertical structures, such as voids or pinnacled rock, but does not resolve horizontal features well (Loke 2004). The strong-gradient array produces a strong signal and requires very few measurements compared to other arrays (AGI 2014). This makes the strong-gradient array suitable for conductive environments and very fast for data collection at the sacrifice of spatial resolution. The surveys presented in this report primarily utilize the dipole-dipole array for its ability to map the vertical structures expected in karst environments. Strong-gradient data is also collected as it runs quickly (about 5-7 minutes) and provides additional data in the case of noisy dipole-dipole data.

ERT has been used successfully by previous researchers to characterize karst environments (e.g. Zhou et al. 2000, Zhou et al. 2002, Carriere et al. 2013). Electrical resistivity measurements are relatively simple to collect and process, but results can often be difficult interpret in karst environments. The resistivity of geologic materials is dependent primarily on their porosity and degree of saturation (Loke 2004). In ERT, sinkhole features tend to have either higher resistivity (e.g., air-filled voids, unsaturated loose unconsolidated sediments in a solution widened joint) or lower resistivity (e.g., water filled voids, saturated loose unconsolidated sediments in a solution

widened joint) than the surrounding soil or parent rock depending on the degree of saturation. The presence of offline conductive structures such as buried utilities or ground loops induced by adjacent powerlines are known to show up in resistivity results at a depth equal to their offline distance (White et al. 2003). Resistivity lines should be placed perpendicular to known conductive structures or moved a distance away that is greater than the expected maximum depth of investigation.

2.4.4 Seismic Methods

Seismic methods use geophones or accelerometers placed on the ground surface to measure vibrations that have passed through the subsurface. A sledgehammer striking a metal plate is typically the source of the vibrations (Figure 2-3). These measurements can be used to map the shear wave velocity of the subsurface and detect areas of significant velocity contrast, such as open voids. Several seismic based methods are available that range in both applicability and complexity. Seismic methods have the advantage that they directly measure the stiffness of the subsurface rather than measuring an indirect property. However, all seismic methods are affected to some degree by ambient noise and vibrations such as traffic noise. Also, processing of seismic data can be quite complex depending on the processing method that is used.

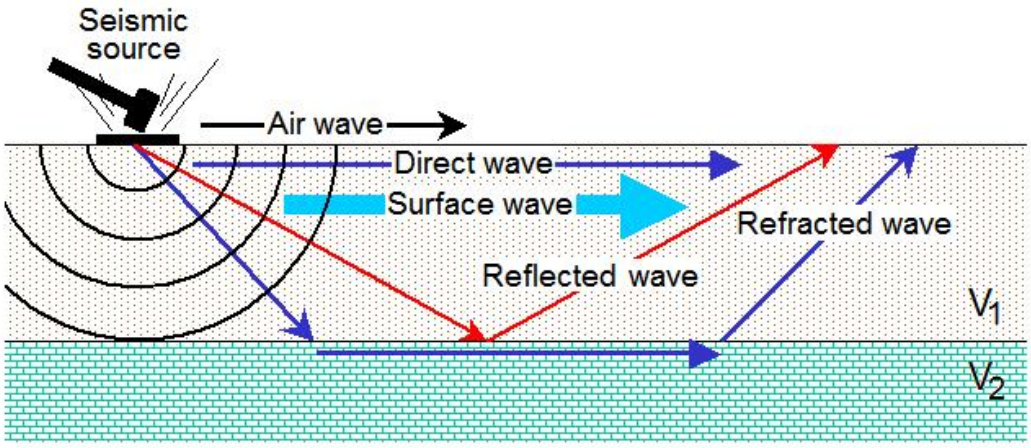

Figure 2-3: Example of seismic waves generated from a hammer striking a metal plate (Park Seismic LLC)

Surface wave based seismic methods are among the easiest seismic methods in terms of both data collection and processing. Also, because surface waves are often the dominant energy source, these methods are the most robust in high noise environments. These methods make use of the dispersive properties of seismic surface waves to develop 1D shear wave velocity profiles.

Multichannel analysis of Surface Waves (MASW) (Park et al. 1999) is the most common surface wave method, being a more advanced version of the older spectral analysis of surface waves (SASW) (Nazarian 1984). For the MASW method, a standard seismic spread is used, while SASW uses only two receivers at a time. The profile that is generated is an average of the area under the spread.

Because these methods only generate 1D profiles, they cannot directly detect lateral heterogeneities such as voids or pinnacled rock. However, it is fairly common to stitch together multiple 1D profiles to form a pseudo-2D or 3D profile (Luo et al. 2008). One method to achieve this it to use a seismic landstreamer where geophones on plates are towed behind a vehicle, allowing many 1D profiles to be collected quickly (Liberty and Gribler 2014). While surface wave methods are fairly robust in the presence of noise, they tend to perform poorly where there is shallow rock (Casto et al. 2010). Surface wave methods have been used with varying degrees of success to map subsurface voids (Xia et al. 2007, Ivanov et al. 2016). It has also been used to successfully map a 2D bedrock surface in karst environments (Parker and Hawman 2012).

The seismic refraction method relies on body waves rather than surface waves, specifically compression waves (also called p-waves). P-waves travel through the subsurface faster than surface waves and will be recorded first. For each seismic trace that is collected, the time from when the source is triggered to the first arrival of the waveform is picked. Automatic methods to perform this picking are available (for example, Lee et al. 2017), but final picks may need to be adjusted manually. The picks of the first arrivals can be interpreted in a variety of ways, from simple layered models (Burger et al. 2006), to more complex ray tracing tomographic methods that can provide 2D or 3D profiles (Sheehan et al. 2005a).

In all cases, however, seismic refraction can have trouble detecting low velocity zones. Because the p-waves that arrive first will always travel along the fastest path, low velocity zones will be masked by surrounding, higher velocity zones (Banerjee and Gupta 1975, Sheehan et al. 2005b). This can leads to issues accurately detecting anomalies, such as voids, that typically have lower velocities. Additionally, because the first arrivals are p-waves that have a much smaller amplitude than the surface waves, noise can make it very difficult to pick the first arrivals, especially at large source-receiver offsets.

In spite of these difficulties, seismic refraction, especially advanced tomographic methods, have seen use in karst environments. For example, Hiltunen and Cramer (2008) used seismic

refraction tomography to estimate the location of the rock surface in a karst area. Cardarelli et al. (2009) also used seismic refraction tomography, in conjunction with electrical resistivity tomography, to detect buried cavities.

The seismic reflection method uses reflected p-waves rather than refracted p-waves. As the p-waves travel through the subsurface, interfaces or others heterogeneities will cause some energy to be reflected back to the surface where they are recorded. These reflections can then be used to estimate the layering of the subsurface (Burger et al. 2006). The reflections often have the smallest amplitude of all the seismic waves, thus a noisy environment can be detrimental to a seismic reflection survey. While it can be used in near surface applications (Steeples et al. 1986, Isiaka et al. 2019), seismic reflections are more commonly used for much deeper, regional explorations (e.g. oil and gas exploration). Processing is very complex and it requires much skill to appropriately interpret seismic reflection data.

A final surface-based seismic method that is relatively new is full waveform inversion (FWI). With full waveform inversion, rather than just targeting a single phase of the seismic wave train, the entire waveform in modeled. This allows full 2D and 3D shear wave velocity profiles to be created, although at quite a bit of computational expense. Data is collected similarly to a seismic refraction survey. This method is very complex as it involves a full simulation of the elastic wavefield. Once the wavefield is simulated, the velocity model is adjusted so that the simulated waveforms match the waveforms that were observed in the field. Virieux and Operto (2009) provide a summary of the state of practice of seismic full waveform inversion, although their focus is primarily on larger scale problems. For near surface problems, Tran et al. (2013) have used seismic FWI for sinkhole detection, and Sullivan et al. (2016) used FWI to detect abandoned mines under a roadway.

CHAPTER 3: SELECTED GEOPHYSICAL METHODS

3.1 Introduction

The literature review has highlighted some of the geophysical methods that can be used to investigate karst features. Based on this review, electrical resistivity and seismic methods were selected as the preferred techniques for this project. The objective of the study was to determine the ease of use for each method, data processing requirements and ability to detect and map the desired features. This chapter will discuss details of the data collection and processing requirements of both the electrical and seismic methods. Field data sheets, used to record important survey information in the field, are included as Appendix A.

3.2 Electrical Resistivity

Electrical resistivity testing was selected for this study due to its history of use in karst and the ease of processing and interpretation (Zhou et al. 2000, van Schoor 2002, Park et al. 2013, Majzoub et al. 2017). For the electrical resistivity method, electrical current is injected into the ground using a pair of electrodes (Figure 3-1). This study is focused on direct current methods, where one of the electrodes is attached to the positive side of the current source (e.g., a battery) and the other to the negative side. Other pairs of electrodes are then used to measure the corresponding changes in electrical potential (voltage). This is analogous to a flow net (Figure 3-1), where the current is represented by water flow and the potential is represented by hydraulic head. By collecting voltage measurements at various distances away from the current electrodes, the shape of the electrical flow net can be determined. These measurements are then used within a numerical analysis to determine the subsurface resistivity profile that would give rise to the measured voltages. This process is called inversion, where numerical models are created and adjusted until the results from the numerical models match the experimental observations within some tolerance. Further details on each of these aspects of testing are discussed in the following sections.

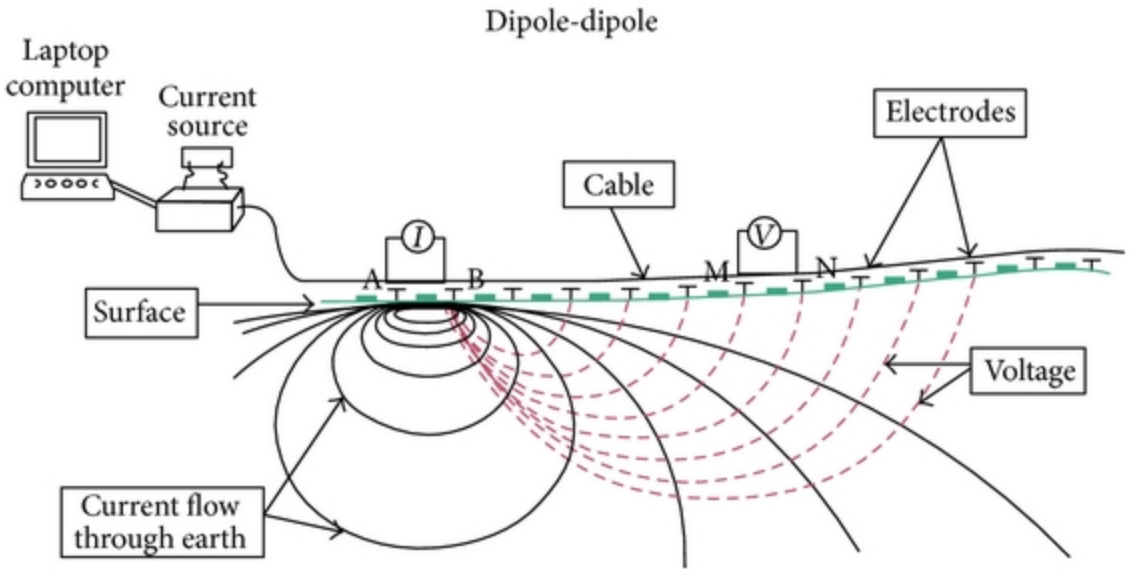

Figure 3-1: Setup for a multichannel dipole-dipole survey (Okpoli 2013).

3.2.1 Data Collection

ERT surveys for this study were performed using a commercial eight channel SuperSting system (AGI 2018). This system consists of the SuperSting instrument that injects current into the ground and measures voltages, a set of stainless steel stakes that serve as electrodes, a set of cables, and a switchbox that controls which electrodes are active. The full system is shown in Figure 3-2. Fifty-six electrodes can be connected to each switchbox and multiple switchboxes can be connected to a single SuperSting. An electrode spacing of up to 16.4 feet [5 meters] may be used depending on the goal of the survey. A larger electrode spacing generally corresponds to a greater depth of investigation and decreased resolution. A smaller electrode spacing will generally have higher resolution (i.e. smaller objects will be able to be seen) but will not have as large a depth of investigation. As a rule of thumb, the maximum depth of investigation will be approximately 1/5 the spread length for surveys with 56 electrodes measured in a dipole-dipole configuration and slightly deeper for strong-gradient measurements.

Electrodes must be hammered into the ground, which can be difficult in areas with significant tree roots, stiff soils or large rocks. In these cases, electrodes may need to be skipped or moved to accommodate the obstacles. The resistivity inversion is also affected by changes in topography. For this reason, topographic surveys are commonly performed to measure the location

and elevation of the electrodes for use in the inversion. For the surveys performed for this study, a total station was used to measure the relative location and elevation of the electrodes when there was significant topography or deviations from standard spacings. Survey data was recorded on the field data sheets included as Appendix A.

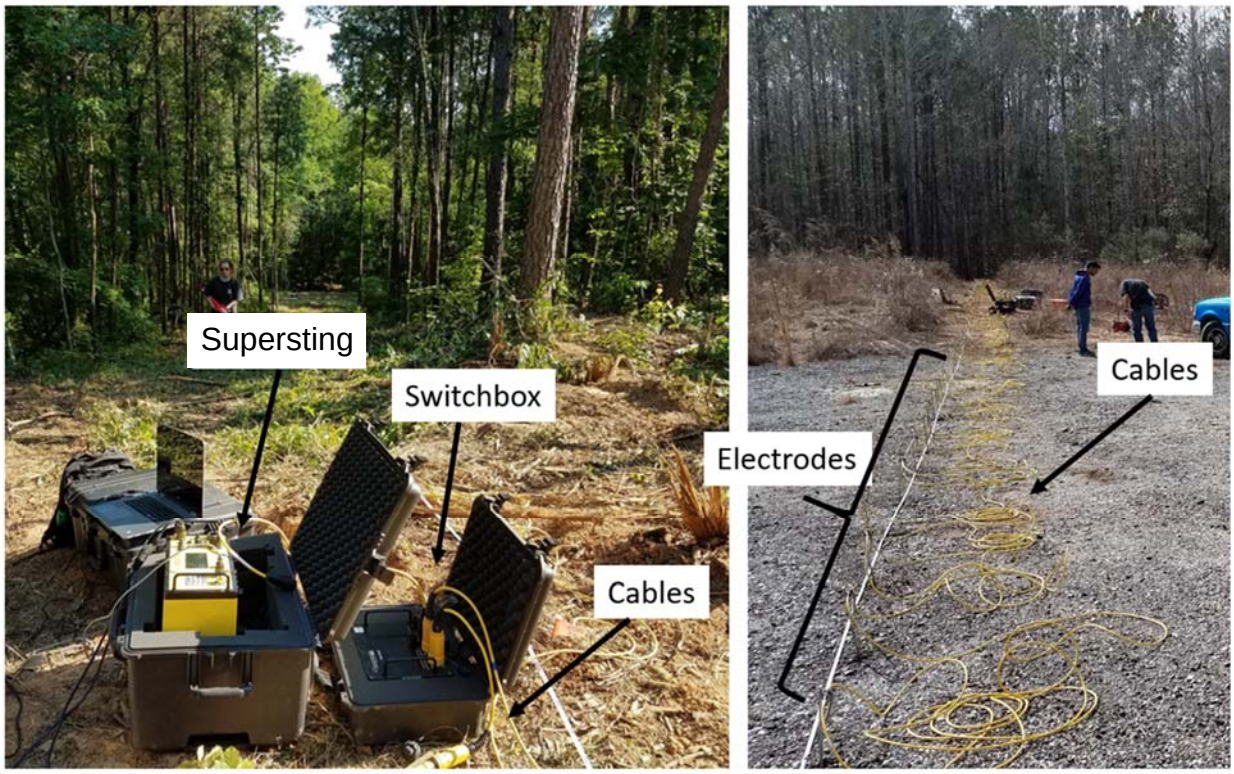

Figure 3-2: SuperSting resistivity imaging system

It is also possible to perform 3D electrical resistivity surveys. In principal, these surveys work the same as 2D surveys, except the electrodes must be arranged in a 2D array rather than a linear array. Including the correct electrode positions and elevations in the inversion is more critical for 3D surveys.

The time to conduct a field survey depends on the number of electrodes used and the number of measurements that are taken. The set-up and break-down time will also increase as the electrode spacing increases. For a typical 56 electrode 2D dipole-dipole survey, the survey will take about 30 - 45 minutes on an 8 channel SuperSting system, excluding set-up and break-down.

3.2.2 Processing and Inversion

Inversion of the resistivity data is performed by converting the measured field data, such as potential difference *(ΔV)* and injected current *(I)*, to an 'apparent' resistivity *(ρ_a=kR)* using the measured resistance *(R=ΔV/I)* value and a geometric factor (*k*) which depends on the geometry of the current *(C1 and C2)* and potential electrodes *(P1 and P2)* (Loke 2004). An example of how *k* is calculated for the dipole-dipole and strong gradient arrays are shown below in Figure 3-3. These calculated ρ_a values represent the resistivity of a homogenous half space that would be measured for a given geometric factor (Loke 2004). Numerical inversion of the measured data is then required to obtain an estimate of the true subsurface resistivity distribution.

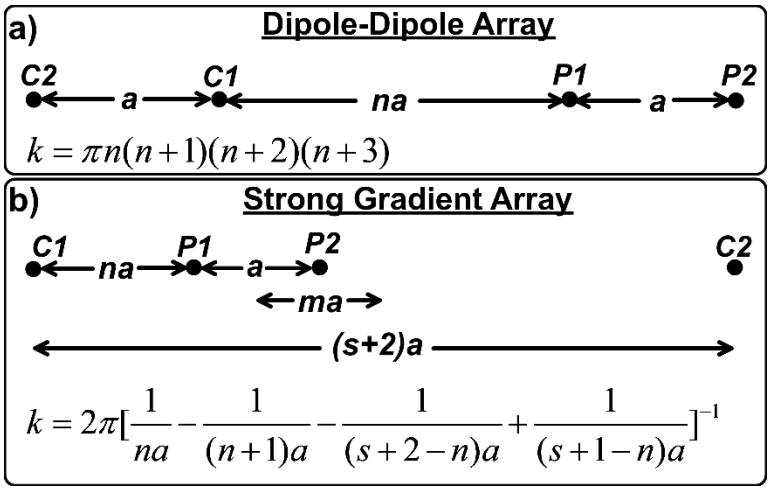

Figure 3-3: Geometric factor for a) dipole-dipole array with dipole separation *'a'*; b) strong gradient array with potential electrode separation *'a'* where $(s+2)a$ is the distance between *C1* and *C2* and ma is measured from the center of *P1/P2* to the center of *C1/C2* (after Loke et al. 2013)

Inversion techniques often seek to find a synthetic subsurface model which produces an apparent resistivity distribution that closely matches the measured data. The starting synthetic model for inversion is typically a homogenous finite element mesh with a resistivity equal to the average of the measured apparent resistivity values. A virtual survey is then performed on the finite element mesh with the same electrode arrangements used in the field. The resistivity of the zones in the mesh are then updated through numerical solution of an inverse problem which considers the current synthetic model and the misfit with the measured data (AGI 2014). This synthetic model is iteratively updated by this process until the data misfit falls below some desired threshold.

The inversion procedure produces a non-unique estimate of the subsurface resistivity distribution as an infinite number of synthetic models may exist which fit the data equally well

(DeGroot and Constable 1990). Constraints are often imposed on the models to produce an optimal outcome, but it is important to understand the solutions are only unique to the parameters chosen (Constable et al. 1987). Resistivity data is commonly inverted using a smoothness-constrained procedure known as Occam's inversion (AGI 2014). Occam's inversion seeks to find solutions which are never more complex than the true subsurface resistivity distribution (Constable et al. 1987) by producing the smoothest possible model whose apparent resistivity distribution fits the measured data to an *a priori* Chi-squared statistic (AGI 2014).

Data from electrical resistivity surveys was inverted using the commercial inversion software EarthImager 2D (AGI 2014). The time required for processing the ERT data is relatively short. Preliminary inverted profiles are generally able to be created in the field. Processing and interpreting the final profile generally requires less than a day of office time to complete.

3.2.3 Appraisal of Results

Along with the subsurface resistivity profile that is generated from an inversion, several measures of the quality of the inversion are available. The RMS misfit and the L2 misfit both provide an indication of the misfit of the measured data to the calculated resistivity profile. A lower number indicates a better fit. Typically, a RMS misfit of less than 5% or a L2 misfit of less than 1 indicate a high quality inversion, although these values may be adjusted depending on the level of noise in the measured data (AGI 2014). To remove some of the noise in the data, it is typical to remove outliers after an inversion and rerun the inversion.

The depth of investigation (DOI) for resistivity surveys can be described as a measure of the sensitivity of the inverted resistivity value to the measured data. DOI depends on the geometry of the electrodes and can be described as a curve at which half the signal contribution comes from above and below (Oldenburg and Li 1999). DOI may also be estimated by identifying regions which are least sensitive to chosen inversion parameters. Calculating the DOI can help identify regions in an inverted section that are more sensitive to the measured data and thus can be interpreted more confidently, as opposed to regions where the inverted resistivity value is sensitive to the starting model.

Oldenburg and Li (1999) proposed a method to calculate a DOI index by comparing the effect of different starting synthetic models on the inversion results. They proposed using two separate homogenous starting models with the resistivity values r_{1r} and r_{2r}, respectively, and inverting the measured data from each starting model to have a similar misfit. This paper uses a

one-sided DOI index approach where r_{1r} was equal to the average of the measured apparent resistivity values and r_{2r} was approximately equal to ten times r_{1r}. The DOI index, $R(x,z)$, is calculated using Equation 1 and can be normalized by its maximum value (Equation 2) to arrive at a normalized DOI index, $R_N(x,z)$. The depth of the finite element mesh used in the inversions was also extended to 3.5 times the maximum depth of the apparent resistivity pseudosection to ensure that cells near the bottom of the mesh are not significantly affected by the measured data as recommended by Marescot et al. (2002).

$$R(x,z) = \frac{|\log[r_2(x,z)] - \log[r_1(x,z)]|}{\log(r_{2r}) - \log(r_{1r})} \tag{1}$$

$$R_N(x,z) = \frac{|\log[r_2(x,z)] - \log[r_1(x,z)]|}{R_{\max}[\log(r_{2r}) - \log(r_{1r})]} \tag{2}$$

Where $R(x,z) =$ DOI index at point (x,z)

$R_{\max} =$ maximum value of $R(x,z)$

$R_N(x,z) =$ normalized DOI index at point (x,z)

r_{1r}, r_{2r} = initial resistivity values for each homogenous starting model

$r_1(x,z)$, $r_2(x,z)$ = Inverted resistivity values at (x,z) from models with resistivities r_{1r}, r_{2r}

Areas which are least affected by the starting model will have a R_N value near zero and may be used more confidently for interpretation. Areas which are most affected by the starting model will have a R_N value closer to one and should be used cautiously when interpreting the inverted profile. Odenburg and Li (1999) used the $R_N=0.20$ contour line as a cutoff value above which inverted data should be interpreted cautiously but also state that regions which are controlled by the measured data and those controlled more by the inversion parameters are typically separated by steep gradients. Further details of this approach are described in Oldenburg and Li (1999), Marescot et al. (2002), Loke (2004), and Tanguy (2011).

3.2.4 Interpretation

The resistivities of some common earth materials are shown in Figure 3-4. As the figure shows, even for a single material, there can be quite a bit of variability in the resistivity. The resistivity of soil and rock is primarily controlled by the amount of water in the soil or rock, which in turn is controlled by the porosity. Clays, as well as shale, claystone, and other similar materials,

generally conduct electricity quite well, and tend to have lower resistivity values, especially if they are saturated. Sandy material above the water table generally has a higher resistivity that decreases below the water table. Rock typically has a higher resistivity than soil due to the fact that it has a lower porosity and therefore lower water content. However, rocks with high secondary porosity (i.e. highly fractured rocks) that are below the ground water table may appear as low resistivity zones.

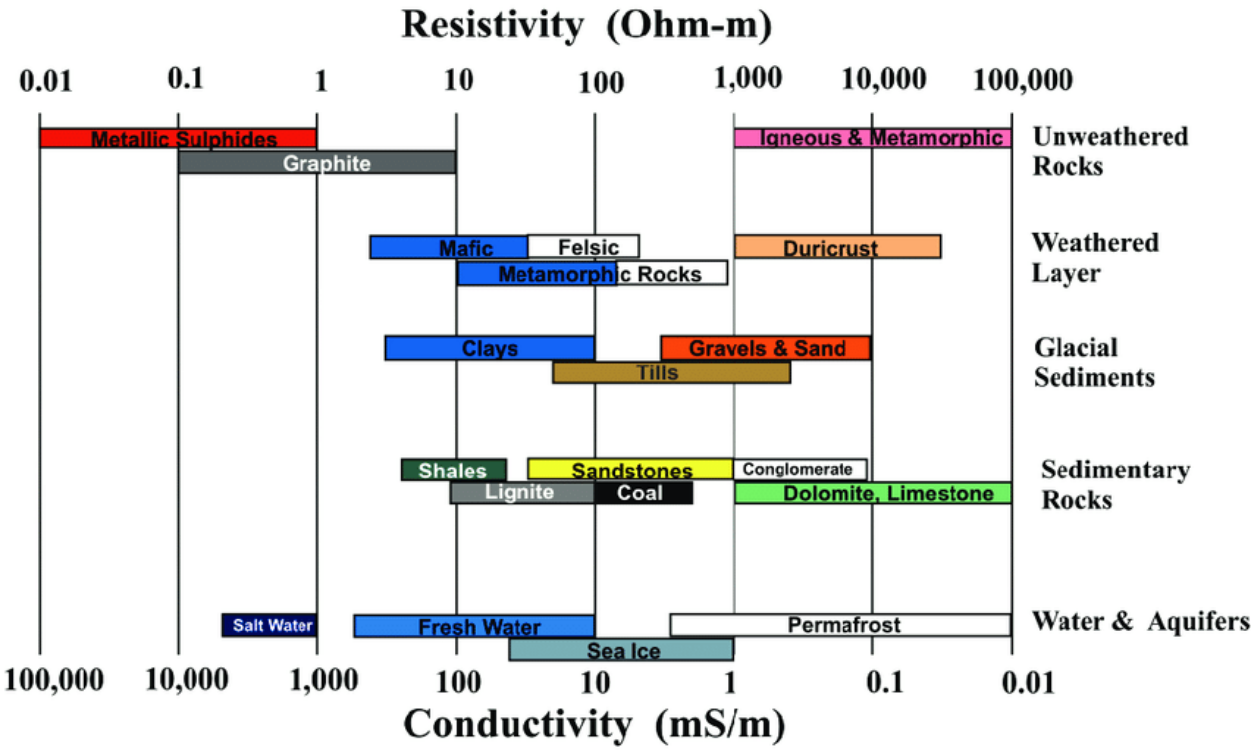

Figure 3-4: Resistivity of common rocks, soils, and minerals (Rosas-Carbajal 2014)

Sinkholes or voids that are filled with loose, unsaturated material or air may appear as high resistivity zones. Sinkholes that are filled with water or saturated material will appear as low resistivity zones. If the limestone bedrock appears as a high resistivity zone, pinnacled rock or solution-widened joints often appear as lower resistivity areas protruding into the high resistivity zone. However, if the limestone has a lower resistivity than the overlying material, then these features will appear as higher resistivity protruding into the lower resistivity rock.

It should be noted that linear, metallic structures can affect resistivity results, even if they are some distance away from the line. Structures such as fences, guardrails, pipes, or power lines that are parallel to a resistivity line can create a preferential flow of current, which makes the

affected area appear to have a lower resistivity. Therefore, resistivity lines should be placed as far away from metallic structures as is reasonably possible, and care should be taken in interpreting resistivity profiles that may be affected. This is generally not an issue for structures that are perpendicular to the line. Additionally, there may be issues inverting and interpreting resistivity lines that go over large, near surface voids (e.g. box culverts).

3.3 Seismic Methods

For seismic methods, a source of seismic waves or vibrations is applied to the ground. For many smaller tests, this source is a sledgehammer (Figure 3-5). The waves travel through the ground and are recorded on receivers, such as geophones. Different types of waves are generated by the hammer impact (Figure 3-5) and will travel at different speeds based on the stratigraphy and the elastic stiffness of the soils and rock at a given site. The shear wave velocity (V_s) is commonly used to measure stiffness of soils and rocks in geotechnical engineering and represents the speed at which an s-wave (or shear wave) travels through the soil. By recording the waves as they move away from the source, information on the structure of the subsurface can be obtained. These measurements are then used within a numerical analysis to determine the subsurface velocity profile that would best match the recordings. This process is called inversion, where numerical models are created and adjusted until the results from the numerical models match the experimental observations within some tolerance. Some seismic analyses only focus on a single type of wave (e.g., surface wave analyses focus on Rayleigh or Love waves), while other methods will utilize multiple types or all of the recorded waves (e.g., full waveform inversion). Further details on each step in performing a seismic survey are discussed in the following sections.

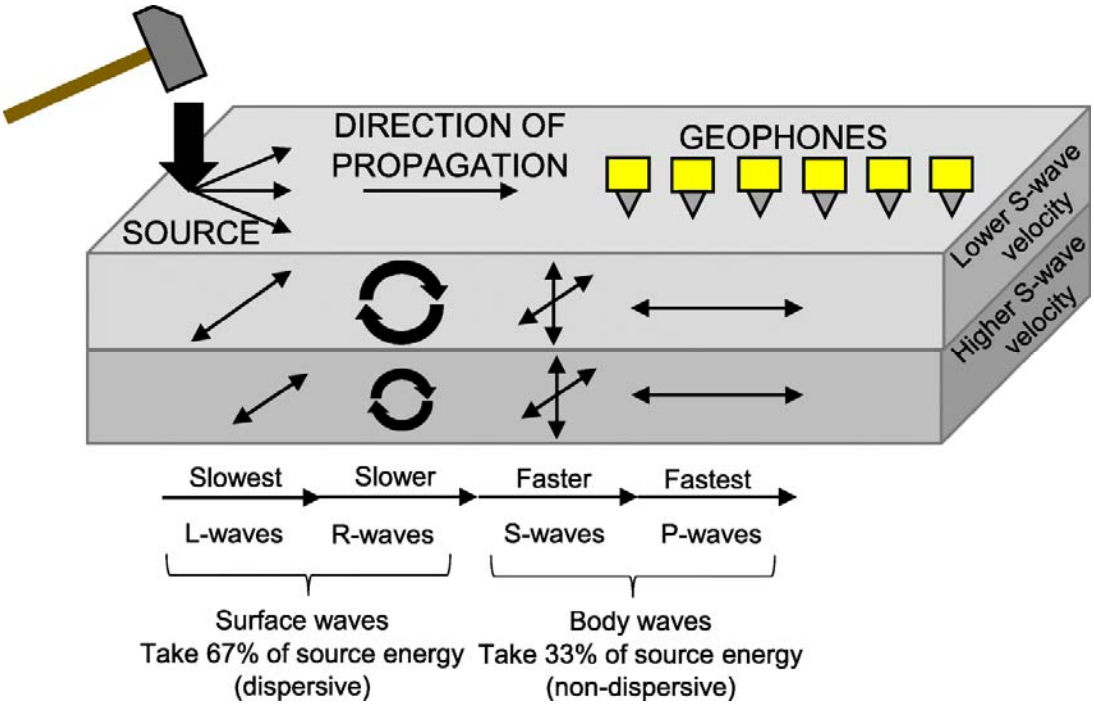

Figure 3-5: Body and surface seismic waves generated by a sledge hammer (seismic source) and received by an array of geophones (receivers). Simplified directions of particle motion in the ground are shown for a two-layer system (Jug et al. 2020).

3.3.1 Data Collection

The seismic data acquisition equipment consists of a Geometrics Geode seismograph connected to a laptop computer, 4.5 Hz geophones, and spread cables. Each Geode can record up to 24 geophones and several Geodes can be connected. The geophones measure seismic waves that are generated by a source, typically a sledgehammer striking a metal plate. Hammers from 10 to 20 pounds [45 to 90 Newtons] are typically used. The Geode seismic data acquisition system is shown in Figure 3-6.

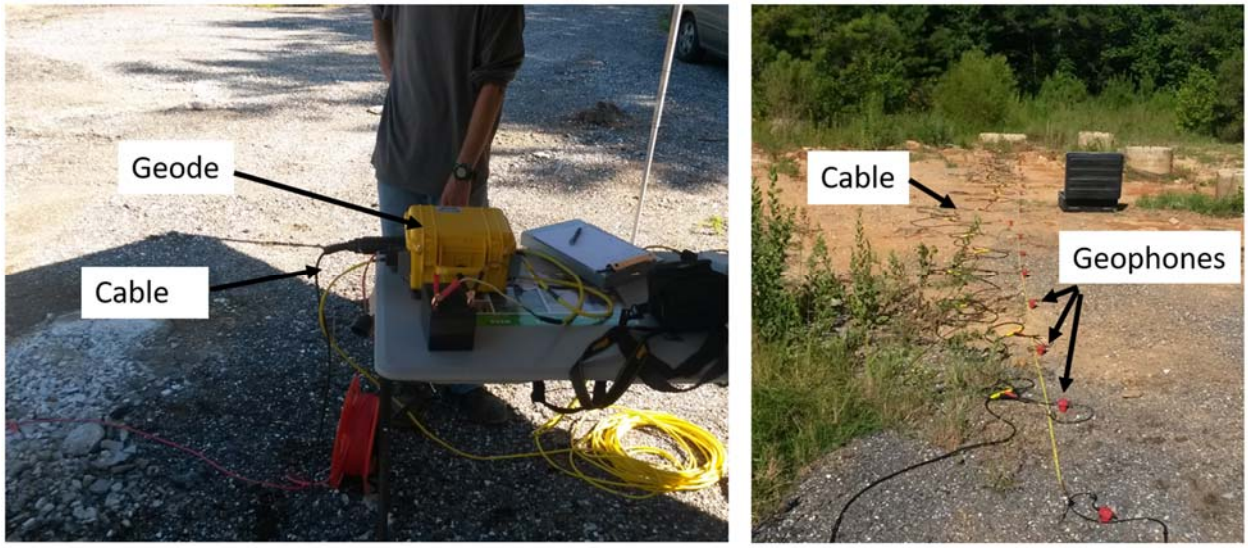

Figure 3-6: Geode Seismic Data Acquisition System

The geophone spacing is variable (typically 3.3-6.6 feet [1-2 meters]). Generally, larger spacings (and therefore longer spread lengths) can provide a greater depth of investigation at the cost of decreased resolution. However, the depth of investigation is also a function of the frequency of the source, so a longer spread does not necessarily guarantee a greater depth of investigation.

The source spacing and location may also vary depending on the survey type and goals. For a multichannel analysis of surface waves (MASW) survey, the sources are placed off the end of the spread, typically at distances of up to half the spread length from the end. To collect data for full waveform inversion (FWI) processing, sources are placed at regular intervals throughout the spread.

3.3.2 Processing and Inversion

(1) Multichannel Analysis of Surface Waves (MASW)

The multichannel analysis of surface waves (MASW) can be used to develop a 1D shear wave velocity model of the subsurface. This method is not as complex as some other seismic processing methods, and data can be processed fairly quickly and easily. A thorough knowledge of seismic wave propagation, signal processing, and nonlinear optimization is not required to use MASW. Because MASW provides a 1D profile, it is unable to directly detect lateral heterogeneities such as sinkholes and pinnacled rock. However, multiple 1D profiles can be combined to create a pseudo-2D profile that may capture lateral variations.

For the MASW technique, various signal processing techniques can be used to transform the field records to show amplitude as a function of frequency and phase velocity. When viewed this way, a curve can be picked that relates the frequency of the surface waves to the velocity at which they travel. This curve is called the *dispersion curve*. Once the dispersion curve is picked, an inversion procedure is used to determine a 1D velocity model that fits the picked dispersion curve, typically in a least squares sense. The workflow for MASW is shown in Figure 3-7. The open-source software Geopsy (Wathelet et al. 2004, Wathelet 2008) was used for MASW processing. The Geopsy software generates many 1D seismic profiles and ranks them based on their fit to the picked dispersion curve. Other MASW software is available that generates a single profile that is the best fit in a least-squares sense. SurfSeis, a software by the Kansas Geologic Survey, is an example of this type of software. This software is typically easier to use than Geopsy but is has the drawback that it does not consider the non-uniqueness that is inherent in the inversion.

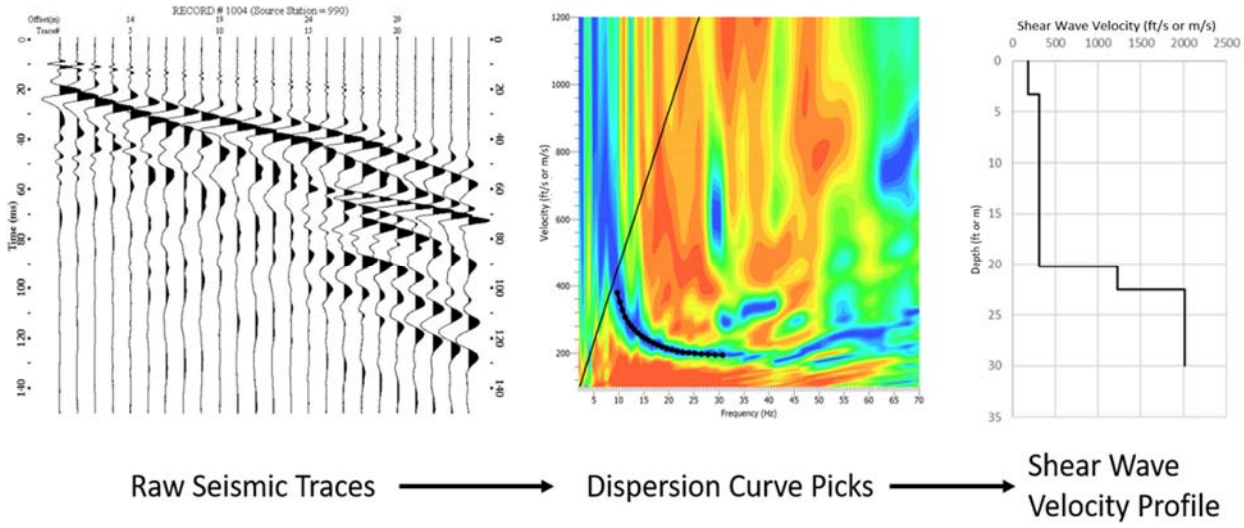

Figure 3-7: MASW processing workflow

(2) Seismic Full Waveform Inversion (FWI)

The FWI processing (Virieux and Operto 2009) begins by selecting a trial subsurface velocity model and then solving the elastic wave equation to generate a set of synthetic seismograms. This is called the forward model. The misfit between the synthetic seismograms in the forward model and the observed (field) seismograms is calculated along with the gradient of the misfit with respect to the parameters used in the velocity model. The gradient and misfit are

then used in a nonlinear optimization algorithm to calculate an updated velocity model so that the misfit is reduced. A new set of synthetic seismograms is calculated for the updated model and the process is repeated until some predefined stopping criteria is reached.

For the current study, the forward modeling was performed using SPECFEM2D (Tromp et al. 2008). This is an open-source, spectral element code that solves the elastic wave equation. SPECFEM2D has been widely used for global, regional, and exploration seismology (e.g., Modrak and Tromp 2016). The forward model provides a set of synthetic seismograms that are then compared to the observed seismograms. This comparison is made in terms of the misfit between the synthetic and observed data and is calculated as the sum of the waveform residual energy over all sources and receivers, (Equation 3).

$$\chi = \sum_{Sources} \sum_{R} \int_{T_0}^{T_1} \left\| s(x_R, t) - d(x_R, t) \right\|^2 dt \tag{3}$$

Where χ = misfit

s = synthetic seismogram

d = observed seismogram

x_R = position of receiver, R

t = time

T_0, T_1 = bounds of time window of interest

Once the misfit is calculated the gradient of the misfit with respect to the model parameters is calculated using the adjoint method described by Tromp et al. (2008). This method essentially solves the wave equation using the time-reversed residuals as simultaneous sources at the receiver locations to develop an “adjoint” wavefield. The gradient is then calculated using the interaction of the adjoint wavefield and the forward wavefield. Details for this calculation can be found in Tromp et al. (2008).

In the current study, a regularization term is added to the misfit function in an attempt to suppress some non-uniqueness and ensure a certain degree of smoothness on the velocity model. A Tikhonov regularization term is used. This term is the squared norm of the spatial gradient integrated over the entire problem domain, as seen in Equation 4. If the velocity model is smoother, this term will be smaller, leading to a lower overall misfit. A regularization parameter, λ, is a small, positive real number that controls how much smoothing is forced on the model.

$$\chi_{reg} = \chi + \frac{\lambda}{2}\int_V \left\|\nabla_x m\right\|^2 dV \tag{4}$$

Where χ_{reg} = regularized misfit

$\nabla_x m$ = spatial gradient of velocity model

V = model domain

λ = regularization parameter

A limited memory Broyden-Fletcher-Goldfarb-Shanno (L-BFGS) quasi-Newton method was used to minimize the misfit (Nocedal and Wright 2006, Modrak and Tromp 2016). This method approximates the inverse Hessian while only storing a few vectors rather than the full matrix. This reduces the computational effort required to perform the inversion. The strong Wolfe conditions were satisfied for each iteration (Nocedal and Wright 2006). The entire inversion procedure was implemented by the authors using Matlab and runs on both high-performance desktop computers and high-performance computing clusters. The time to perform FWI is currently on the order of hours, but this processing time will likely decrease as the technology matures and as the codes are further optimized.

One issue that arises when using a 2D numerical model is that the source function in the numerical model is inherently a line source. Because a point source is used in the field (i.e., hammer impact), there is a phase and amplitude difference in the synthetic and observed seismograms due to the different types of sources. To account for this, the corrections given by Schafer et al. (2012) are used. The observed data is first convolved with $t^{(-1/2)}$ to correct the phase. The amplitude is then corrected using an empirical factor of the form Ar^{α} where r is the source-receiver distance. The values of A and α are determined by minimizing the energy of the residual waveform (that is, the difference between the synthetic and observed data). To calculate the source-time function, a method similar to that used by Ernst et al. (2007) is employed. For this study, an impulse response of the trial model is calculated and then deconvolved from the observed data to give an approximate source-time function.

3.3.3 Appraisal of Results

The quality of a seismic inversion is usually appraised by qualitatively comparing the modeled data to the observed data, although quantitative measures of the misfit are available and

are useful for ranking various models. For MASW, the calculated dispersion curve is compared to the dispersion curve picks that were generated from the field data as shown in Figure 3-8.

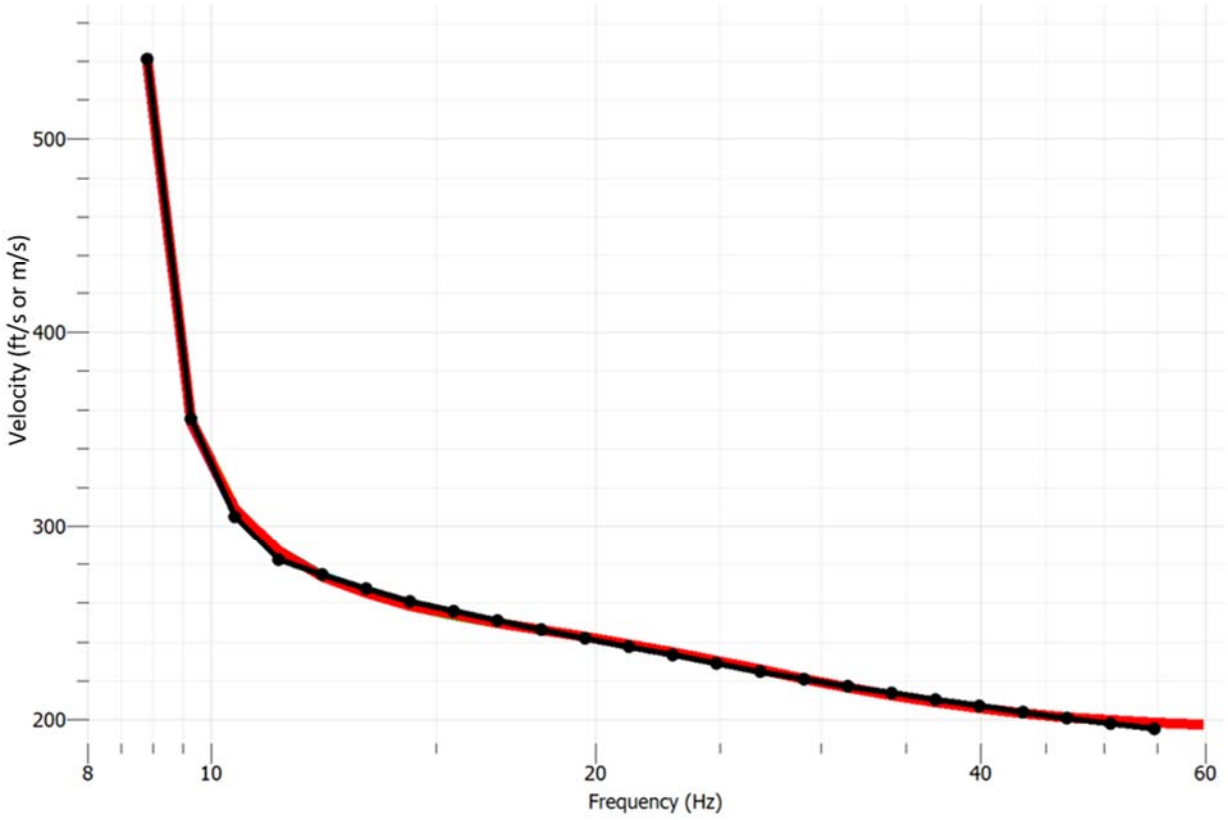

Figure 3-8: Calculated (red) and picked (black) dispersion curve

To appraise full waveform inversion results, the calculated seismic traces are compared with the target traces. As with MASW, a qualitative measure of the misfit is most useful for comparing two possible models. An example of the resulting traces from the full waveform inversion algorithm is shown in Figure 3-9, along with the recorded traces. Several points about the data collection and FWI algorithm are illustrated in this figure. First, peaked traces near the source have been removed, as have traces far from the source that have a low signal-to-noise ratio. Second, although there is traffic noise in the observed data from the adjacent interstate, the surface waves do not seem to be significantly affected by this. The FWI algorithm is able to match the observed surface waves fairly well, but there is more mismatch associated with some of the higher frequency body waves.

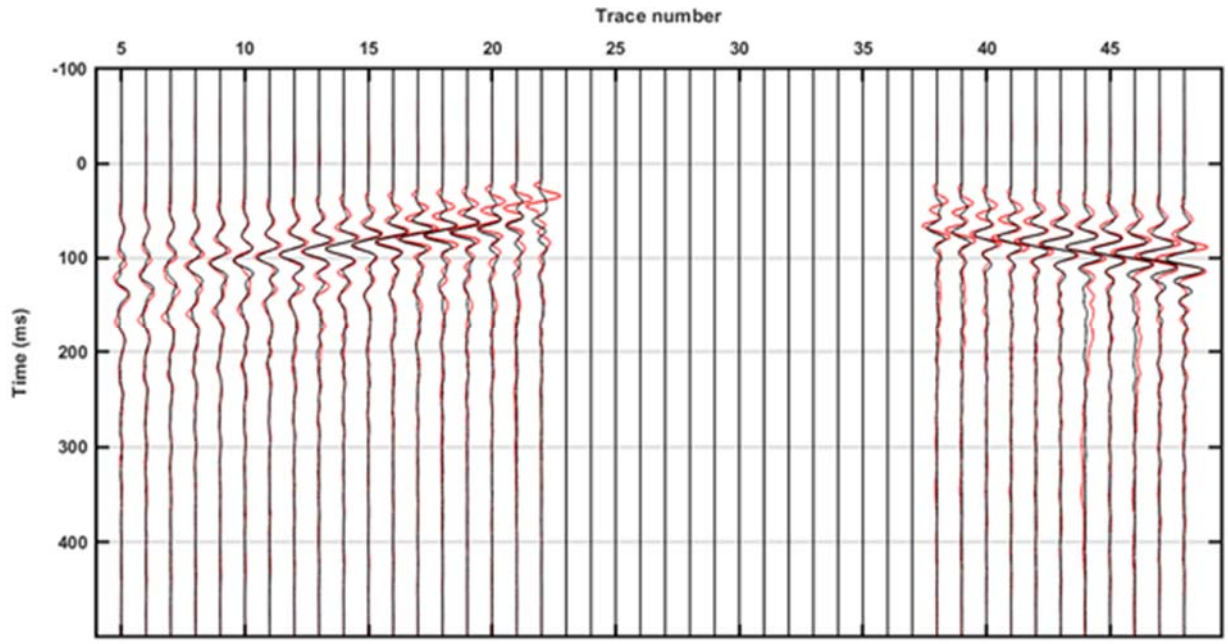

Figure 3-9: Observed (red) and simulated (black) seismic traces from Full Waveform Inversion (FWI) algorithm. Note that receivers close to the source have been removed from the inversion as these receivers reached their peak response

3.3.4 Interpretation

Table 3-1 shows the shear wave velocities that are used in the IBC/ASCE 7 (ASCE 2010) to distinguish different seismic site classes. This table includes generic material descriptions for the shear wave velocities that are averaged over the upper 100 feet [30 meters]. These descriptions often provide a good starting point for developing geologic interpretations from seismic data. As the table shows, shear wave velocities generally correspond to the soundness of the material.

Table 3-1: Seismic site class and descriptions used in the IBC (after ASCE 2010)

Site Class	**Generic Description**	**Shear Wave Velocity (Vs30)**
A	Hard rock	>5000 ft/s [1500 m/s]
B	Rock	2500-5000 ft/s [760-1500 m/s]
C	Very dense soil and soft rock	1200-2500 ft/s [360-760 m/s]
D	Stiff soil	600-1200 ft/s [180-360 m/s]
E	Soft soil	<600 ft/s [180 m/s]

Because seismic velocities correspond to material stiffness, the rock surface can often be identified as the transition from a lower velocity layer to a higher velocity layer. One dimensional methods such as MASW, provide data only at discrete points. Because it is a 2D method, FWI can provide a continuous rock surface, which is often more useful in areas with pinnacled rock or other karst features. Generally, sinkholes or voids will appear as a low shear-wave velocity zone. This is the case for voids filled with water or air, as well as loose or soft soil.

Both MASW and FWI seem to perform poorly in areas where the rock is within about 10 feet [3 meters] of the ground surface. Where the rock is known to be relatively shallow, other investigation methods should be given preference over surface wave based seismic methods. Additionally, seismic methods generally perform poorly in noisy environments, such as near busy interstate highways. However, MASW seems to be fairly robust even in the presence of noise, although noise can decrease the depth of investigation.

3.4 Joint Interpretations

Interpretation of the electrical resistivity and seismic geophysical tests in karstic geology can be challenging due to the highly heterogeneous environments and limitations inherent to each method. Electrical resistivity tomography (ERT) and seismic methods are often used together to overcome these individual limitations and reduce uncertainty in the interpretation of results (e.g., Sumanovac and Weisser 2001, Cardarelli et al. 2009, Margiotta et al. 2015). For example, a high resistivity zone could be interpreted as an air-filled void or as rock, but when combined with seismic results, it can be identified with less uncertainty.

Practically, this can be achieved by creating a scatter plot of electrical resistivity versus shear wave velocity as shown in Figure 3-10. In this figure, the rock shows up as the group of points at the top right that have high resistivity and high shear wave velocity. The overburden appears as the cluster at the top left, points that have lower velocities and moderate to high resistivities. The sinkhole feature appears as the cluster on the lower left, a zone of low resistivity and low velocity. This type of analysis can often be useful if one of the geophysical methods is difficult to interpret.

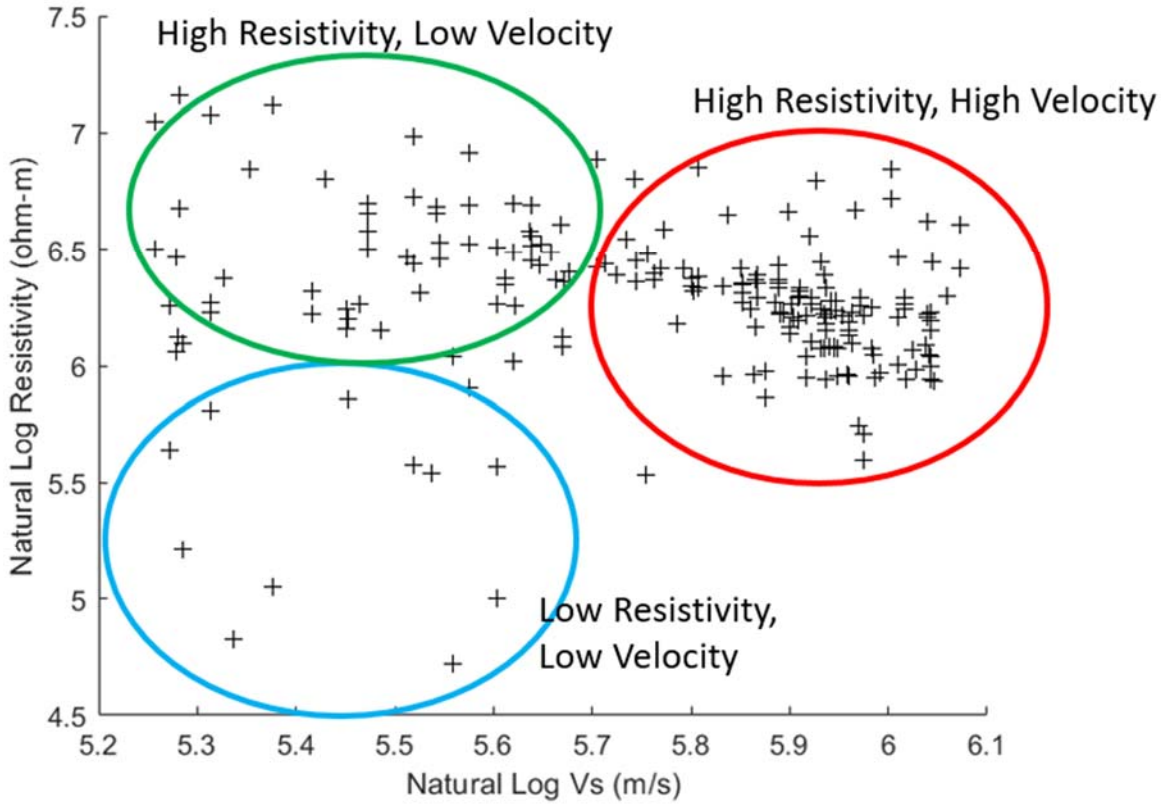

Figure 3-10: Scatter plot of normalized electrical resistivity versus normalized shear wave velocity

Other sources of information should also be included in geophysical interpretations. This includes information from geologic maps, aerial photos, and nearby outcrops, as well as any available borings. Much of this information could be gathered before any geophysical surveys have been completed. In this way, a hypothesis of the subsurface structure could be developed and then rationally updated through the interpretation of the geophysical results. This in turn would inform the selection of the locations and types of insitu tests to be completed. As the subsurface information is gathered, the conceptual model of the subsurface should be incrementally updated in a way that all available information is included.

CHAPTER 4: GEOPHYSICAL SURVEYS

4.1 Introduction

One of the key tasks in the current project was the development and implementation of a geophysical field testing program at karst sites across the state. The objective of this program was to determine advantages and limitations of the selected geophysical methods and to provide training to ALDOT personnel on the performance and interpretation of the test results. This field testing program was implemented at eight sites with either active (open) sinkholes, repaired sinkholes, or pinnacled rock that was leading to subsidence. This chapter provides an overview of the field testing program and the sites where geophysical surveys were performed and discusses some key findings from each of the different types of sites.

4.2 Overview of Sites

The locations of the geophysical surveys were mapped (Figure 4-1) in relation to geologic units (Tew 2006) with carbonate rocks (i.e., limestone, dolostone, and marble). These units are expected to be the most susceptible to sinkhole development, although other regions of the state also have a significant number of sinkholes (Figure 2-1) due to both buried carbonate rocks and non-karst sources of sinkhole development. A summary of the tests performed at each site along with the selected category is provided in Table 4-1. The tests followed the procedures discussed in the previous chapter.

Table 4-1: Geophysical survey locations

Site	Approximate Coordinates	Category	Electrical Resistivity	Seismic FWI
Talladega CR-2	33.145848°, -86.355152°	Repaired Sinkhole	X	
I-65	33.208924°, -86.795281°	Repaired Sinkhole	X	X
Logan Martin	33.433431°, -86.336917°	Active Sinkhole	X	X
Spring Villa	32.596391°, -85.304354°	Active Sinkhole	X	X
SR-275	33.412646°, -86.132528°	Active Sinkhole	X	
SR-21	33.367164°, -86.170198°	Possible Sinkhole	X	
Centreville	32.941597°, -87.085996°	Pinnacled Rock	X	
I-59/20	33.519557°, -86.858681°	Pinnacled Rock	X	

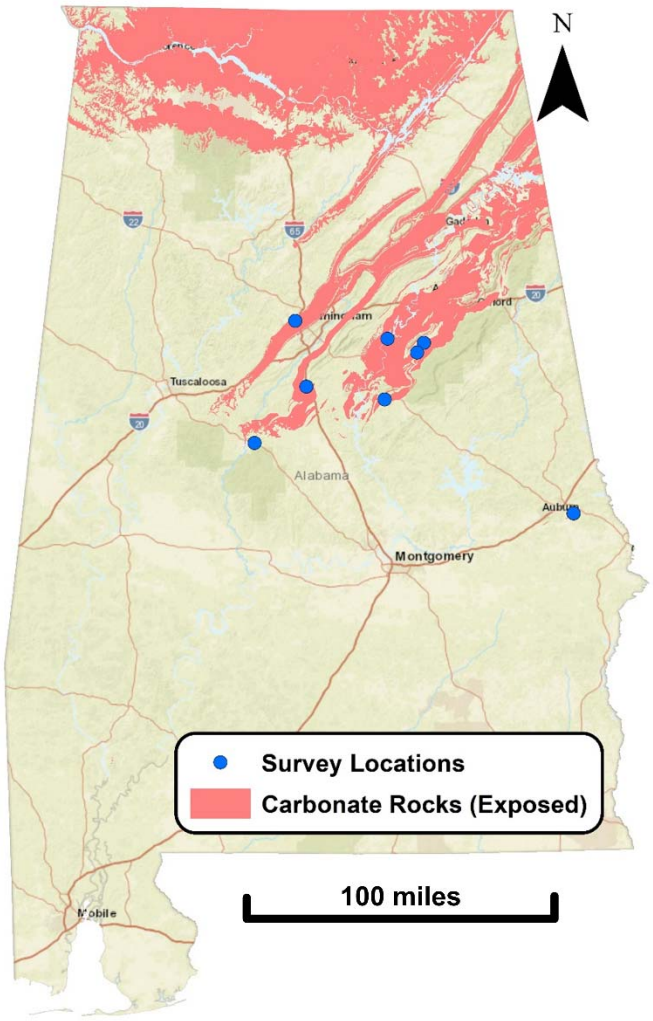

Figure 4-1: Locations of geophysical surveys in relation to exposed geologic units containing carbonate rocks (i.e., limestone, dolostone, and marble). Geologic units from GSA (2006).

4.3 Surveys at Repaired Sinkholes

Geophysical surveys were performed at two sites (Talladega County Road 2 and I-65 near the Shelby County Airport) where sinkholes had occurred and been repaired prior to the survey (Table 4-1). Both repairs were completed by filling the hole with a mixture of rock and/or flowable fill. Resistivity tests were performed at both sites, while seismic FWI was only performed at the site along I-65. The goal of the surveys at these sites was to try and map the bedrock surface and to identify any features, which may have contributed to the formation of the sinkholes. Some results from each of the sites are discussed below along with some general findings concerning surveys at repaired sinkholes.

4.3.1 Talladega CR-2

An electrical resistivity survey was performed along CR-2 in Talladega County near a recently repaired sinkhole to investigate possible karst features and determine depth to rock. The location of the electrical resistivity line is shown in

Figure 4-2 in relation to existing sinkhole repairs. The survey line had to be performed on the side of the road opposite the sinkhole repair due to the presence of power lines, which could negatively influence the geophysical results. The survey was performed on 7/26/2019. The geology near the site is complex, but the sinkhole and survey line appear to be in the Shelvin Rock Church formation (Whiting 2009). The site also lies very close to the Gooch Branch Chert formation and the Gantt's Quarry formation. Each of these formations contain dolomitic marbles that are potentially karstic and have a history of sinkhole formation in the Sylacauga area (Ruffin-Bass 1996).

The inverted resistivity profile is shown below in Figure 4-3. The results show a layer with a mix of low to high resistivities at the surface underlain by a higher resistivity layer to depths of about 25-75 feet. These upper layers are interpreted as overburden soils which may be unsaturated. A deeper low resistivity layer (200-400 ohm-m) is also apparent in the results which is interpreted as the surface of the marble unit. These resistivity values are consistent with marble which is reported to exhibit resistivities as low as 100 ohm-m (Loke 2004). The interpreted rock surface appears to be at a depth of about 70 feet in the vicinity of the recently repaired sinkhole and varies between depths of about 30-75 feet over the length of the survey line. Due to the large depth to the rock surface, seismic methods were not used at this site as they were not expected to give enough resolution at those depths.

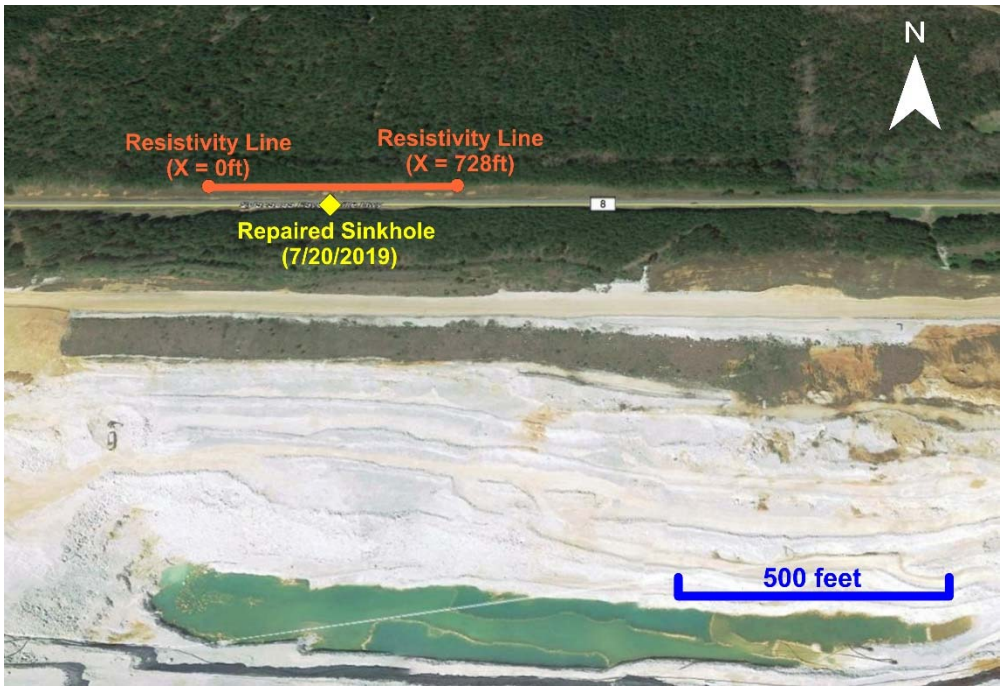

Figure 4-2: Site map showing location of resistivity line and recently repaired sinkhole along Talladega CR-2.

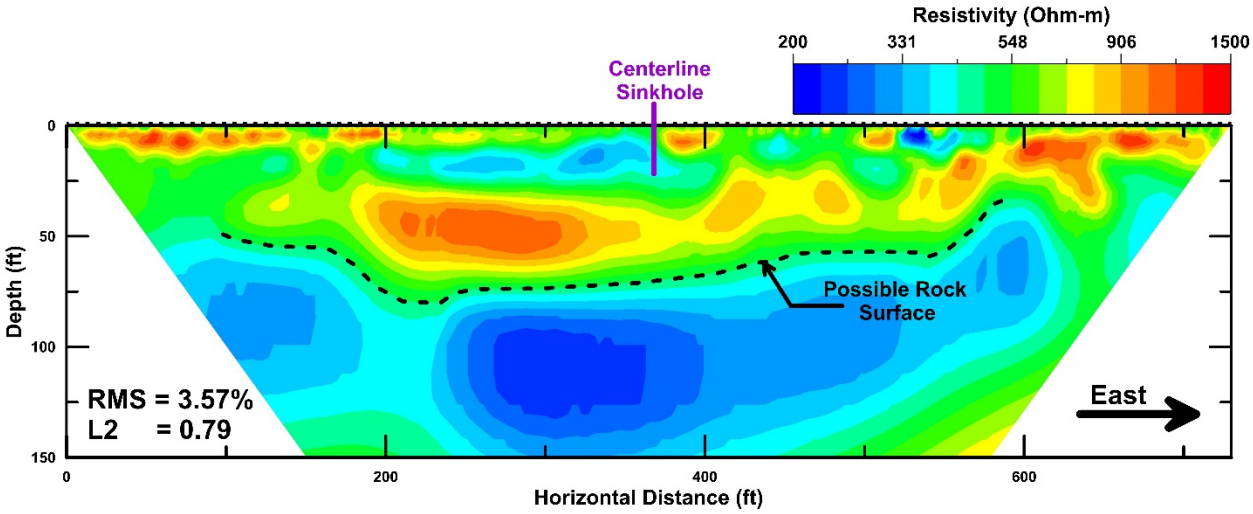

Figure 4-3: Inverted resistivity profile with interpreted potential rock surface for Talladega CR-2.

4.3.2 I-65 at MP 236.5

A geophysical investigation was conducted along the shoulder of I-65 Northbound (NB) near MP 236.5 on January 7, 2019. The site lies along a boundary of between two carbonate rock units (undifferentiated Chepultepec and Copper Ridge dolomites and Longview and Newala limestone). Several limestone quarries exist in the area with the closest active quarry sitting only

1700 feet [520 meters] northwest of the site. Sinkhole activity near the site has been reported previously requiring repairs along the interstate. The most recent, was a small sinkhole (roughly 1 meter in diameter) that was reported on the shoulder of the roadway (Figure 4-4) in the spring of 2011. A drilling program was then implemented by ALDOT near the reported sinkhole lasting for 6 days. Soils with an SPT N-value less than or equal to 6 were considered soft soils (Figure 4-5). The drilling program revealed a vertical zone of soft soils extending down to rock between boreholes B2 and B5.

The purpose of the geophysical surveys was to identify any potential sinkhole features using geophysical methods and then compare these results with the boring information previously acquired at the site. The geophysical investigations performed consist of 2D seismic and electrical resistivity surveys. The resistivity survey was performed closer to line A-A' and the seismic survey was performed closer to line B-B' (Figure 4-4). Both surveys were roughly centered on the zone of soft soil identified in the borings and both were performed within a few hours of each other. The time required to collect both the resistivity and seismic data was approximately 2 hours each using a four-person crew. This is significantly less time than required for the drilling program (approximately 6 days to complete 10 borings) and the geophysical surveys were able to be completed without any disruption to traffic on the interstate.

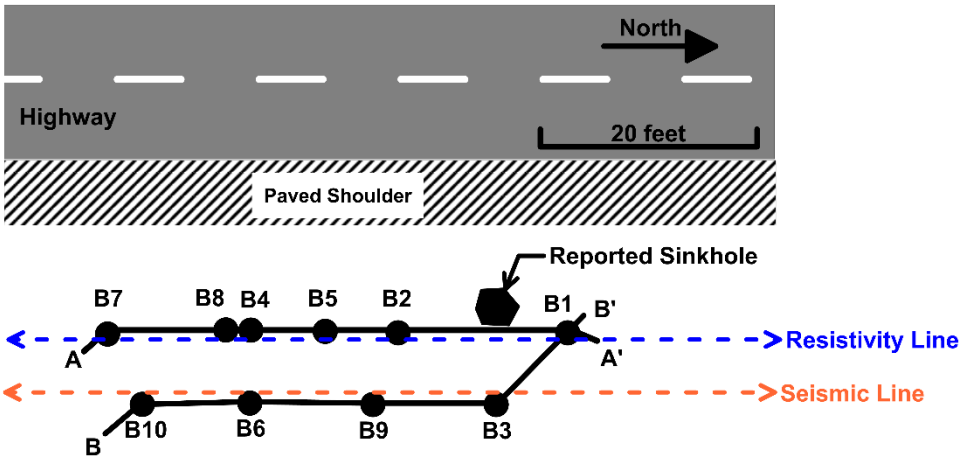

Figure 4-4: Site map with locations of borings and reported sinkhole along NB I-65 at MP 236.5.

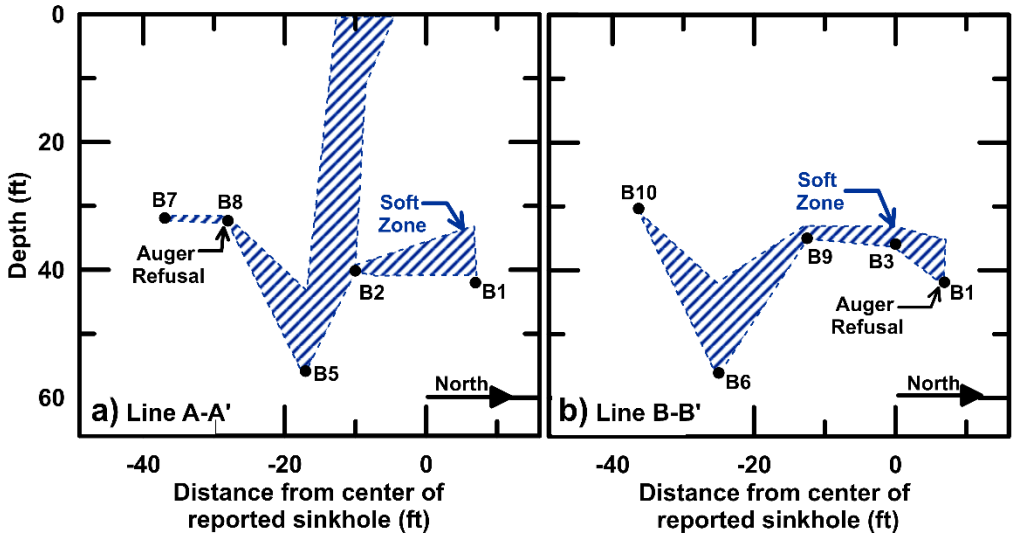

Figure 4-5: Soft soils and auger refusal surface encountered during drilling for lines a) A-A' and b) B-B' as shown in Figure 4-3.

The results of the geophysical tests are compared with the boring information in Figure 4-6. The interpreted auger refusal surface from the ERT results is shown in Figure 4-6a. Regions where the data was most uncertain were blanked out using the depth of investigation (DOI) parameter as described by Oldenburg and Li (1999). The ERT results provide a continuous representation of the auger refusal surface over along a length of about 230 feet [70 meters]. The ERT results show a break in the interpreted low resistivity auger refusal material at the same location as the interpreted solution widened joint along line A-A'. The width of the solution feature is difficult to determine based on the ERT results alone, but the gap in the interpreted rock surface is approximately 55 feet [17 meters] wide. The minimum depth to the interpreted auger refusal surface was about 30 feet [9 meters] but its maximum depth was difficult to estimate from the ERT results as the surface of the interpreted low resistivity auger refusal material is not identifiable within the limits of the solution widened joint.

The interpreted auger refusal surface from the seismic FWI results are shown in Figure 4-6b. The seismic FWI data provided a continuous representation of the auger refusal surface over a length of about 100 feet [30 meters]. The seismic data shows a dip in the interpreted high velocity auger refusal surface near the location of the solution widened joint from line B-B, but the velocity contrast is not very high. The width of the solution widened joint based on the seismic FWI results is about 13 feet [4 meters] and the depth of the interpreted high velocity auger refusal material varies from 23 to 36 feet [7 to 11 meters] which is shallower than suggested by the borings. The

location of the solution widened joint from the seismic FWI results is also located to the left of the feature identified in the borings.

The interpreted surfaces from the geophysical investigations are compared with the auger refusal points from the drilling program in Figure 4-6c. The resistivity line was placed along line A-A' and the seismic line was placed closer to line B-B' (Figure 4-4), so data from both lines is shown in Figure 4-6c. All three investigation methods show a break in the rock surface at the approximate location of the sinkhole. The ERT results show a much wider feature than the other two, but this is expected from using a smoothness-constrained inversion technique, which will tend to blur sharp changes in layering. The FWI results were the most difficult to interpret, primarily because they were rather limited in depth. Outside of the sinkhole area all three methods show a similar depth to rock with both the ERT and FWI providing continuous measurements over a larger area than the borings. While the preceding discussion has focused on interpreting the different results independently, a more complete picture of the subsurface can be obtained by integrating the results of all three investigation methods.

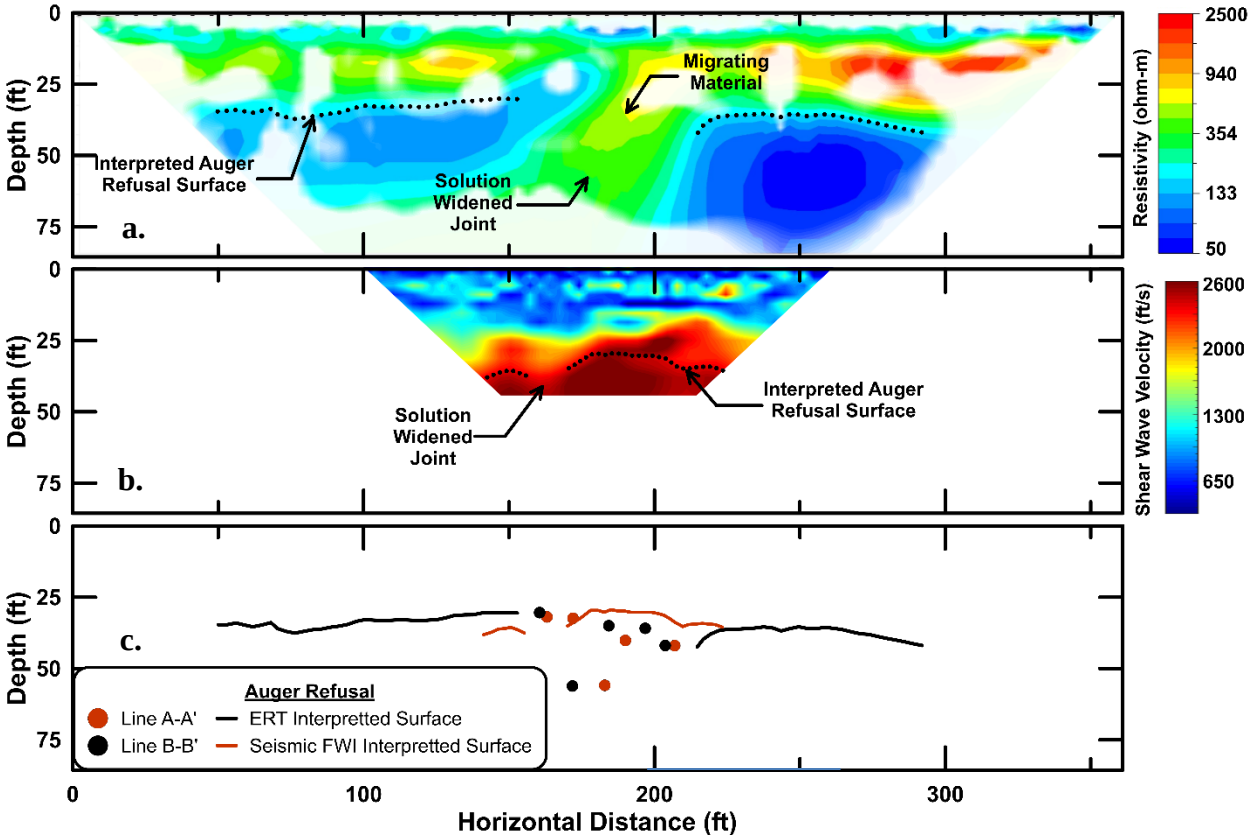

Figure 4-6: Interpreted profiles from the (a) inverted resistivity section, (b) seismic FWI results and (c) rock surfaces from all three investigation methods.

4.3.3 Lessons Learned from Repaired Sinkholes

The two surveys described above both attempted to map the bedrock surface in the vicinity of a repaired sinkhole. Electrical resistivity was able to map the rock surface at both sites which showed up as a low resistivity layer below the higher resistivity surface materials (primarily cherty clay). At the site along I-65, the resistivity survey was also able to map a gap in the interpreted rock surface at the approximate location of the sinkhole, which is believed to be a solution widened joint. The FWI results were only used at the site along I-65, but showed a clear transition in velocity at the rock surface and the direct measurement of an engineering property (elastic stiffness) allowed the soil and rock layers to be identified without relying on the borings for confirmation. However, the area near the sinkhole showed only a slightly lower shear wave velocity, which likely would not have been interpreted as a significant result were it not for the presence of the sinkhole in this location. The seismic FWI results were also limited in resolution both laterally and with depth, which was why this technique was not used at Talladega CR-2 where the depth to rock was too great.

4.4 Surveys at Active Sinkholes

Three surveys were performed at sites with active sinkholes (defined as sinkholes that were open at the ground surface) and one survey was performed at a site where subsidence was observed and a sinkhole is suspected. The goal at these sites was to map both the bedrock surface and any open voids in the subsurface. Surveys at active sinkholes required additional work to deal with safety concerns associated with working around active sinkholes and a need to place the surveys adjacent to the open void rather than centered on the feature of interest, as can sometimes be done at a repaired site. A summary of the surveys at Spring Villa and Logan Martin are presented here. A report describing the surveys along SR-275 and SR-21 are included as Appendix B.

4.4.1 Logan Martin

This survey was performed about 0.5 miles north of the Logan Martin Dam on the St. Clair County side of the Coosa River. The site contains a sinkhole feature which has been active since at least 2006. At the time of the investigation the sinkhole was over 40 feet wide. Onsite personnel have been attempting to fill the sinkhole with rock and concrete for years, but subsidence continued. A line of ground subsidence was also observed extending from the sinkhole to the southwest (Figure 4-7). The subsidence line and sinkhole perimeter were surveyed with a total station. The sinkhole is primarily located within the Knox Group, which consists of dolostone,

dolomitic limestone, and limestone; and is characterized by abundant light-colored chert. Both resistivity tests and seismic FWI were performed at this site.

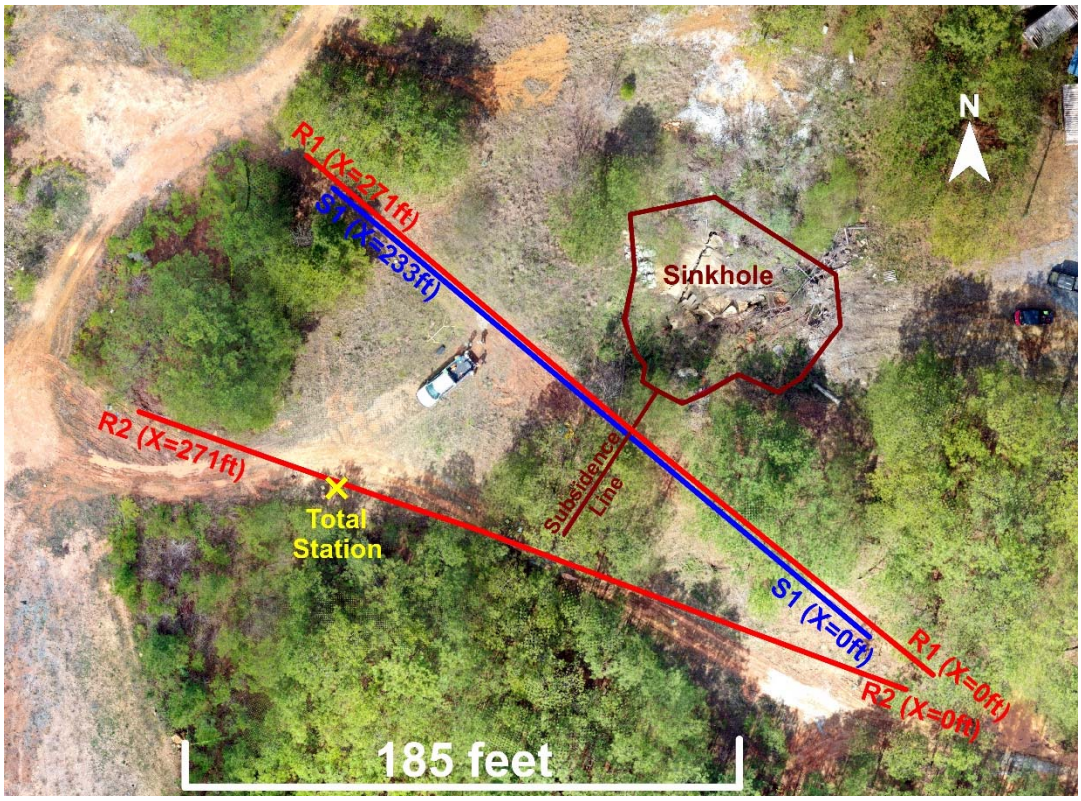

Figure 4-7: Site map for the surveys at Logan Martin with geophysical survey (resistivity lines R1 and R2 and seismic line S1) and sinkhole feature locations indicated.

The inverted resistivity sections for lines R1 and R2 are shown in Figure 4-8. An abrupt change in resistivity is observed at a depth of about 5 to 10 feet in survey R1. An abrupt change in resistivity is also observed in R2 at depths of about 5 to 8 feet. A dip in this transition is observed at X = 130 feet in survey R1 and at X = 140 feet in R2. The low point in the higher resistivity surface corresponds well with the location of the potential solution widened joint from the resistivity results. There is a second transition from higher to lower resistivity at depths ranging from 20-30 feet to as deep as 50 feet near X = 200 feet on line R1. The resistivity of this lower layer is more consistent with values typically observed for wet dolostones (Figure 3-4). From the resistivity results alone, it is very difficult to determine where the rock surface is, so seismic FWI was used to try to determine which of these regions corresponded to rock.

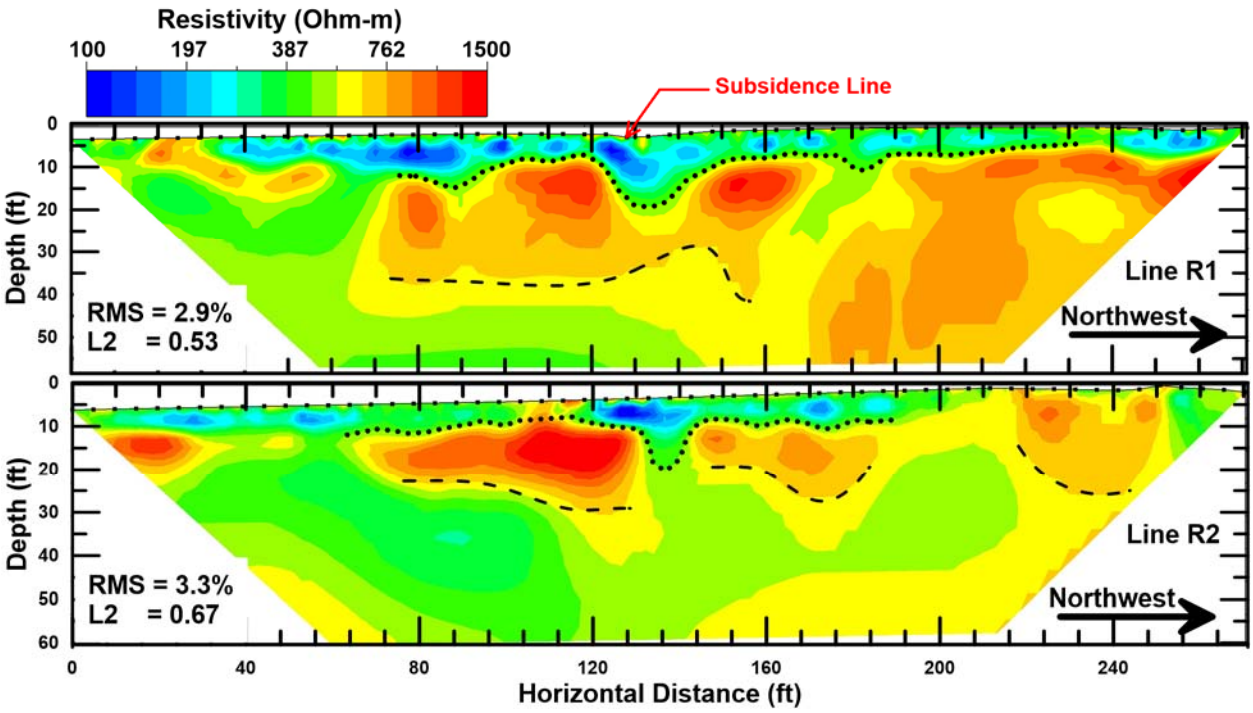

Figure 4-8: Inverted resistivity sections for lines R1 and R2 at Logan Martin. Two layer changes are identified using dashed and dotted lines, but the types of materials cannot be identified from the resistivity alone.

The results from the seismic full waveform inversion are shown in Figure 4-9. The results show an upper layer with velocities in the 700 – 900 ft/s range and then a transition to stiffer material between about 20 and 30 feet. An estimation of the potential rock surface is shown on the seismic velocity profile, although the velocity values are on the lower end for rock (V_s = 1000-1500 ft/s), so this interpretation should be confirmed with borings or other in-situ testing. The subsidence area appears as the low velocity zone at around X=125 feet, consistent with surface observations.

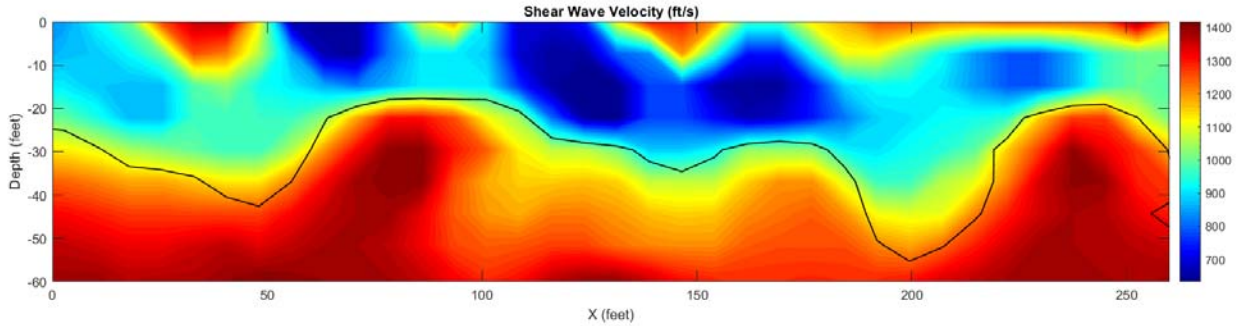

Figure 4-9: Shear wave velocity profile from seismic full waveform inversion

A joint interpretation can be formed by considering the resistivity profile from line R1 and the FWI profile together. Figure 4-10 shows a scatter plot where the resistivity has been plotted against the shear wave velocity (this methodology was previously discussed in Chapter 3.4). In this figure, several groups can be picked based on the combination of resistivity and velocity. What has been interpreted as rock shows up as the group of points at the top right that have high resistivity and high shear wave velocity. The overburden appears as the cluster at the top left, points that have lower velocities and moderate to high resistivities. The sinkhole feature appears as the cluster on the lower left, a zone of low resistivity and low velocity. The spatial locations of these groups is shown in Figure 4-11. The location of the subsidence feature from the joint interpretation is consistent with surface observations. However, this interpretation should be confirmed with in-situ testing.

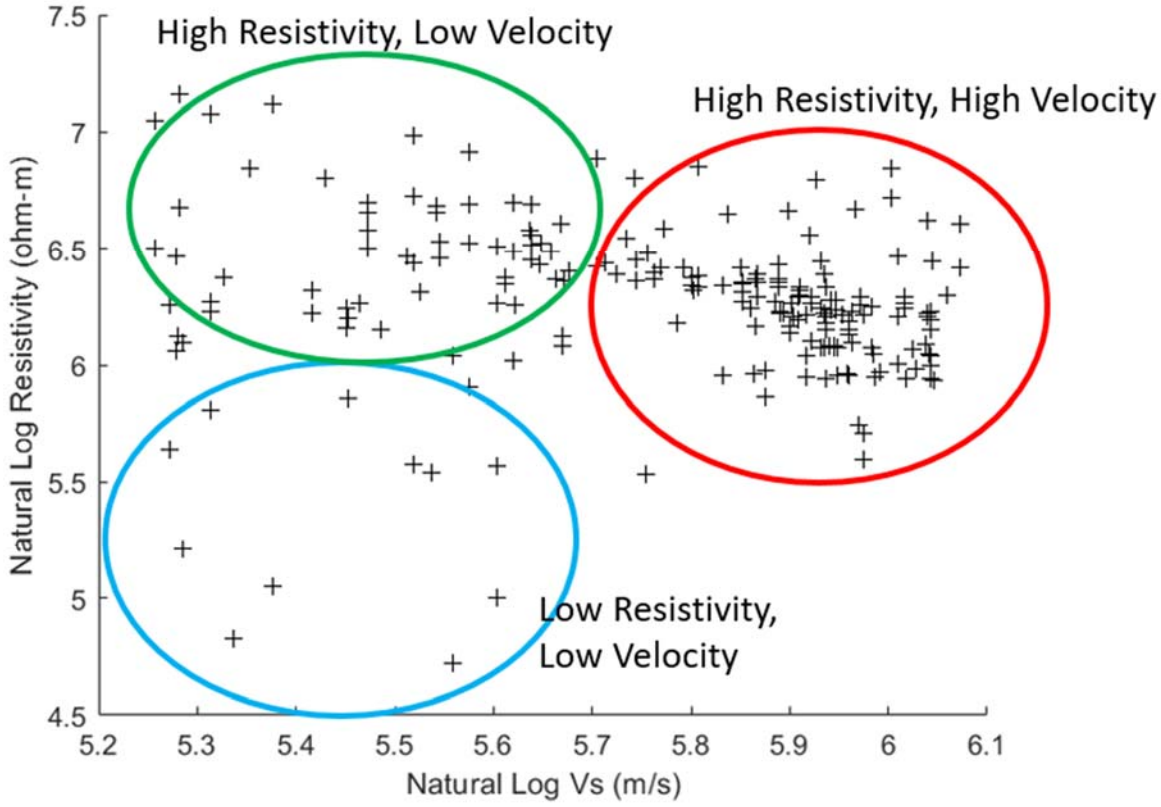

Figure 4-10: Scatter plot of resistivity versus shear wave velocity from lines S1 and R1 at Logan Martin.

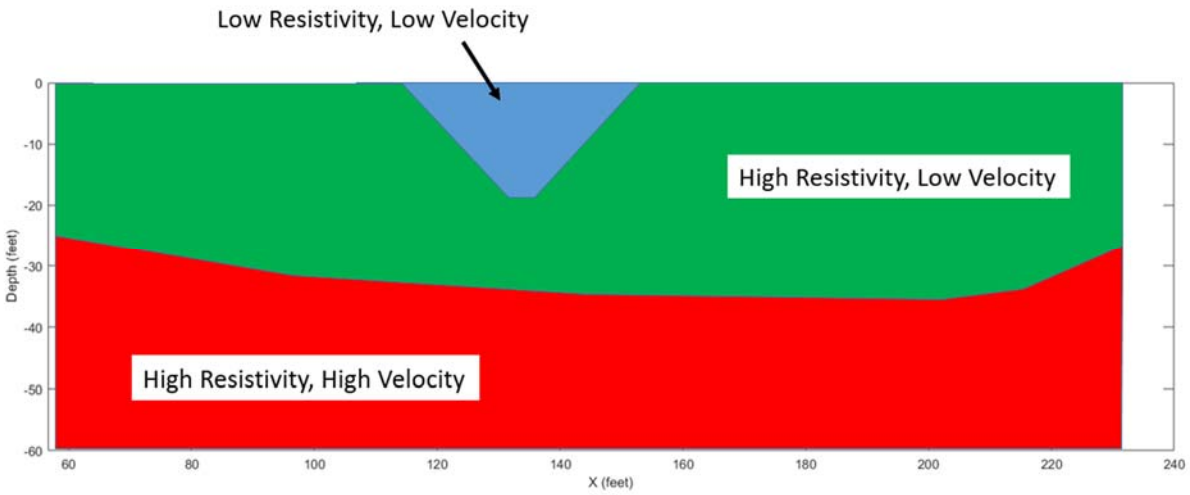

Figure 4-11: Approximate spatial locations of the material groups from Figure 4-10.

4.4.2 Spring Villa

Spring Villa is a small community near Opelika, Alabama that has a history of sinkholes associated with quarry activity. The area is underlain by Chewacla Marble. The surveys for this project were performed adjacent to a water filled sinkhole (Figure 4-12) that likely opened sometime between 2006 and 2011 according to historical aerial images of the site. The sinkhole is approximately 130 feet [40 meters] in diameter and about 26 feet [8 meters] deep in the deepest portion (measured using a depth finder, contours shown in Figure 4-13). Geophysical surveys were performed along the southern and eastern edges of the sinkhole (Figure 4-12), which is located in a heavily wooded area. Three resistivity and two seismic surveys were performed at this site and the results were combined along with the depth information into a 3D visualization program to produce the results shown in Figure 4-13 and Figure 4-14.

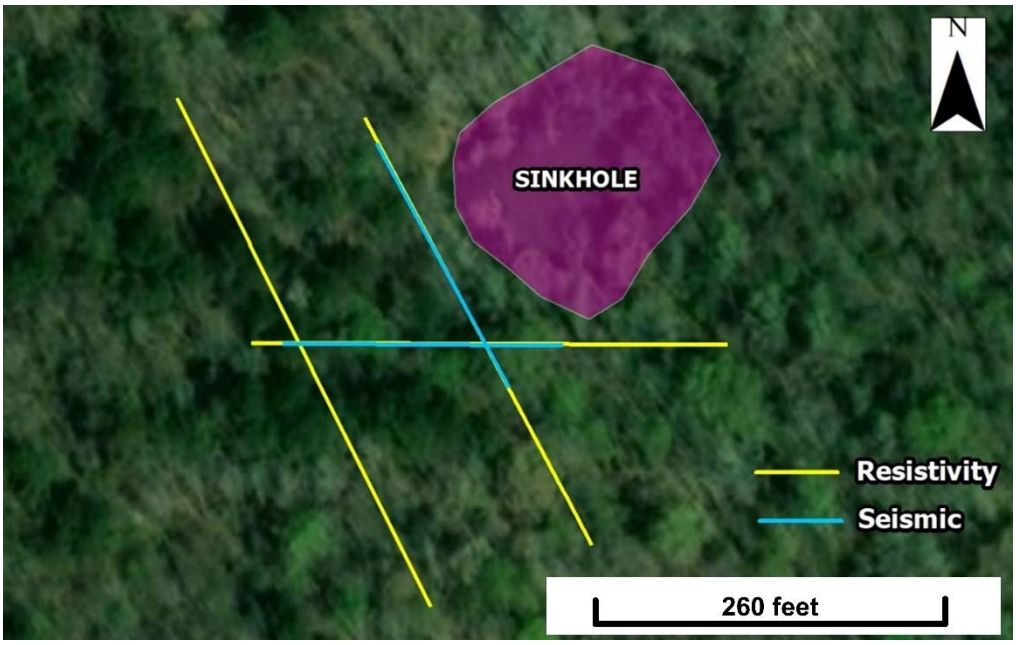

Figure 4-12: Location of the sinkhole relative to the geophysical survey lines.

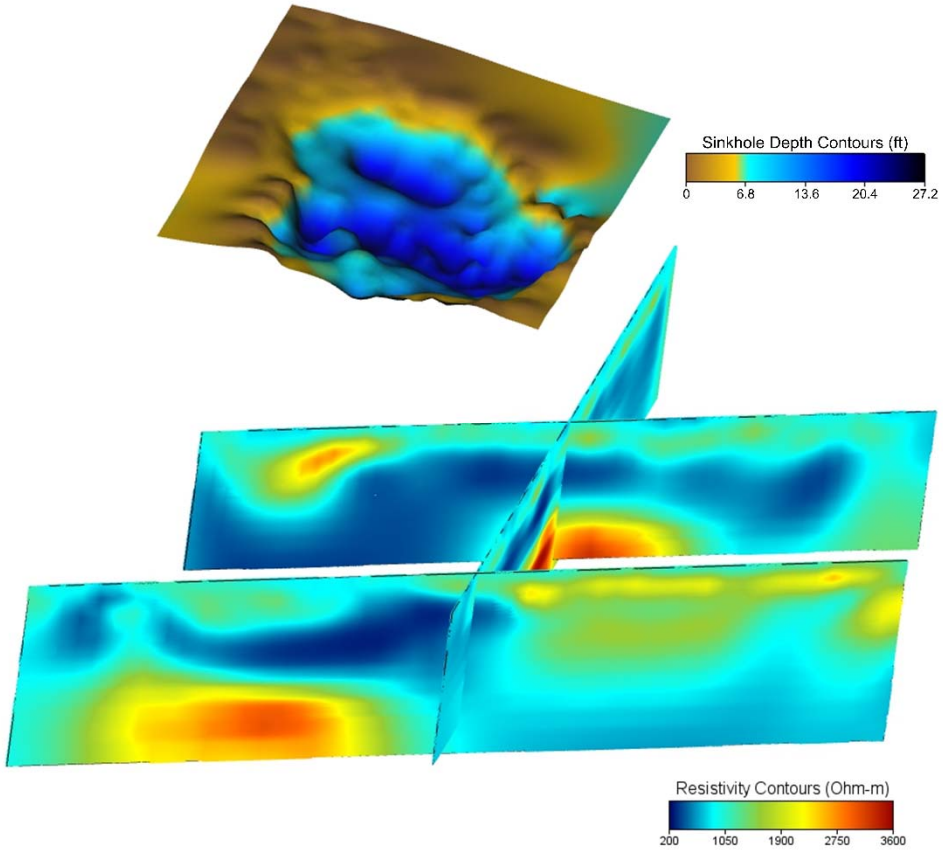

Figure 4-13: Electrical resistivity results from the three lines performed at Spring Villa, along with depth contours measured within the water-filled sinkhole.

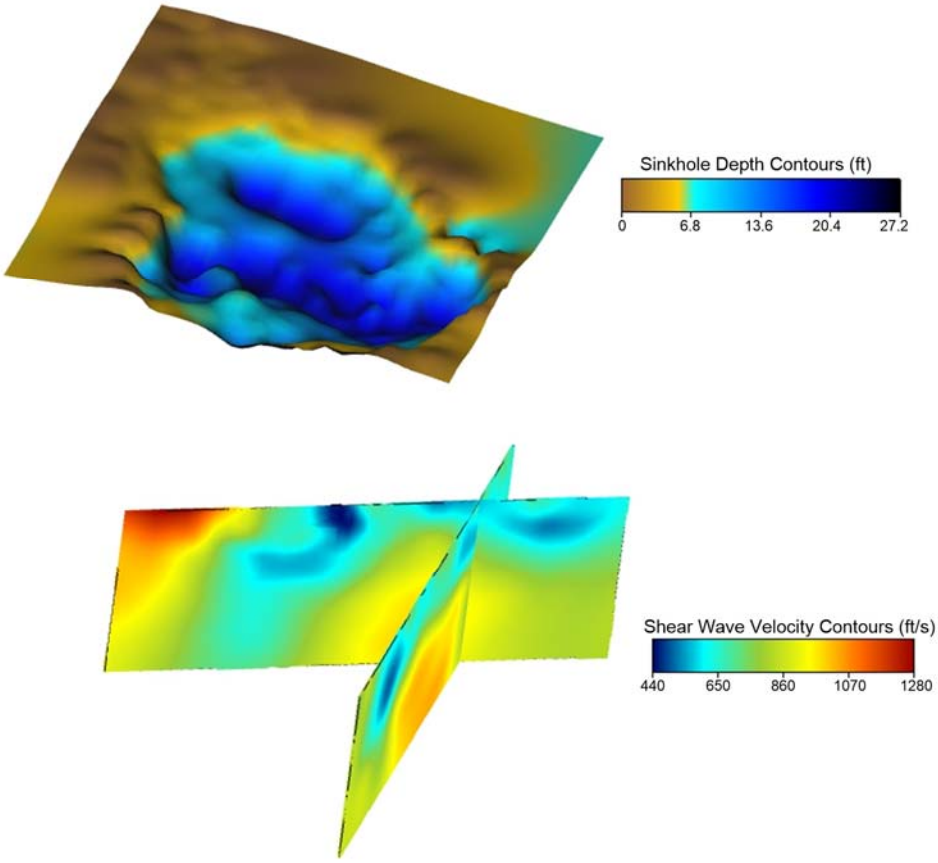

Figure 4-14: Electrical resistivity results from the three lines performed at Spring Villa, along with depth contours measured within the water-filled sinkhole.

The electrical resistivity results (Figure 4-13) showed a large region of low resistivity material near the sinkhole at depths ranging from 16 to 36 feet [5 to 11 meters], which is similar to the deeper regions of the sinkhole. The shear wave velocity results (Figure 4-14) also showed a lower velocity zone in parts of this region. These areas of low velocity and low resistivity are interpreted as being zones of heavily fractured, saturated rock that is serving as the erosion conduit for the sinkhole. Due to the heavily wooded nature of this site, it was not possible to get boring information to confirm this in the region of the surveys.

4.4.3 Lessons Learned from Active Sinkholes

Three active sinkhole sites and one possible sinkhole site with active subsidence were surveyed during this project (see Appendix B for information on surveys at SR-21 and SR-275). Several important lessons were learned from these surveys. There was no boring information available at any of the sites, so no "ground truth" was available to judge the accuracy of the results. Despite this, features consistent with either dipping rock or saturated, fractured rock were observed

in the areas around the sinkholes at the sites with confirmed sinkholes. The surveys at SR-21 were more difficult to interpret primarily due to interference from the buried box culvert that was located at the subsidence area (Appendix B). Results from the resistivity tests and the seismic FWI had to be integrated to identify the likely solution features at Logan Martin and Spring Villa. This is an important conclusion from this work and highlights the need to use more than one investigative technique in order to accurately assess the subsurface. For example, the resistivity results at Logan Martin provide a full picture of the subsurface but selecting a resistivity contour to represent the rock surface is almost impossible without using the seismic data. Boring data would also have been able to serve this purpose if it were available.

4.5 Surveys at Sites with Pinnacled Rock

Two sets of surveys were performed at sites with deep pinnacled rock profiles. These types of features are common in karstic areas in central Alabama, where the depth to competent rock can change by tens of feet in a very short distance. These types of profiles can have multiple geotechnical hazards including subsidence, sinkhole development, and challenges in investigation and construction due to the irregular rock surface. Drilling programs to investigate pinnacled rock sites are especially challenging and often expensive due to the need to have closely spaced borings to accurately map the rapid changes in the rock surface. Geophysical techniques offer a potential tool to assist with these investigations. Electrical resistivity was selected for this task due to the large depths to rock, which were not likely to be visible in the seismic results.

4.5.1 Old US-82 in Centreville

Two electrical resistivity surveys have been performed along Montgomery Road (Old US-82) in Bibb County, Alabama. The surveys were performed near a repaired sinkhole to determine the depth to rock and identify any potential karst features. Both survey lines were performed on the north side of the road roughly centered over the sinkhole repair. The surveys were completed approximately 10 feet off of the edge of pavement to avoid a concrete box culvert. Resistivity survey R1 was performed on 7/25/2019 and survey R2 was performed on 8/1/2019. A site map containing the locations of the resistivity lines and the sinkhole repair are shown in Figure 4-15. Geologic maps of the area (Szabo et al. 1988) indicate that there are several formations containing limestone or dolostone within 2 to 5 miles [3 to 8 kilometers] of the site, although the surface geology is mapped as alluvium. At least eight sinkholes have been previously reported within a ten 10 mile [16 km] radius of the site.

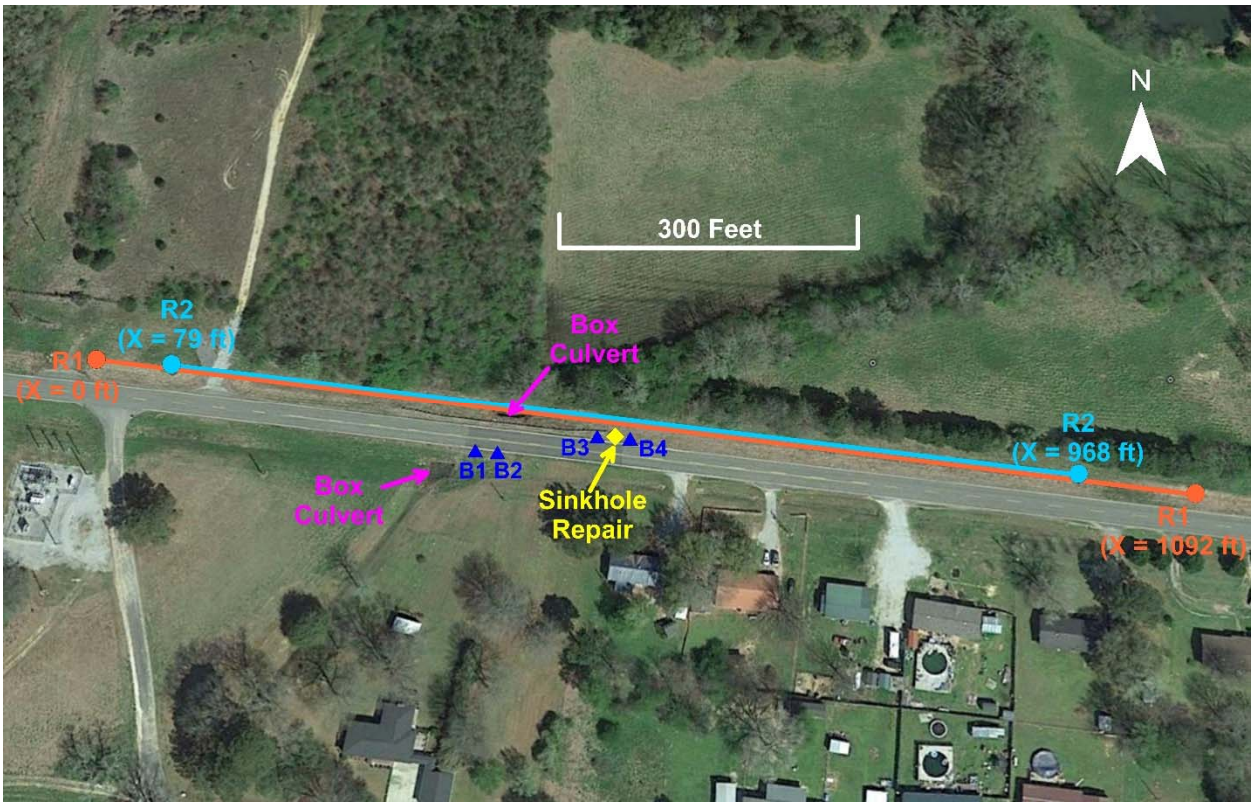

Figure 4-15: Site map with locations of resistivity lines, sinkhole repair and approximate locations of boreholes in Centreville.

Four boreholes were drilled near the repaired sinkhole in 2016. Two boreholes were drilled on the south side of the road just east of the box culvert and two boreholes were drilled on the north side of the road on either side of the sinkhole repair. The exact locations of the boreholes were not surveyed, but their approximate locations are shown in Figure 4-15. The boreholes indicate predominantly sand with some silt, clay and gravel to the drilling depths of 45-55 feet. These borings do not indicate depth to rock or auger refusal. Logs were also examined from two nearby water wells that were drilled for the City of Centreville in 1992, but the exact locations of the two wells are not known. The logs from these wells show the overburden soils consisting of sand, gravel, and clay overlying chert and limestone rock. The depth to rock was found to vary between 68-80 feet between the two well locations. The report also indicates a void present in the rock at a depth of 187 feet, which produced approximately 300 gallons per minute of water. This likely indicates a karst feature.

The interpreted results from electrical resistivity surveys R1 and R2 are shown below in Figure 4-16 and Figure 4-17 respectively. Note that survey line R2 runs from X= 79 feet [24 m] to X= 981 feet [299m]. The results show a low resistivity layer (< 500 ohm-m) in the upper 40-80 feet [12-24 m] which is interpreted as overburden soil. This upper layer is underlain by a higher resistivity layer (> 1000 ohm-m) which is interpreted as the limestone and chert rock. These depths to rock are fairly consistent with the depths reported as part of the well drilling program. The resistivity of this layer is higher than some of the previous sites investigated in this report (primarily dolostone and marble), but is well within the range of resistivities expected for limestone (Figure 3-4). Figure 4-18 compares the interpreted rock surface from surveys R1 and R2. The interpreted rock surfaces from each survey are in reasonable agreement near the edges of each line. The largest difference between the interpreted rock surfaces is observed between X=300-500 ft [91-122m]. This also coincides with the location of the culvert where the data was of the poorest quality.

The results from each survey also show three features of interest near the sinkhole repair. A vertically oriented zone of high resistivity (labeled Feature 1 in Figure 4-16 to Figure 4-18) is present directly below the location of the sinkhole repair. This may indicate raveling soils, which are a common indication of an active sinkhole, or features leftover from the sinkhole repair. Feature 1 appears at X=525 feet [160m] between depths of 20 feet and 65 feet [6 to 20 meters] on survey R1 and it appears at X=538 feet [164 m] between depths of 25 feet and 70 feet [8 to 21 meters] on survey R2. Another feature of interest (labeled Feature 2 on Figure 4-16 to Figure 4-18) is observed just east of Feature 1. Survey R1 indicates a vertical discontinuity in the interpreted bedrock layer near X=500 feet [152 m]. The deeper survey (R2) does not show any discontinuity in the rock at this location, but does show a lower resistivity zone in this same location and the bedrock below this location has a lower resistivity than along the eastern and western edges of the survey. This feature may indicate a dip in the rock surface or could potentially indicate a zone of fractured limestone. Additional investigations are needed to determine the exact nature of Feature 2. The last feature of interest (Feature 3) is low resistivity area present in the results of both surveys at about X=700-800 feet [213-244 m] and starting at a depth of about 120 feet [36.6m] and extending to the bottom of the surveys. The lower resistivity associated with Feature 3 may indicate a zone of fractured, saturated limestone. The depth of Feature 3 is similar to the flowing, open voids encountered during the well drilling program at a depth of 187 feet [57 m]. The close

location of Feature 3 to the previously repaired sinkhole may indicate that soils are being eroded into these voids leading to the voids at the ground surface. However, the interpretations provided in this report are based primarily on the resistivity data and further investigations are required to confirm these conclusions.

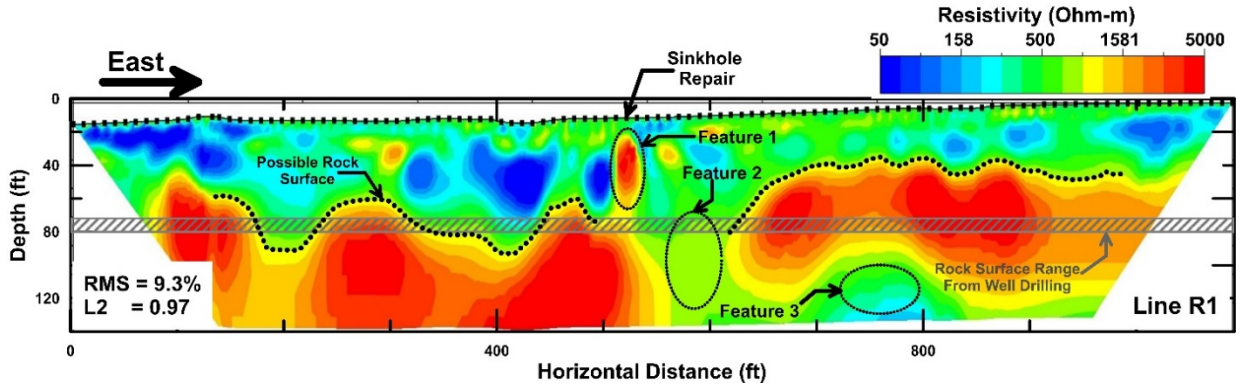

Figure 4-16: Interpreted results from electrical resistivity line R1 at Centreville. The dotted line indicates the surface of the limestone/chert layer (higher resistivity).

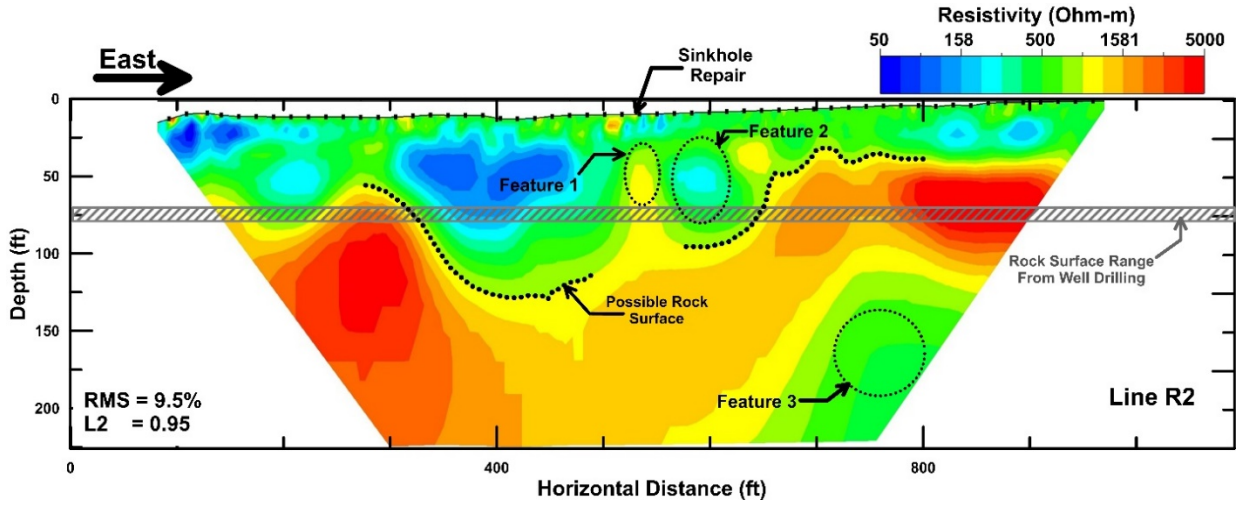

Figure 4-17: Interpreted results from electrical resistivity line R2 at Centreville. The dotted line indicates the surface of the limestone/chert layer (higher resistivity).

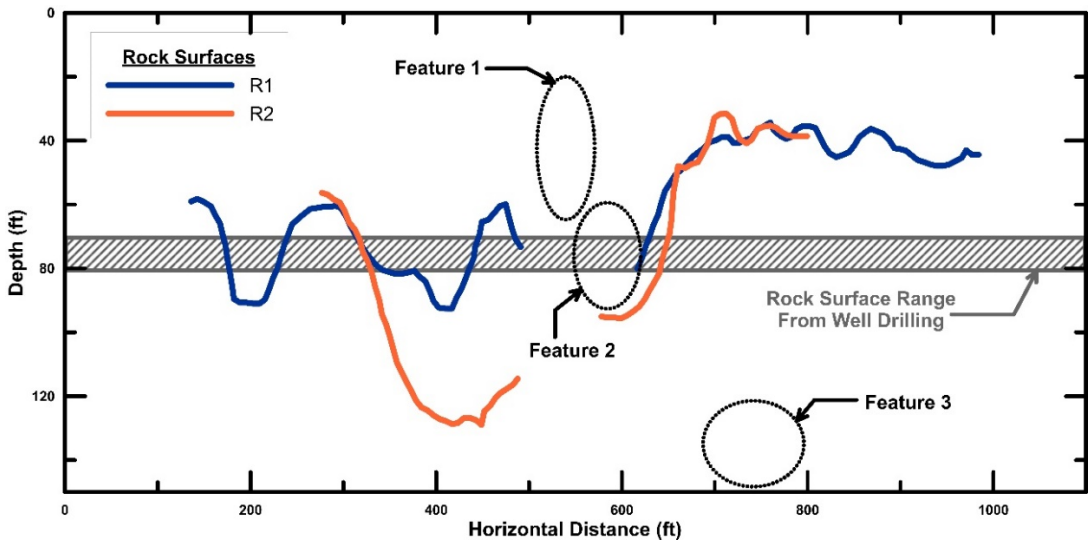

Figure 4-18: Comparison of interpreted rock surfaces from resistivity surveys R1 and R2 at Centreville (locations of features are interpreted jointly from surveys R1 and R2)

4.5.2 I-59/20 near Arkadelphia Road

Electrical resistivity testing was performed along a frontage road adjacent the SB lanes of I-59/20. This section of the interstate is adjacent to a limestone quarry and has a history of subsidence and sinkholes. A drilling program (Figure 4-19) revealed that depth to rock varied drastically over short lateral distances. Seismic and resistivity surveys were performed just off the roadway. The seismic data was difficult to interpret due to the large amount of traffic noise, so only the resistivity results were considered in this study.

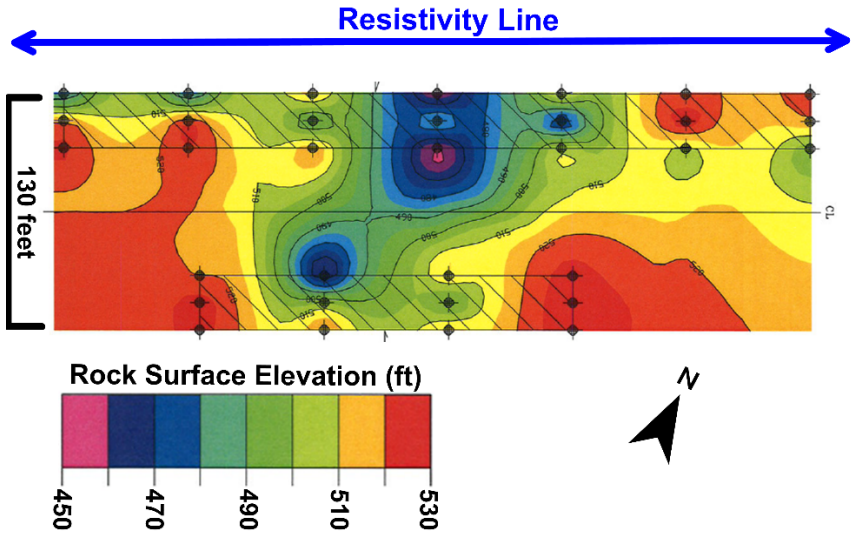

Figure 4-19: Rock contours from an ALDOT drilling program in the SB lanes at I-59/20

The interpreted resistivity results are shown in Figure 4-20. They reveal a low resistivity surficial layer overlying a high resistivity layer that is interpreted as the rock surface. This is in contrast to some of the previous sites where the rock has been visible as lower resistivity, but at this site, the water table in the rock is very deep due to dewatering at the adjacent quarry. There are likely perched water tables within the shallow clayey soils, which may account for some of the pockets of lower resistivity material in this zone. The interpreted rock surface from the resistivity test is highly variable in elevation and consistent with the results from the boring program (Figure 4-19). The results from the borings close to the resistivity line have been projected onto the resistivity results in Figure 4-20. These results give similar surfaces, but it is important to remember that direct comparisons between the borings and resistivity values are difficult at this site as they were not performed in the same location and the rock surface is highly variable.

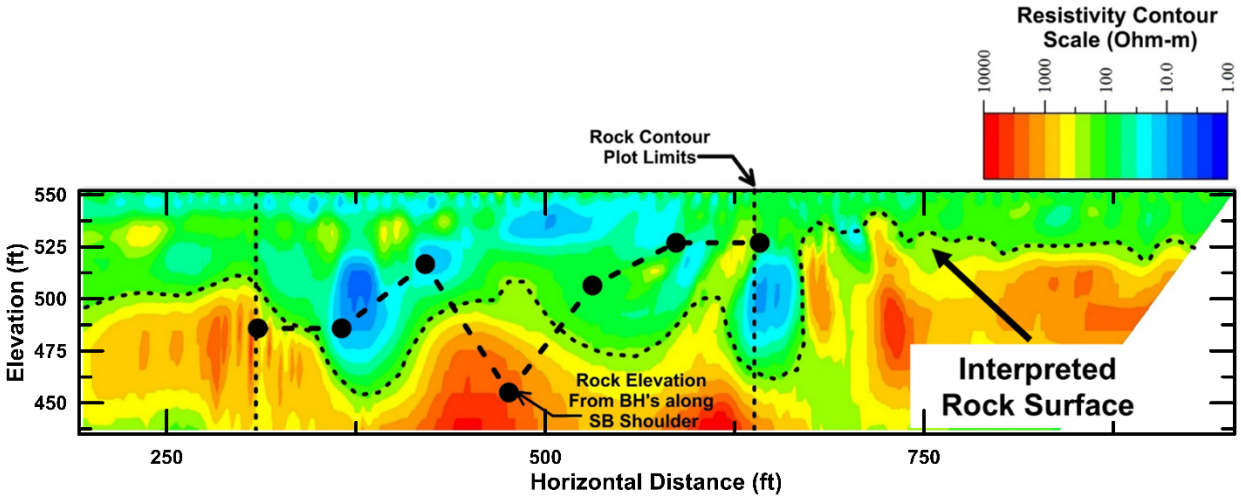

Figure 4-20: Comparisons of electrical resistivity results with borings at I-59/20.

4.6 Findings from Case Histories

The previous section has summarized findings from surveys performed at eight sites with a variety of karstic features including repaired sinkholes, active sinkholes, and sites with pinnacled rock. Some important findings from these case histories are:

- Resistivity and seismic based surveys were able to identify karst features at the selected sites and results compared well with available site information.
- Resistivity may not be able to identify features beneath large concrete structures, such as box culverts, or in areas with significant utility conflicts.

- Seismic methods may not be practical in areas with large vibrational noise such as busy interstates.
- Joint interpretation can reduce uncertainty and overcome limitations of the individual methods.
- Geophysical methods should be used with borings to verify interpretations. They should ideally be performed prior to drilling to optimize boring locations.

These lessons have been used to develop a sinkhole investigation plan, which is discussed in the next chapter.

CHAPTER 5: SINKHOLE INVESTIGATION PLAN

5.1 Introduction

This chapter presents a recommended investigation plan for sinkhole sites based on the investigation methods reviewed in Chapter 3 and the different types of sites (e.g. sites with repaired sinkholes, active sinkholes, and pinnacled rock) reviewed in Chapter 4. Lessons learned from the case histories have been applied to the development of this plan. The plan is first reviewed, followed by a cost comparison between traditional investigations (involving only borings) and the proposed investigation plan involving both geophysical surveys with optimized boring locations.

5.2 Recommendations for Future Surveys

The recommend investigation plan involves five stages: desk investigation, site inspection, geophysical surveys, drilling program, and integrated characterization. Each of these stages is discussed below.

5.2.1 Desk Investigation

The first step in any site characterization program should be a desk investigation. The purpose of the desk investigation is to gather site specific information and create preliminary plans for the geophysical surveys and the drilling program prior to visiting the site. Recommended action items for the desk investigation are outlined in the list below.

i. Review any known information related to geology and sinkhole activity at, or near, the site
   - Review any previous maintenance records, email correspondence or pictures related to sinkhole activity at the site.
   - Identify potential sinkhole features/ repairs from satellite image or LiDAR data if possible.
   - Review site geology and previous investigations to identify if carbonate rocks exist at site.
   - Estimate size and depth range of expected sinkhole features from available information.
   - Identify if any quarries exist near the site and confirm whether they are actively dewatering. Active quarries are known to accelerate sinkhole formation.

ii. Create preliminary geophysical survey plan
   - Determine geophysical survey objectives.
   - Estimate type and number of geophysical surveys needed (resistivity and seismic).
   - Identify potential locations for geophysical surveys.

- Underground utility surveys should be performed by an independent firm prior to performing the geophysical surveys. This action item is required prior to any drilling. This action item may be performed prior to the geophysical surveys and used to confirm or adapt the preliminary survey plan. If information from the utility survey is not available prior to performing the geophysical surveys, the utility locations will still be helpful for interpreting the geophysical results after the surveys are performed.
- Identify any conductive features which may influence resistivity results (i.e., power lines, electric conduits, metal fence, metal pipes). Resistivity survey line should be placed at an offline distance from conductive features equal to the expected maximum depth of investigation.
- Identify potential for vibrational noise at the site which may influence seismic results (i.e., large trucks). If survey lines must be placed near roadway, hammer shots may need to be timed to occur when large trucks are not driving by. This may add time to survey.
- Determine allowable survey lengths based on site constraints.
- Estimate topography and associated challenges. Sites with significant topography (vertical elevation changes larger 2-3 feet) will need to be surveyed using a total station to estimate topography for inversion.

iii. Create preliminary boring plan (optional at this stage)

- Estimate number of borings based on areas that need hard confirmation of depth to rock.
- Select locations based on accessibility, existing infrastructure, geophysical survey locations.
- Creating the boring plan can also be done after geophysical surveys are performed to optimize boring locations based on areas where ground truth will be most useful.

5.2.2 Physical Site Inspection

The second step in the recommended site characterization program is to physically visit and inspect the site, if possible. The purpose of the physical site inspection is to confirm information gathered in the desk investigation and gather any additional information that may affect the preliminary geophysical plan. The physical site inspection may be performed on the

same site visit used to perform the geophysical surveys and the preliminary geophysical survey plan may be altered in the field, if needed. Recommended action items for the physical site inspection are outlined in the list below.

i. Confirm locations and sizes of sinkhole features identified in desk investigation and identify any other sinkhole features at the site. These may include areas of subsidence (often identified by ponded water), open voids, or damage to paved areas or concrete structures.
ii. Confirm locations of any conductive features identified in desk investigation and identify if any other conductive features exist at the site.
iii. Take photos of any visible sinkhole activity or conductive features the site.
iv. Confirm or adapt preliminary geophysical survey plan based on site inspection.

5.2.3 Geophysical Surveys

The next recommended step in the site characterization program is to prepare and perform the geophysical surveys. For each geophysical method, there a few pre-survey items that may be performed the same day as the geophysical survey, or in the office prior. The electrical resistivity and seismic surveys may be performed simultaneously or the electrical resistivity can be performed first, and the preliminary field results may be used to guide seismic survey plan. Recommended action items for performing the geophysical surveys are outlined in the bulleted list below.

- Electrical Resistivity Survey

i. Pre-survey Items:
    - Determine survey line lengths, locations and electrode layouts
    - Determine arrays to be used for electrical resistivity surveys. It is recommended to use dipole-dipole and strong-gradient arrays for sinkhole sites.
    - Create any resistivity command files and upload to device if needed.
    - Forward models (i.e., a numerical simulation of a survey at the proposed site to predict how results will look) may also be run during this stage if sufficient information from previous investigations exists. Results from forward models can help guide the preliminary survey plan.
ii. Survey:
    - Place the electrodes in as close as a straight line as practicable (for a 2D survey). The spacing between electrodes should ideally be at regular intervals, but this is not always

possible due to obstructions. Adjustments can be made after the survey is performed to account for actual electrode locations, but these must be carefully recorded.

- Perform electrical resistivity survey first as it is quick to perform, and preliminary results are available in the field. A brief discussion on performing the surveys is included in Chapter 3.2, but detailed instructions should be obtained from the equipment manufacturer.
- Perform topographic survey, if needed. A survey should be used if elevation changes of more than 2-3 feet occur across the site or if the topography is irregular. Sites with a constant slope likely will not require a survey, although an estimate of the total elevation change across the site should be done. This survey can be performed while the resistivity surveys are running.
- A preliminary inversion should be performed in the field to confirm that the data was collected correctly and that the results look reasonable. Topography and irregular spacing will not likely be able to be included in this inversion, so any interpretation should be limited. Based on the results of this inversion, it may be necessary to re-run a test or to run a different type of array.

iii. Post-Survey Items

- Invert measured data after making any necessary adjustments for irregular spacing or topography. Some discussion of the inversion process is Chapter 3.2, but detailed instructions should be obtained from the software publisher.
- The preliminary results can be used to guide a seismic survey or seismic can be performed alongside resistivity. Details for the seismic surveys are discussed in the next section.
- Once all geophysical surveys have been completed, a joint interpretation can be completed to identify potential rock surface and/ or sinkhole features. This can be an informal interpretation as was performed for Spring Villa (Chapter 4.4.2) or a more formal clustering approach as was performed for Logan Martin (Chapter 4.4.1).
- The processed results can then be used to guide the development of a drilling program (Chapter 5.2.4).

- Seismic Survey

  i. Pre-survey:

- Determine required survey type based on overall objectives
    - If only the depth to rock at discrete locations is required, MASW may be used
    - If a full 2D profile is required, seismic FWI should be used. Note that MASW data is typically only used to produce 1D profiles that can be contoured together to create a pseudo-2D profile.
- Select line locations, geophone spacing (desired depth), and shot locations
    - Use preliminary electrical resistivity results to guide seismic survey. Or perform seismic at same time as resistivity using desk investigation and site inspection to guide survey layout.

i. Survey

- Place the geophones in as close as a straight line as practicable. The spacing between geophones should ideally be at regular intervals, but this is not always possible due to obstructions. Adjustments can be made after the survey is performed to account for actual geophone locations, but these must be carefully recorded.
- Perform seismic survey with source locations as determined pre-survey. If necessary, source locations can be adjusted in the field, but the locations must be carefully recorded. A brief discussion on performing the surveys is included in Chapter 3.3, but detailed instructions should be obtained from the equipment manufacturer.
- Perform topographic survey, if needed. A survey should be used if elevation changes of more than 2-3 feet occur across the site or if the topography is irregular. Sites with a constant slope likely will not require a survey, although an estimate of the total elevation change across the site should be done. This survey should not be performed while the seismic survey is being conducted to avoid creating extra noise.
- Preliminary inversions in the field are typically not possible in the field. However, preliminary dispersion curves can be created in the field to estimate the frequency content and surface wave quality of the data. If time permits, these dispersion curves can be inverted in the field.

ii. Post-Survey Items

- Invert measured data after making any necessary adjustments for irregular spacing or topography. Some discussion of the inversion process is Chapter 3.3, but detailed instructions should be obtained from the software publisher. Note that MASW

inversions can typically be completed in less than a day, but FWI may take several days to complete.

- Once all geophysical surveys have been completed, a joint interpretation can be completed to identify potential rock surface and/ or sinkhole features. This can be an informal interpretation as was performed for Spring Villa (Chapter 4.4.2) or a more formal clustering approach as was performed for Logan Martin (Chapter 4.4.1).
- Use processed seismic data, along with resistivity results, to help guide drilling program if seismic results are available prior to drilling (Chapter 5.2.4).

5.2.4 Drilling Program

The drilling program should ideally be performed after the geophysical surveys as the results will aid in identifying optimal borehole locations. Cone penetration tests can be used to assess depth to rock, but special care must be taken to avoid damaging the cone tip. Standard penetration tests can be very useful to identify soft zones, which may represent migrating material, and obtain samples of the soils. If augers are used for drilling through the soil, rock coring should be continued for at least 10 feet to determine if the auger refusal material is indeed carbonate rock. Alternative drilling methods like sonic drilling should strongly be considered for these investigations as they can provide continuous cores of both the soil and rock.

Boring locations should be determined based on areas where the interpretation of the geophysical tests is uncertain or to confirm the location of identified features, such as gaps in the rock surface or unexpected zones of low velocity. The number and depth of the borings will need to be determined based on the individual details of each site, but it is recommended that at least 10’ of coring be performed below the rock surface to confirm that drilling has not been impeded by an isolated boulder and to gather samples of the rock. These samples will be important to confirm that the rock is carbonate and to compare the rock type to established correlations for shear wave velocity and electrical resistivity (e.g., Figure 3-4). The drilling program should also confirm the depth of the water table (and the presence of any perched water tables), which will affect both the resistivity and compression wave velocity.

5.2.5 Integrated Site Characterization

The final step in the recommended site characterization program is to integrate the results of all of the investigation methods in order to develop a ground model that honors each of the sources of data while recognizing the uncertainties present in each. For example, ERT data can

quickly and easily provide continuous profile across hundreds of feet of a site, but from this data alone, it is not possible to determine whether the layers are rock or soil. This is because different types of rocks and soils can have similar resistivity values (Figure 3-4), and the resistivity can be affected by changes in water content or chemical composition of the pore water. Common resistivity inversion techniques also lead to smooth profiles that may mask or smear sharp features like voids. Seismic data on the other hand can reliably distinguish between soil and rock, but FWI results are sensitive to noise and require a significant amount of processing that is not currently practical for routine surveys. Data gathered from boring logs can be used to confirm interpretations from the geophysical results and to assist with interpreting zones where the tests may disagree or where the data is uncertain. Borings are especially useful for identifying depth to water table, depth to auger refusal and soil types at the site. Rock cores can then be used to confirm that auger refusal materials are indeed rock, determine rock type, and to assess fractures and weathering.

5.3 Cost Estimates for the Proposed Investigation Plan

Integrating geophysical methods into sinkhole investigations provides two main benefits. The first is more complete data can be obtained by measuring continuous profiles of the subsurface as opposed to collecting data at discrete points. The second benefit is that geophysical data can generally be collected at a lower cost than borings reducing the overall cost of an investigation program. The following sections attempt to quantify this cost benefit by comparing the costs associated with performing geophysical surveys combined with drilling versus the cost of drilling alone. Information on actual drilling costs were available for one site discussed in Chapter 4 (I-65 at MP 236.5) and so a direct cost comparison can be made between the actual investigation and estimated costs for the geophysical surveys. Hypothetical costs for drilling only and an integrated characterization at two additional sites were developed using average consultant rates provided by ALDOT.

5.3.1 I65 Sinkhole repair at MP 236.5

Details on this site are provided in I-65 at MP 236.5 (Chapter 4.3.2). Ten boreholes were drilled at this site over a period of 6 days prior to the geophysical surveys being performed. The ten boreholes consisted of 378 feet of drilling and cost approximately $18,000 (internal ALDOT costs). The geophysical surveys required approximately four field hours to complete both the resistivity and seismic data collection (approximately two hours each). The geophysical surveys were also non-invasive and did require a shoulder closure but did not cause any disruption to the

flow of traffic on the interstate. The geophysical surveys were completed as part of a research project, so a direct cost comparison was not available. Expected ALDOT costs were estimated for the geophysical surveys by assuming each test would require two hours to collect the data with a four-person crew with an additional two hours of driving time to get to the site. Resistivity and seismic data collection are therefore assumed to each require 4 hours from all onsite personnel. Daily rental rates provided by the manufacturers are used to estimate geophysical equipment costs assuming a full day (8 hour) rental is required for all equipment. Additional time for processing and interpretation by a senior geologist is also considered. Costs are compared for each investigation method in Table 5-1.

A detailed cost breakdown for the 2D resistivity and seismic with FWI are shown in Table 5-2 and Table 5-3, respectively. The resistivity data required about 4 hours of processing. The total cost of the 2D resistivity survey was calculated to be $1,696 and it was estimated to take about 2 full days to deliver processed data (Table 5-1). The FWI processing for the seismic data required approximately 30 hours to complete, but approximately 25 of these hours were computational time so the amount of user interaction was comparable to resistivity. These computations were performed on the Hopper HPC cluster at Auburn University. A HPC cluster would not likely be available in-house at a DOT or consulting firm, so the cost for these 25 hours of purely computational time was estimated using current rental rates for cloud-based HPC (e.g., an Amazon Web Services EC2 compute instance). The current on-demand pricing for an equivalent computational instance to that used on the Hopper cluster is about $2.50 per hour, which was included in the cost estimate for the FWI. The total cost of the seismic survey with FWI processing was calculated to be about $2,020 and estimated to take about 4 full days to deliver processed results. Using these estimates, the combined costs for the combined geophysical surveys would be approximately $3,700. This cost is significantly lower than the drilling costs, but some drilling would likely be needed to confirm the results of the geophysical surveys. The full costs of the integrated characterization approach are explored through two hypothetical sites discussed next.

Table 5-1**:** Comparison of total cost and time to collect and process data for each investigation technique

Investigation Technique	Total Cost
ALDOT Drilling Program	$ 18,000
2D Electrical Resistivity	$ 1,696
Seismic with FWI	$ 2,021

Table 5-2**:** 2D resistivity cost summary

Item	QTY	Hourly Rate	Data Collection Hours	Data Processing Hours	Cost
Lead Engineer/ Geologist	1	$ 70	4	4	$ 560
Assistant Engineer/ Geologist	1	$ 58	4	0	$ 232
Field Worker	2	$ 24	4	0	$ 192
Equipment Rental	1	$ 64	8	0	$ 512
Traffic Control	1	$ 50	4	0	$ 200
		Totals	**24**	**4**	**$ 1,696**

Table 5-3: Seismic with FWI cost summary

Item	QTY	Hourly Rate	Data Collection Hours	Data Processing Hours	Cost
Lead Engineer/ Geologist	1	$ 70	4	5	$ 630
Assistant Engineer/ Geologist	1	$ 58	4	0	$ 232
Field Worker	2	$ 24	4	0	$ 192
Equipment Rental	1	$ 88	8	0	$ 704
Traffic Control	1	$ 50	4	0	$ 200
Computation Only	1	$ 2.50	0	25	$ 63
		Totals	**24**	**30**	**$ 2,021**

5.3.2 Theoretical Site on Pinnacled Rock

The first site considers exploration costs associated with investigating a site with deep pinnacled rock. Information from the I-59/20 survey (Chapter 4.5.2) will be used to guide the study. Drilling was performed at this site through the existing roadway, but the geophysical surveys were performed along a frontage road adjacent to the interstate. As the costs of drilling on an active interstate are very different than drilling on the shoulder, hypothetical costs were estimated using average rates from ALDOT consultants (Table 5-4). The depth of the borings was estimated using the rock surface determined from the resistivity data (Figure 4-20). For a drilling only investigation it was assumed that borings would be evenly spaced at 40 feet, 60 feet and 100 feet. It was also assumed that 10 feet of rock coring would be performed in every boring. An

average drilling rate of 60 feet per day is estimated based on the drilling program from I-65 discussed in the previous section. Mobilization costs were estimated assuming the drill rigs were travelling from Montgomery, AL and it was assumed that a water truck would be needed each day.

Table 5-4: Estimated Consultant Drilling Rates

Item	Rate
Auger Drilling Rate (per foot) (Including One SPT Every 5 feet)	$ 16.00
Rock Coring Rate (per 5 foot core)	$ 50.00
Drilling Rig Mobilization Rate (per mile) ($371 minimum)	$ 3.57
Water Truck (per day)	$ 217.00

Costs for the integrated characterization approach proposed in this report are estimated first. It is assumed that the project requires information on the subsurface to be characterized over a horizontal distance of 600 feet (between X = 200 and 800 feet in Figure 5-1). A resistivity survey is performed first to estimate the depth to the rock surface. The cost to perform and process one resistivity survey is assumed to be equal to $1,696 as estimated in section 5.3.1. The resistivity survey is then used to select locations for borings. It assumed that for a site this large, four borings will be needed to provide adequate ground truth for the resistivity results. Seismic results will not be collected at this site due to the large depths to rock. The cost for the four borings is estimated using the itemized costs in Table 5-4 to arrive at a total investigation cost of $8,211 (Table 5-5).

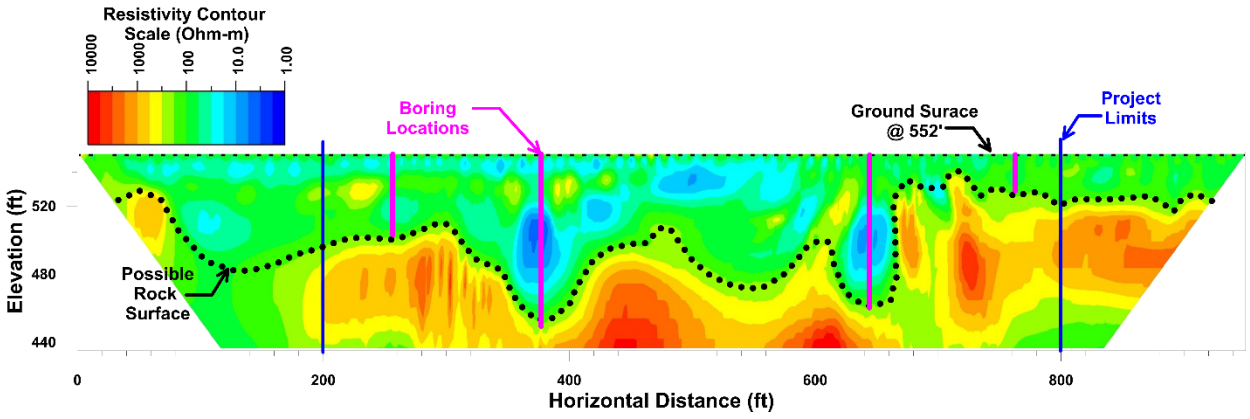

Figure 5-1: Boring locations using 4 borings to confirm ERT results

Table 5-5: Estimated cost to perform geophysics and a drilling programs consisting of 5 borings (auger depths estimated from Figure 5-1)

	Resistivity and 4 Borings	
Item	QTY	Cost
Total Auger Depth (ft)	272	$ 4,352
Total 5 Foot Rock Cores	8	$ 400
Water Truck Days Required	5	$ 1,085
Drilling Equipment Mobilization (per mile)	190	$ 678
Seismic Surveys Required	0	$ -
Resistivity Surveys Required	1	$ 1,696
Totals		$ 8,211

Potential boring locations for a drilling only program with borings evenly spaced at 40 feet, 60 feet and 100 feet are shown below in Figure 6. The borings that were actually performed at this site within the roadway had a spacing of approximately 50 feet. A boring spacing of 40 feet appears necessary to accurately represent the interpreted rock surface. A boring spacing of 100 feet misses the two locations where the rock surface is the deepest as well as the pinnacle at 500 feet. A boring spacing of 60 feet misses the deep rock at 650 feet and the pinnacle at 500 feet. The cost associated with completing drilling only programs with borings spaced evenly at 40 feet, 60 feet and 100 feet are shown in Table 5-6. The cost of performing and processing one resistivity survey and four borings is estimated to be comparable to a drilling only program consisting of seven borings spaced at 100 feet on center. The cost is estimated to be almost 60% less than a drilling only program consisting of sixteen borings spaced at 40 feet on center, which would be required to adequately map the rock surface without integration of geophysics. These cost estimates do not account for the extra value provided by the continuous results from the geophysical surveys.

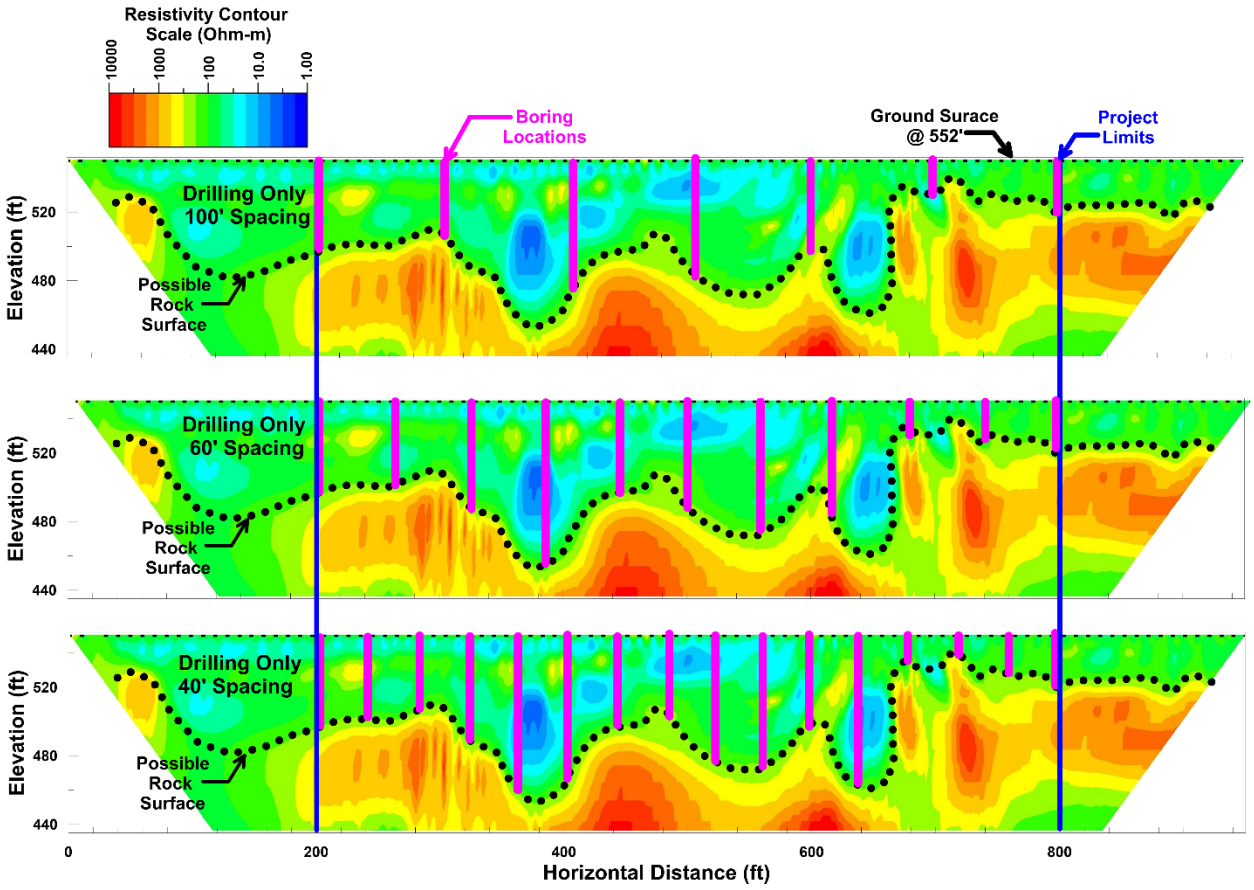

Figure 5-2: Boring locations for drilling only with borings evenly spaced at 100 feet (top), 60 feet (middle) and 40 feet (bottom)

Table 5-6**:** Estimated cost to perform drilling programs with borings evenly spaced at 40 feet, 60 feet and 100 feet (auger depths estimated from Figure 5-2)

	40' Boring Spacing		60' Boring Spacing		100' Boring Spacing	
Item	QTY	Cost	QTY	Cost	QTY	Cost
Total Auger Depth (ft)	900	$ 14,400.00	623	$ 9,968.00	367	$ 5,872.00
Total 5 Foot Rock Cores	32	$ 1,600.00	22	$ 1,100.00	14	$ 700.00
Water Truck Days Required	15	$ 3,255.00	11	$ 2,387.00	7	$ 1,519.00
Drilling Equipment Mobilization (per mile)	190	$ 678.30	190	$ 678.30	190	$ 678.30
Totals		$ 19,934		$ 14,134		$ 8,770

The previously described scenario represents one 2D line of borings and geophysical surveys. Karst environments, however, represent a 3D challenge to geologists and engineers. The I-59/20 sinkhole site used as the basis for this theoretical cost analysis required multiple lines of borings spaced at roughly 55 feet on center and very dense boring grids near subsidence areas (Figure 4-19). An average boring spacing of about 40 feet along a given line therefore seems to be a reasonable representation of current ALDOT practice for a site similar to I-59/20. For this type of site, implementing the current investigation program is estimated to save up to 60% on investigation costs. Cost savings are likely to be much greater if a dense grid of borings (as compared to a single line) is required.

5.3.3 Theoretical Site Near Active Sinkhole

The second theoretical site examined was assumed to be adjacent to an active sinkhole. Information from the Logan Martin Dam survey (Chapter 4.4.1) will be used to guide the study. The Logan Martin site contains an active sinkhole with a line of ground subsidence extending away from the sinkhole towards the southwest (Figure 4-7). No drilling has been performed at this site. The geophysical data at this site took one day to collect, so the total cost to perform and process geophysical test is assumed to be the same as described in Section 5.3.1. The drilling rates described in Section 5.3.2 are also assumed to apply to this site. The drilling rate is again assumed to be an average of 60 feet per day with one water truck required for each day of drilling.

For the purposes of this comparison, it is assumed that the subsurface is to be characterized over a horizontal distance of 160 feet (X = 60 to 220 feet in Figure 5-3). For the integrated characterization, it is assumed that both a resistivity and a seismic test are performed at the same time. The rock surface identified from the combined resistivity and seismic interpretation (Figure 4-11) is assumed to be correct, although this rock surface is smoothed due to the clustering approach and likely misses some small scale variations. It is assumed that two borings would be needed to provide verification of the geophysical results, given the simple rock surface. One boring would be drilled around the subsidence and the other would be drilled in the area of the deepest estimated depth to rock. The samples collected from these borings would allow the geophysical results to be correlated with the soil/rock type and extrapolated across the length of the site. The cost of integrating ERT and seismic with drilling is shown in Table 5-7.

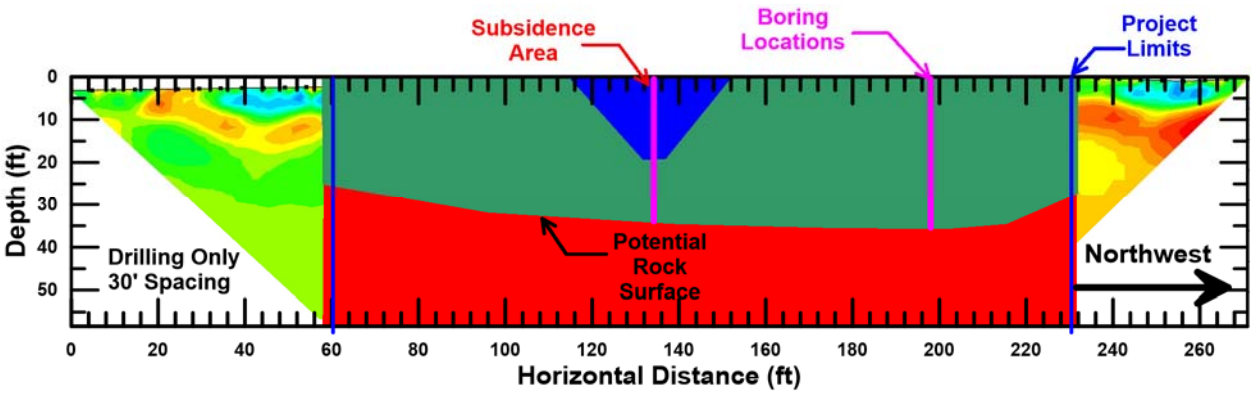

Figure 5-3: Boring locations using 2 borings to confirm geophysical results

Table 5-7: Estimated cost to perform geophysics and a drilling programs consisting of 5 borings (auger depths estimated from Figure 5-3)

	Resistivity, Seismic and 5 Borings	
Item	QTY	Cost
Total Auger Depth (ft)	72	$ 1,152
Total 5 Foot Rock Cores	4	$ 200
Water Truck Days Required	1	$ 217
Drilling Equipment Mobilization (per mile)	180	$ 643
Seismic Surveys Required	1	$ 2,021
Resistivity Surveys Required	1	$ 1,696
Totals		$ 5,928

Potential boring locations for a drilling only program with borings evenly spaced at approximately 16 feet, 20 feet and 30 feet are shown below in Figure 5-4. It was assumed that all spacings would place two boreholes in subsidence and a borehole at each end of the project. A boring spacing of 16 feet is slightly longer than the spacing used at the active sinkhole along I-65, so it seems to be a reasonable representation of current ALDOT practice for active sinkhole investigations. For the current site, the interpreted bedrock profile is fairly simple, but it is important to note that this would not be known without performing the geophysical surveys beforehand. The cost associated with completing drilling only programs are shown in Table 5-8. The borings at this site are relatively shallow compared with the pinnacled rock site explored in

the last section, so the costs of the drilling program are significantly less. The cost of the largest spacing is approximately half of the smallest spacing, but would provide far fewer data points than is typically needed to characterize an active sinkhole. At this site, the assumed rock surface is relatively simple, so the larger spacing would likely be sufficient, but there would be no way to know that without the geophysical data. The cost of performing the geophysical surveys and two borings would fall between the cost of drilling borings on a 20 foot and 30 foot spacing. It is approximately 34% less than the cost associated with the closest spacing, which is consistent with current ALDOT practice at sinkhole sites.

The cost savings of the integrated characterization compared with current ALDOT practice for this hypothetical site is approximately 60% of the pinnacled rock site, primarily due to the shallow rock surface. Integrating resistivity and seismic results in this scenario was estimated to be comparable to a drilling only program with borings spaced at between 20 and 30 feet, which would be about twice the spacing currently used by ALDOT at active sinkhole sites. However, it is important to note that the combination of the geophysical data with the borings give far more subsurface information than the borings alone, which would allow for more targeted repairs to be designed. The cost savings of using the geophysical methods would also be even more cost effective if a grid of borings was planned as was at the sinkhole along I-65 (Chapter 4.3.2).

5.3.4 Cost Comparison Conclusions

The previous three sections compared the cost of performing drilling only programs with an integrated site characterization program incorporating both geophysics and borings. The first comparison shows that the direct costs of geophysical surveys are significantly lower than current ALDOT drilling costs. This comparison however does not include the costs associated with gathering ground truth for the geophysical results. In order to examine this, cost estimates were developed for two hypothetical sites, a site with deep pinnacled rock and an active sinkhole site with shallow rock, using average consultant drilling rates provided by ALDOT. The proposed characterization approach was shown to be approximately 60% less expensive than current ALDOT practice at the pinnacled rock site and 34% less expensive at the active sinkhole site. These cost comparisons do not include the extra value provided by the more detailed characterization offered by the integrated approach.

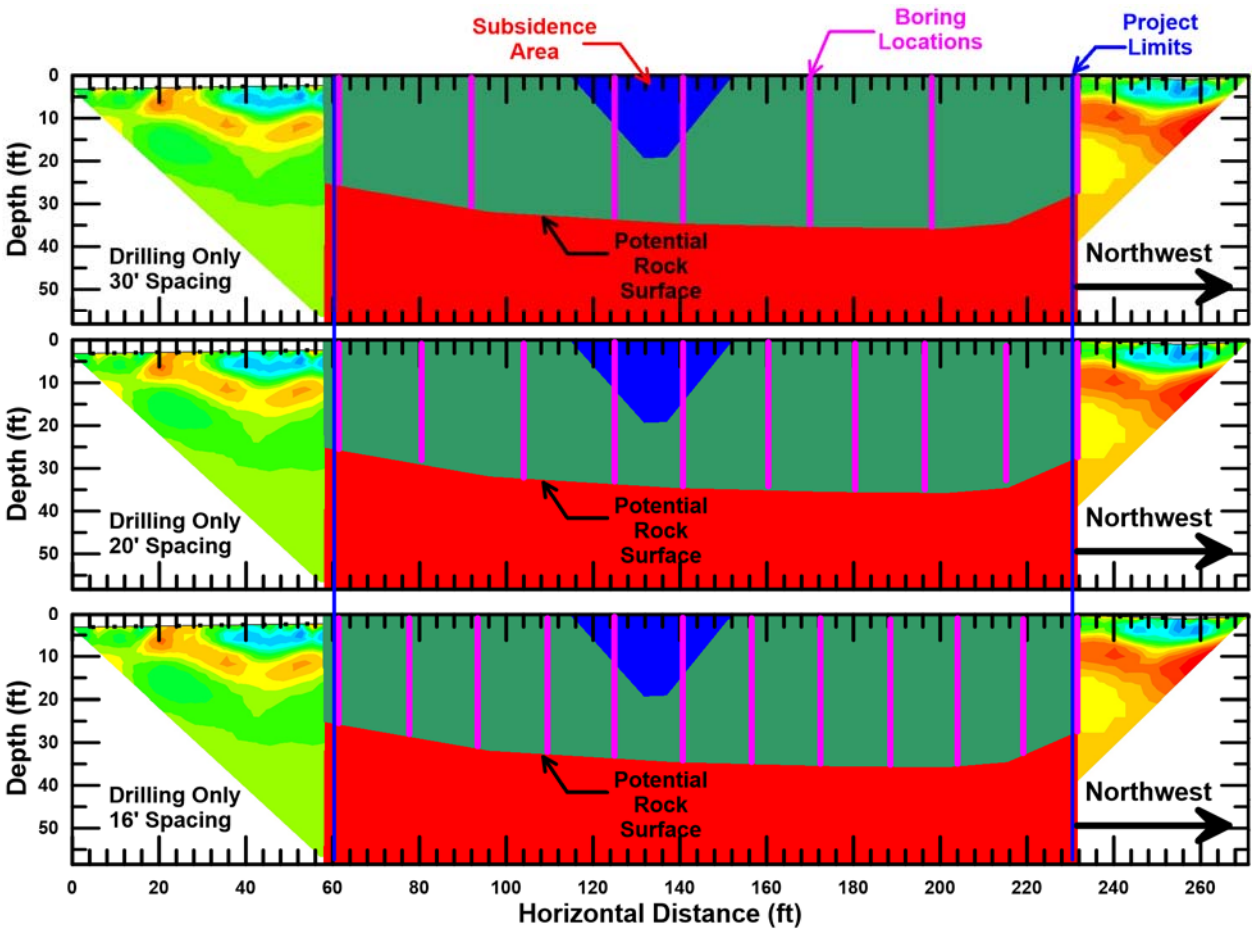

Figure 5-4: Boring locations for drilling only with borings evenly spaced at 30 feet (top), 20 feet (middle) and 16 feet (bottom).

Table 5-8: Estimated cost to perform drilling programs with borings evenly spaced at 16 feet, 20 feet and 30 feet (auger depths estimated from Figure 5-4)

	16' Boring Spacing		20' Boring Spacing		30' Boring Spacing	
Item	QTY	Cost	QTY	Cost	QTY	Cost
Total Auger Depth (ft)	361	$ 5,776	293	$ 4,688	166	$ 2,656
Total 5 Foot Rock Cores	22	$ 1,100	18	$ 900	10	$ 500
Water Truck Days Required	7	$ 1,519	5	$ 1,085	3	$ 651
Drilling Equipment Mobilization (per mile)	180	$ 643	180	$ 643	180	$ 643
Totals		$ 9,038		$ 7,316		$ 4,450

CHAPTER 6: CONCLUSIONS AND RECOMMENDATIONS

6.1 Summary

Sinkholes along highways pose a significant challenge for state and federal transportation agencies, including significant repair costs, and indirect costs associated with traffic delays and lane and road closures. When a sinkhole or area of subsidence is identified, current practice is to investigate the area with a dense grid of borings to establish the location of voids or soft zones in the soil and to map the rock surface. Repairs are then completed by excavating and backfilling the sinkhole, which may involve a large amount of earthwork depending on the size of the hole and the depth to rock. Auger borings and rock coring provide information at discrete points and so a large number are needed to get an adequate understanding of the rock surface. This can require an expensive and time-consuming investigation program and the lack of continuous data also means that features may be missed.

Surface-based geophysical methods can overcome some of these limitations by providing continuous profiles of the subsurface in less time and at a far lower cost than typical drilling programs. Geophysical methods typically used for sinkhole investigations include electrical resistivity, seismic methods, gravity measurements, and ground penetrating radar (GPR). Out of these methods, electrical resistivity and seismic methods were considered the most reliable for use along Alabama highways, where clayey soils often limit the depth of GPR surveys and highway-related noise and infrastructure can adversely affect gravity measurements. Geophysical measurements cannot directly determine soil and rock type and so must be correlated with other types of data including borings.

The current study evaluated the use of electrical resistivity tomography (ERT) and seismic full waveform inversion (FWI) to evaluate karst sites in Alabama. Surveys were performed at sites with repaired sinkholes, active (open) sinkholes, and sites with deep pinnacled rock profiles. The goal of the surveys was to compare the geophysical results with available boring information and surface observations to determine the strengths and limitations of each method for use in Alabama. It was found that each method was able to identify shallow karst features, but the seismic FWI was limited to depths of 30-40 feet. The ERT surveys were able to reach depths of more than 100 feet, but it is difficult to determine which zones represent soil or rock without incorporating either the seismic data or information from nearby borings. The most complete characterizations were made by integrating data from all available sources.

The findings from the surveys performed at karst sites were used to develop an integrated sinkhole investigation plan for sinkhole sites that utilizes existing information (e.g., geologic maps, aerial imagery, previous investigations), geophysical testing, and targeted borings. Recommended steps for gathering information from each of these sources was presented in Chapter 5. The use of the proposed integrated investigation plan was demonstrated through example investigations at two hypothetical sites based on surveys performed for this project. The integrated investigation plan was found to offer potential costs savings of between 34% and 60% compared with current practice. The cost savings were greatest for sites with deeper irregular rock profiles and less for sites with shallow, simple rock surfaces. These cost savings do not account for extra value provided by the continuous geophysical surveys or the additional savings that would be realized if a grid of borings was required as opposed to a single line, as was considered in these examples.

6.2 Conclusions

The overall purpose of this research was to provide ALDOT engineers with guidance on surface-based geophysical methods that can be used to investigate the extent of sinkholes and assess changes over time. The geophysical surveys performed for this project used ERT and seismic FWI to image the subsurface and the results were compared to borings, if available. Both geophysical methods were successful in identifying karst features at the sites where they were used, although each survey method had its own limitations. Borings continue to provide the most reliable information on depth to rock but were only able to provide information at a limited number of discrete points and at a significantly greater cost.

The electrical resistivity survey was able to provide the most complete image of the subsurface, but the inversion tended to smooth layers making the potential joint feature appear larger than the other methods would suggest. This method was also the simplest and fastest in terms of data collection and inversion. One of the significant limitations with ERT is that resistivity alone is not sufficient to determine whether a layer is soil or rock and so other results are needed. Electrical resistivity surveys can also be affected by the presence of linear conductive structures such as power lines or pipes that are common along roadways. No such conductive features are known to exist at any of the sites where testing was performed, but it was found that buried concrete culverts also posed a barrier to resistivity testing. Future users should be aware of this limitation when using resistivity testing along highways.

The seismic FWI method was able to provide good data on the upper 35 feet [11 meters] of the sites where it was used and showed clear increases in velocity at the rock surfaces estimated from the borings. The ability to detect joint features in the rock surface was more limited as these were present near the edge of the depth range of this method. For seismic surveys along highways, traffic noise will be present in the seismograms. This can obscure the desired data, especially if the primary target is body waves (i.e., P- or S-waves) generated from an active source, which tend to have lower amplitudes. Although some of the traffic noise will inevitably affect the results, this can be partially overcome by using the higher amplitude surface waves observed on receivers close to the active source as the primary target. These signals generally have a high enough signal-to-noise ratio that the traffic noise is not detrimental to the final inverted profile. The effects of traffic noise can also be reduced by timing shots to come between large vehicles, as was done in the current study. Despite these efforts traffic noise was still present in the records from this site, but the presence of the noise did not seem to significantly affect the final inversion for any of the sites.

A major limitation for both seismic and resistivity inversions is the non-uniqueness that is inherent in inverse problems. Given a set of field observations, there are many seismic or resistivity profiles that would fit the data equally well. A regularization scheme, such as those used in both the seismic and resistivity inversions in this study, can aid in suppressing some of this non-uniqueness by forcing the model to vary smoothly or applying some other constraint to the model. However, these constraints can be thought of as simply ignoring certain classes of models, such as those that do not have a certain level of smoothness, which may not be appropriate in all circumstances. Therefore, it is imperative that any previous information about the geology or subsurface (i.e., from borings) be incorporated into the constraints and starting model.

The limitations of the geophysical methods described above can be overcome by using them as part of an integrated characterization program. This type of characterization seeks to integrate the results of all the investigation methods in order to develop a ground model that honors each of the sources of data while recognizing the uncertainties present in each. Geophysical data can be used to quickly develop 2D or 3D profiles to develop a preliminary model of the subsurface that is consistent with the field observations and site geology. Locations for borings can then be identified based on areas of interest or greatest uncertainty in the preliminary model. Borings are especially useful for identifying depth to water table, depth to auger refusal and soil types at the site. Rock cores can then be used to confirm that auger refusal materials are indeed rock, determine

rock type, and to estimate the degree to which the rock is fractured. All of these will affect the geophysical results and constraining this information will help to develop a more reliable ground model.

6.3 Recommendations for Implementation

The primary conclusion from this work is that 2D surface-based geophysical methods are an effective investigation tool for karst sites along Alabama highways. Electrical resistivity was found to be the simplest test to perform and process, and so should be considered as a primary investigation method for sinkhole sites. Seismic FWI has provided very useful results, but the data processing and interpretation requirements are significant and likely more than could be done for routine ALDOT projects. FWI is a focus of on-going research at multiple universities and is expected to be become more useful to practice as it continues to develop. GPR is a valuable technique for identifying voids beneath pavement, but its depth of investigation is limited in areas with significant clayey soils as are typically found at karst sites in Alabama. Using these geophysical techniques will require trained personnel or working with outside entities that can provide the necessary expertise to process and interpret the results.

The second major conclusion from this work is that an integrated characterization approach can bring significant value to ALDOT sinkhole investigations, including a reduction in costs (estimated as 34-60%) and more complete subsurface profiles. This value comes from the continuous nature of the geophysical surveys, which allows for detailed profiles to be developed with only a few borings as opposed to the large number of borings that are needed without including geophysics. It is anticipated that the improved characterization will also help with designing more targeted repairs, which could also lead to significant cost savings.

Implementing an integrated characterization program will require an ability to combine information from different characterization sources into a common spatial coordinate system. For this research, this was done using ArcGIS and Google Earth and surveys were performed using a combination of handheld GPS units, a total station, and unmanned aerial vehicles (UAVs). This method of data collection is less precise than that provided by ALDOT surveyors but has the advantage of being able to be collected at the same time as the geophysical data. Future geophysical surveys should consider using similar survey tools to get approximate locations and using a total station (or equivalent method) to collect topography data at the time of the survey when necessary.

6.4 Future Studies

The current study has focused on characterizing sites with karst features, such as sinkholes, but has not explored how improved characterization will affect the design of repairs. The use of geophysical methods offers the potential for repeated monitoring over time, which may enable a more performance-based design approach to sinkholes, in which repairs are designed to limit damage to highway infrastructure, but do not require complete excavation and backfilling of the sinkhole. These types of repairs have the potential to offer significant cost-savings, but this was beyond the scope of the current project. Future research may explore these alternative repair methods and associated monitoring requirements.

The presentation and storage of geophysical results has not been standardized for DOTs. This leads to differences in the way results are plotted and presented, and complicates sharing of results between different entities. Data standards have been developed for other types of geotechnical data (e.g., SPTs, lab tests), but standards for geophysical data are still lacking. This is an important area for future research in order to standardize the presentation of geophysical data and allow for different organizations to easily share and transfer the results of these investigations.

This study has demonstrated the potential of seismic FWI to map irregular rock surfaces at depths of less than 35 feet. This sort of rock mapping has applications far beyond sinkhole investigation, including foundation design, determining the rippability of rock, slope design, and estimating variability in soil properties. This technique has the potential to be used at larger depths, but this will require different types of sources (i.e., controlled vibratory sources) and improvements to the current inversion techniques. This is a promising area for future research.

One of the limitations of resistivity testing is the uncertainty in correlating the resistivity of a material to the soil type or rock type. Generic correlations have been developed based on international datasets, but these correlations often span several orders of magnitude. Correlations developed specifically for Alabama soils and rocks would likely have significantly less uncertainty and may allow resistivity results to be used more directly to identify soil and rock types. Developing this correlation will require compiling a large dataset of ERT results in different geologies across the state and correlating these results with soil and rock samples. The current study represents a first step in this direction, but significantly more data would be needed to generate reliable correlations.

REFERENCES

Advanced Geosciences Inc. (AGI) (2014). *EarthImager 2D Manual*. Austin, TX

Advanced Geosciences Inc. (AGI) (2018). *SuperSting Earth Resistivity, IP & SP System with Wi-fi: Instruction Manual*. Austin, TX

American Society of Civil Engineers (ASCE) (2010). *ASCE 7-10: Minimum Design Loads for Buildings and Other Structures*. American Society of Civil, Reston, VA.

ASTM D6429-99 (2011). "Standard Guide for Selecting Surface Geophysical Methods." ASTM International, West Conshohocken, PA.

Banerjee, B., and Gupta, S.K. (1975). "Hidden Layer Problem in Seismic Refraction Work." *Geophysical Prospecting*, 23(4) 642-652. DOI 10.1111/j.1365-2478.1975.tb01550.x

Bullock, P.J. and Dillman, A. (2003). "Sinkhole Detection in Florida using GPR and CPT." In *Proc. Int. Conf. on Applied Geophysics* (ICAG) (pp. 1-12).

Burger, H.R., Sheehan, A.F., Jones, C.H. (2006). *Introduction to Applied Geophysics*. W.W. Norton & Company, New York.

Cardarelli, E., Cercato, M., Cerreto, A., Di Filippo, G. (2009). "Electrical resistivity and seismic refraction tomography to detect buried cavities." *Geophysical Prospecting* 00, 1-11. DOI 10.1111/j.1365-2478.2009.00854.x

Carrière, S. D., Chalikakis, K., Sénéchal, G., Danquigny, C., and Emblanch, C. (2013). "Combining Electrical Resistivity Tomography and Ground Penetrating Radar to study geological structuring of karst Unsaturated Zone." *Journal of Applied Geophysics*, 94, 31–41.

Casto, D.W., Calderon-Macias, C., Luke, B., Kaufmann, R. (2010). "Improving MASW Results for a Site with Shallow Bedrock Through the Use of Higher-Mode Data." GeoFlorida 2010, Orlando Florida. DOI 10.1061/41095(365)136

Constable, S.C., Parker, R.L. and Constable, C.G. (1987). "Occam's inversion: A practical algorithm for generating smooth models from electromagnetic sounding data." *Geophysics*, 52, 289-300.

Degroot-Hedlin, C., and Constable, S. (1990). "Occam's inversion to generate smooth, two-dimensional models from magnetotelluric data." *Geophysics*, 55(12), 1613–1624.

De Waele, J. D., Plan, L., and Audra, P. (2009). "Recent developments in surface and subsurface karst geomorphology: An introduction." *Geomorphology*, 106(1-2), 1–8.

Dojack, L. (2012). *Ground Penetrating Radar Theory, Data Collection, Processing, and Interpretation: A Guide for Archaeologists*, Report, University of British Columbia.

Ernst, J.R., Green, A.G., Maurer, H., Holliger, K. (2007). "Application of a new 2D time-domain full-waveform inversion scheme to crosshole radar data." *Geophysics*, 72(5). 10.1190/1.2761848

Foose, R. M., and Humphreville, J. A. (1979). Engineering geological approaches to foundations in the karst terrain of the Hershey valley. *Bulletin of the Association of Engineering Geologists*, xvi (3), 355–381.

Ford, D. C., and Williams, P. W. (2007). *Karst hydrogeology and geomorphology*. John Wiley & Sons, Chichester, England.

Geological Survey of Alabama (GSA) (2006). "Digital Geologic Map of Alabama." Geological Survey of Alabama, Tuscaloosa, AL.

Geological Survey of Alabama (GSA) (2010). "Sinkholes and Sinkhole Density Across Alabama." Geological Survey of Alabama, Tuscaloosa, AL.

Hiltunen, D.R. and Cramer, B.J. (2008). "Application of Seismic Refraction Tomography in Karst Terrane." *Journal of Geotechnical and Geoenvironmental Engineering*, 134(7), 938-948. DOI 10.1061/(ASCE)1090-0241(2008)134:7(938)

Hoover, R.A. (2003). "Geophysical Choices for Karst Investigations." Ninth Multidisciplinary Conference on Sinkholes & the Engineering and Environmental Impacts of Karst, Huntsville, Alabama. DOI 10.1061/40698(2003)48

Isiaka, A.I., Durrheim, R.J., Manzi, M.S.D. (2019). "High-Resolution Seismic Reflection Investigation of Subsidence and Sinkholes at an Abandoned Coal Mine Site in South Africa." *Pure and Applied Geophysics* 176, 1531-1548. DOI 10.1007/s00024-018-2026-3

Ismail, A. and Anderson, N. (2012). 2-D and 3-D Resistivity Imaging of Karst Sites in Missouri, USA. *Environmental & Engineering Geoscience*. Vol. XVIII(3) 281-293

Ivanov, J., Miller, R., Peterie, S. (2016). "Detecting and delineating voids and mines using surface-wave methods in Galena, Kansas." *SEG Technical Program Extended Abstracts*: 2344-2350 DOI 10.1190/segam2016-13967007.1

Jol, H. M. (2009). *Ground Penetrating Radar: Theory and Applications*. Elsevier, Oxford, UK.

Jug, J., Stanko, D., Grabar, K., Hrzenjak, P. (2020). "New approach in the application of seismic methods for assessing surface excavatability of sedimentary rocks." *Bulletin of Engineering Geology and the Environment,* https://doi.org/10.1007/s10064-020-01802-1

Kaufmann, O., and Quinif, Y. (1999). "Cover-collapse sinkholes in the 'Tournaisis' area, southern Belgium." *Engineering Geology*, v. 52, nos. 1&2, pp. 15-22.

Lamoreaux, P. E., and Newton, J. G. (1986). "Catastrophic subsidence: An environmental hazard, Shelby County, Alabama." *Environmental Geology and Water Sciences*, 8(1-2), 25–40.

Langer, W. H. (2001). "Potential environmental impacts of quarrying stone in karst - a literature review." US Geological Survey Open-File Report OF-01-0484.

Lee, M., Byun, J., Kim, D., Choi, J., Kim, M. (2017). "Improved modified energy ratio method using a multi-window approach for accurate arrival picking." *Journal of Applied Geophysics* 139, 117-130. DOI 10.1016/j.jappgeo.2017.02.019

Liberty, L.M, and Gribler, G. (2014). "Development of land streamer technologies for estimating shear wave velocities in an urban environment." Center for Geophysical Investigation of the Shallow Subsurface, Technical Report 14-02, Boise, Idaho.

Loke, M.H. (2004). "Tutorial: 2-D and 3-D Electrical Imaging Surveys." Geotomo Software. www.geoelectrical.com.

Loke, M., Chambers, J., Rucker, D., Kuras, O., and Wilkinson, P. (2013). "Recent developments in the direct-current geoelectrical imaging method." *Journal of Applied Geophysics*, 95, 135–156.

Luo, Y., Xia, J., Liu, J., Xu, Y., Liu, Q. (2008). "Generation of a pseudo-2D shear-wave velocity section by inversion of a series of 1D dispersion curves," *Journal of Applied Geophysics* 64, 115-124. DOI 10.1016/j.jappgeo.2008.01.003

Majzoub, A.F., Stafford, K.W., Brown, W.A., Ehrhart, J.T. (2017). "Characterization and Delineation of Gypsum Karst Geohazards Using 2d Electrical Resistivity Tomography in Culberson County, Texas USA." *Journal of Environmental and Engineering Geophysics*, 22(4), 411-420. DOI 10.2113/JEEG22.4.411

Marescot, L., Loke, M., Chapellier, D., Delaloye, R., Lambiel, C., and Reynard, E. (2002). "Assessing reliability of 2D resistivity imaging in mountain permafrost studies using the depth of investigation index method." *Near Surface Geophysics*, 1(2), 57–67.

Margiotta, S., Negri, S., Parise, M., and Quarta, T. A. M. (2015). "Karst geosites at risk of collapse: the sinkholes at Nociglia (Apulia, SE Italy)." *Environmental Earth Sciences*, 75(1).

Modrak, R. and Tromp, J. (2016). "Seismic waveform inversion best practices: regional, global, and exploration test cases." *Geophys. J. Int.* 206, 1864-1889. 10.1093/gji/ggw202

Nazarian, S. (1984). "In Situ Determination of Elastic Moduli of Soil Deposits and Pavement Systems by Spectral-Analysis-Of-Surface-Waves Method." Ph.D. Dissertation, The University of Texas at Austin.

Newton, J. G. (1987). "Development of sinkholes resulting from man's activities in the Eastern United States." US Geological Survey Circular 968.

Nocedal, J. and Wright, S.J. (2006). *Numerical Optimization*. 2nd ed. Springer, New York.

Okpoli, C. C. (2013). "Application of 2D Electrical Resistivity Tomography in Landfill Site: A Case Study of Iku, Ikare Akoko, Southwestern Nigeria." *Journal of Geological Research,* http://dx.doi.org/10.1155/2013/895160.

Oldenburg, D.W. and Li., Y., (1999). "Estimating depth of investigation in DC resistivity and IP surveys." *Geophysics*, 64, 403-416.

Orange, B. and Smith, D. (2014). "AL-21 Sinkhole remediation Talladega County." 57th Annual Transportation Conference, Auburn University. Retrieved August 2016. http://eng.auburn.edu/2014TransConf/SinkholeRemediationTalladegaCounty.pdf

Park, C.B., Miller, R.D., Xia, J. (1999). "Multichannel analysis of surface waves." *Geophysics* 64(3), 800-808.

Park, M.K., Park, S., Yi, M., Kim, C., Son, J., Kim, J., Abraham, A.A. (2013). "Application of electrical resistivity tomography (ERT) technique to detect underground cavities in a karst area of South Korea." *Environ Earth Sci* 71, 2797–2806. DOI 10.1007/s12665-013-2658-7

Park Seismic LLC. "What is seismic survey?" Retrieved July 2020. http://www.masw.com/Whatisseismicsurvey.html

Parker, E.H. and Hawman, R.B. (2012). "Multi-channel Analysis of Surface Waves (MASW) in Karst Terrain, Southwest Georgia: Implications for Detecting Anomalous Features and Fracture Zones." *Journal of Environmental and Engineering Geophysics* 17(3), 129-150.

Rosas-Carbajal, M. A. (2014). "Time-lapse and probabilistic inversion strategies for plane-wave electromagnetic data." Dissertation. National University of La Plata, Argentina.

Roth, M., and Nyquist, J. (2003). Evaluation of Multi-Electrode Earth Resistivity Testing in Karst.

Geotechnical Testing Journal, 26(2), 10475.

Ruffin-Bass, N. (1996). "Sinkholes in the marble and dolostone karst of Sylacauga, Alabama." Thesis. University of Alabama.Schafer, M., Groos, L., Forbriger, T., Bohlen, T. (2012). "On the effects of geometrical spreading corrections for a 2D full waveform inversion of recorded shallow seismic surface waves." 74th EAGE Conference & Exhibition incorporating SPE EUROPEC 2012 Copenhagen, Denmark, 4-7 June 2012. 10.3997/2214-4609.20148327

Sheehan, J.R., Doll, W.E., Mandell, W.A. (2005a). "An Evaluation of Methods and Available Software for Seismic Refraction Tomography Analysis." *Journal of Environmental and Engineering Geophysics* 10(1), 21-34. DOI 10.2113/JEEG10.1.21

Sheehan, J.R., Doll, W.E., Watson, D.B. Mandell, W.A. (2005b). "Application of Seismic Refraction Tomography to Karst Cavities," U.S. Geological Survey Karst Interest Group Proceedings, Rapid City, SD. Scientific Investigations Report 2005-5160.

Sirles, P. C. (2006). *Use of geophysics for transportation projects (Vol. 357).* Transportation Research Board.

Steeples, D.W., Knapp, R.W., McElwee, C.D. (1986). "Seismic reflection investigations of sinkholes beneath Interstate Highway 70 in Kansas." *Geophysics* 51(2), 295-301.

Sullivan, B., Tran, K.T., Logston, B. (2016). "Characterization of Abandoned Mine Voids under Roadway with Land-Streamer Seismic Waves." *Transportation Research Record*, 2580, 71-79. DOI 10.3141/2580-09

Šumanovac, F., and Weisser, M. (2001). "Evaluation of resistivity and seismic methods for hydrogeological mapping in karst terrains." *Journal of Applied Geophysics*, 47(1), 13–28.

Szabo, M.W., Osborne, E.W., Copeland, C.W. Jr., and Neathery, T.L., (1988). *Geologic Map of Alabama,* Geological Survey of Alabama Special Map 220, scale 1:250,000

Tanguy, R., Dassargues, A., Brouyère, S., Kaufmann, O., Hallet, V., and Nguyen, F. (2011). "Assessing the contribution of electrical resistivity tomography (ERT) and self-potential (SP) methods for a water well drilling program in fractured/karstified limestones." *Journal of Applied Geophysics*, 75(1), 42–53.

Thomas, B., and Roth, M. (1999). "Evaluation of site characterization methods for sinkholes in Pennsylvania and New Jersey." *Engineering Geology*, 52, 147-152.

Tran, K.T., McVay, M., Faraone, M., Horhota, D. (2013). "Sinkhole detection using 2D full seismic waveform tomography." *Geophysics* 78(5), R175-R183. DOI 10.1190/GEO2013-0063.1

Tromp, J., Komatitsch, D., Liu, Q. (2008). "Spectral-element and adjoint methods in seismology." *Communications in Computational Physics*, Vol. 3, No. 1, pp. 1-32.

Van Schoor, M. (2002). "Detection of sinkholes using 2D electrical resistivity imaging." *Journal of Applied Geophysics*, 50(4), 393-399. DOI 10.1016/S0926-9851(02)00166-0

Virieux, J. and Operto, S. (2009). "An overview of full-waveform inversion in exploration geophysics." *Geophysics*, 74(6), WCC1-WCC26. DOI 10.1190/1.3238367

Wathelet, M. (2008). "An improved neighborhood algorithm: parameter conditions and dynamic scaling." *Geophysical Research Letters*, 35, L09301.

Wathelet, M., Jongmans, D., and Ohrnberger, M. (2004). "Surface wave inversion using a direct search algorithm and its application to ambient vibration measurements." *Near Surface Geophysics*, 2, 211-221.

White, R.M.S., Collins, S., and Loke, M.H. (2003). "Resistivity and IP arrays, optimised for data collection and inversion." ASEG Extended Abstracts, 2003:2, 1-4, DOI: 10.1071/ASEG2003ab182

Whiting, S. E. (2009). "Geology of the Talladega slate belt and the foreland fold-and-thrust belt, Talladega County, Alabama." Dissertation. Florida State University

Xia, J., Nyquist, J.E., Xu, Y., Roth, M.J.S., Miller, R.D. (2007). "Feasibility of detecting near-surface feature with Rayleigh-wave diffraction." *Journal of Applied Geophysics*, 62, 244-253. DOI 10.1016/j.jappgeo.2006.12.002

Zhou, W., Beck, B. F., and Stephenson, J. B. (2000). "Reliability of dipole-dipole electrical resistivity tomography for defining depth to bedrock in covered karst terranes." *Environmental Geology*, 39(7), 760–766.

Zhou, W., Beck, B., and Adams, A. (2002). "Effective electrode array in mapping karst hazards in electrical resistivity tomography." *Environmental Geology*, 42(8), 922–928.

Appendix A: Geophysical Field Survey Sheets

Geophysics Equipment Check List

General (aquire day before survey)			
ITEM	**QTY**	**OUT**	**IN**
Truck keys	1		
Credit Card	1		
Splicing Tools (INF Electrode)			
Water			
Inverter	1		
GPS	1		
Measuring Tape	2		
Measuring Wheel	1		

Resistivity			
ITEM	**QTY**	**OUT**	**IN**
Deep Cycle Battery	2		
Cable Reel	2		
Super Sting	1		
Switch Box	1		
Electrodes	56		
Hammer	2		
Infinity Cable	4		
Infinity electrode	1		
PC Com Cable	1		
Battery Power Cable	1		
Boost Battery Cable	1		
2 meter Switch Box Cable	2		
Male-Male Cable Adapter	1		
Antenna	1		
Android Tablet	1		
Resistivity Checklist + Notes	4		

Seismic			
ITEM	**QTY**	**OUT**	**IN**
Geode	2		
Small Yellow Pelican Case	1		
Computer + Charger	1		
Small 12V Battery	2		
Trigger Cable	1		
12 Lb Hammer	1		
20 Lb Hammer	1		
Auto-Hammer	1		
Plates	3		
Big Pelican Case	1		
Black Spread Cable	1		
Orange Box	1		

Date:

Project:

Notes:

Electrical Resistivity Survey Data Sheet

Date:	**CRS:**
Project Number:	
Purpose:	
Specific Location:	
Line Orientation:	
Line Bearing:	**Notes:**
Arrays Used:	
# Electrodes and Spacing:	
Roll-Along?	
CMD Files:	
Data Files:	

Electrical Resistivity Survey Data Sheet

Date:
Date Surveys are Performed

Project Number:
Internal Project Number

Purpose:
Purpose of Geophysical Surveys
Example: Map Sinkhole Features

Specific Location:
Specific Location of Each Survey Line
Example:
R1- East side of sinkhole repair near NB lanes

Line Orientation:
General Orientation of Survey Line
Example:
R1- South (electrode 1) to North (electrode 56)

Line Bearing:
Rough Bearing Estimate of Survey Lines
This helps for plotting survey lines on maps
Example: R1- 28° NE

Arrays Used:
Arrays Used for Each Survey Line
Example:
R1- dipole-dipole, strong-gradient

 # Electrodes and Spacing:
Number of Electrodes and Spacing for Each Survey Line
Example:
R1- 56 electrodes spaced @ 2m

Roll-Along?
Was a Roll-Along Performed for any Surveys?
Example:
R1- No

CMD Files:
Command Files Used for Each Survey
Example: R1- DD56E.cmd ; SG56E.cmd

Data Files:
Names of Data Files for Each Survey Line and Array
Example-
R1- 2006R1DD.dat ; 2006R1SG.dat

CRS:

Notes from Contact Resistance Test
Example:
R1- electrodes w/ high contact resistance
E8 - E11 ; E22 - E25 ; E43 - E49

Notes:

Notes for Each Resistivity Line Should Include:

- Locations of sinkhole repairs or features along each line
- Locations of borings along each survey line
- Locations of identifiable landmarks in relation to survey lines
- Any other important information related to each survey
- Illustrations are often helpful

Example:
R1- Sinkhole repair @ X=52m
B1 @ X=10m ; B2 @ X=27m ; B3 @ X=46m ; B4 @ X=62m
Electrode 1 @ 4m from NB fog line
Electrode 56 @ 7.5m from NB fog line

Electrical Resistivity Survey Data Sheet

DOI = 70ft ≈ 230'

Date: 2/17/2021

Project Number: 2001 – US 31 Slide

Purpose: Map subsurface at Landslide

Specific Location: NB and SB sides of Road

Line Orientation:
R1 – SW (E_1) → NE (E_{112})
R2

Line Bearing:
R1
R2

Arrays Used:
DD

 # Electrodes and Spacing:
112 @ 2m → R1

Roll-Along?
No

CMD Files:
2001R1 (Don't use 2001R1DD)
2001R1S (Don't use 2001R1S6)

DD
S6

Data Files:

CRS:
R1
⇒ ≈ 3K E98-104

R2

Notes:

R1 → distance off edge of curb → E_1 = 1.25' / E_{111} = 3' / E_{48} = 3.25'
E_{70} = 5.5' / E_{102} = 24'

South edge of pavement removal @ X = 13m | North edge @ X = 202m (E_{102})

B4 stake @ X = 46m (E_{24}) | B5 stake @ X = 93m |

Stations → 888+75 @ X = 4m (E_3) | 890+80 @ X = 66m (E_{34}) | 893+85 @ X = 156m (E_{74})

Road Bends @ ≈ X = 118m (E_{60})

Guardrail starts @

Water flowing @ 60m out of In Colluvator pit

Guard rail = 29m for x=0

Electrical Resistivity Survey Data Sheet

Date: 2/17/2020

Project Number: 2021 – Line R2

Purpose:

Specific Location: 0.1 North side of Road

Line Orientation: 90 SW (E11) → NE (E117)

Line Bearing:

Arrays Used:

 # Electrodes and Spacing:

Roll-Along?

CMD Files:

Data Files:

CRS:

41-42 – 5 m

75 –

104-112 – 35 m

~~*~~ Subtract 2m from each X-distance

Notes:

B1 @ X = 58 m (E29) (X = 56 m)
B2 @ X = 116 m (E58) (X = 114 m)
B3 @ X = 172 m (E86) (X = 170 m) ≈ same Elev. as R2

"Bump" sign @ X = 97 m (X = 95 m)

South edge pavement removal @ X = 12 m (E6) (X = 10 m)

R1 cracks → N

Flow water @ 60m

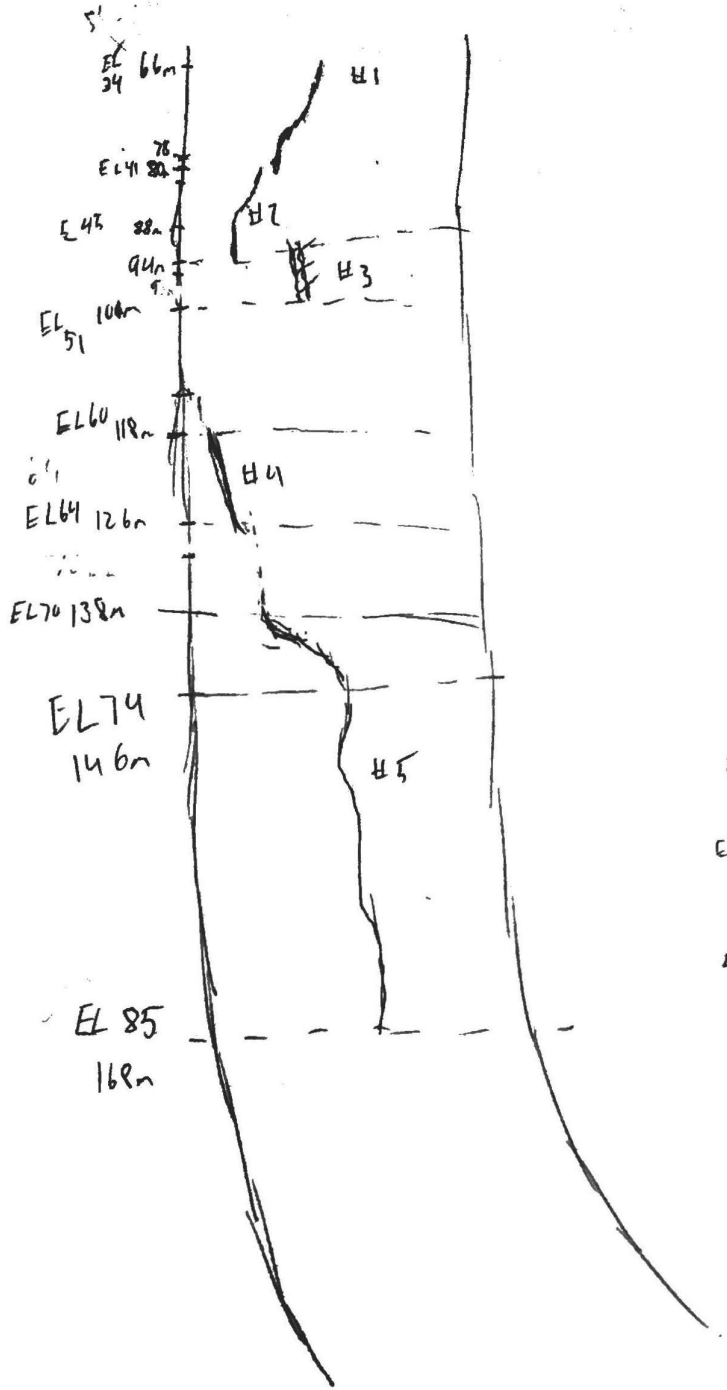

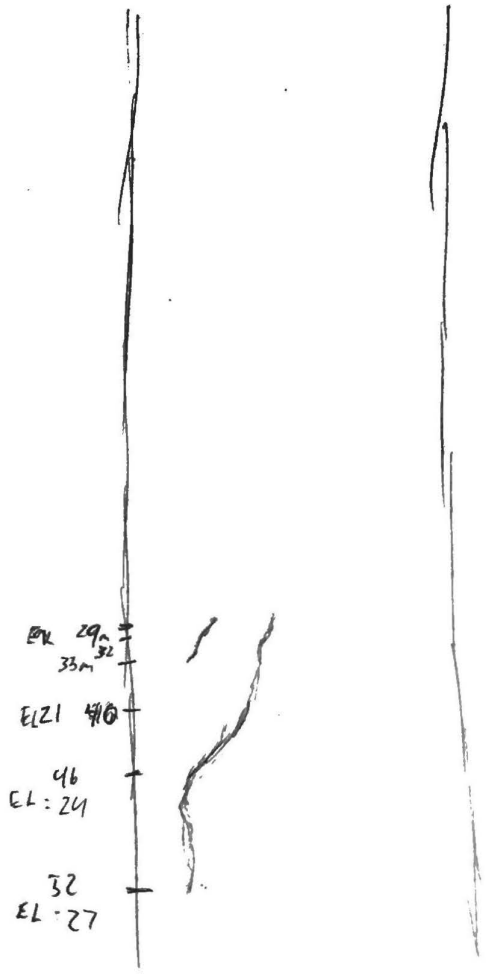

Project #:	2001	Date:	2/17/20	H_{instr}:	5.06'	Tripod Location #:
Survey #:	R1	Zero Bearing:	0°N	H_{rod}:	6.0'	

Record	Northing N	Easting E	Elevation Z	X- coordinate Location	Electrode #	Notes
Initial				X= m	EL	
Final						
1	-35.506	49.343	-0.590	0 m	1	
2	-1.956	113.020	-5.511	22m	12	
3	37.037	188.667	-12.154	48	25	
4	46.820	209.980	-14.826			X= R1 mid X
5	77.478	263.307	-18.766	74	38	
6	117.411	338.261	-23.311	100	51	
7	152.661	401.411	-27.515	122	62	
8	222.684 ?	587.187 ?	-38.369 ?	199 ?	84 ?	
9	209.682	504.435	-36.378	138	80	
10	239.042	555.500	-40.154	176	89	
11	258.515	589.515	-43.914	188	95	
12	281.803	628.752	-48.488	202	102	
13	~~284.944~~	~~634.088~~	~~-47.854~~	~~204~~	~~103~~	
14	284.945	633.865	-49.822	204	103	RH = 8.0'
15	289.562	638.031	-49.278	206	104	
16	292.434	644.879	-50.816	208	105	
17	295.129	651.056	-52.267	210	106	
18	301.871	662.199	-52.938	214	108	
19	318.311	680.631	-54.337	222	112	
20						
21	162.582	293.032	-23.677	B5		
22	110.018	215.243	-17.699	ST 890+80		
23	80.695	159.023	-13.813	B4		
24	12.013	37.040	-1.854	STA 988+75		
	-34.761	-56.601	3.085	Start G.R.		

Project #:	2001	Date:	2/17/20	H_{instr}:	5.06'	Tripod Location #:	X = 11m
Survey #:	R2/S2	Zero Bearing:	0° N	H_{rod}:	6.0'		15m right

Record	N	E	Z	Location	Notes
Initial					
Final				X: m EL	
1	121.856	-58.516	-24.164	@ 2m 1	ST1 / R1/S1 top stick
2	129.214	-30.593	-25.825	x: ~~*~~(11m) TS #2 ~~(x=0m, y=2m)~~	
3	154.198	-1.804	-29.966	20 11	
4	240.538	83.379	-43.478	B1	
5					
6	-4.774	-28.630	1.392	2 1	R2/S2
7	25.084	36.822	-4.953	24 12	
8	28.444	42.485	-7.137	26 13	
9	45.047	77.729	-13.494	38 19	
10	70.673	130.194	-17.374	66 28	
11	110.215	212.950	-20.580	84 32	
12	170.182	336.884	-28.306	156 63	
13	235.948	472.025	-38.365	172 86	
14	280.506	559.948	-43.978	202 101	
15	312.527	624.149	-48.634	224 112	
16					
17	239.298	470.746	-38.392	B3 52020	
18	267.349	546.984	-42.365	End Sign BLMP	
19	-57.870	-117.160	10.350	Begin Sign +	
20					
21					
22					
23					
24					

* Subtract 2m from R2 X= (coordinates)

Project #:	Date:	H_{instr}:	Tripod Location #:
Survey #:	Zero Bearing:	H_{rod}:	

Record	N	E	Z	Location	Notes
Initial					
Final					
1					
2					
3					
4					
5					
6					
7					
8					
9					
10					
11					
12					
13					
14					
15					
16					
17					
18					
19					
20					
21					
22					
23					
24					

Appendix B: Geophysical Investigations at SR-21 And SR-275

Geophysical Investigation Report 1909:

SR-21 and SR-275 Sinkholes

Prepared by

Michael Kiernan

Dan Jackson

Jack Montgomery

November 2019

Department of Civil Engineering

Samuel Ginn College of Engineering

DISCLAIMERS

All interpretations in this report are opinions based on inferences from geophysical tests or other measurements. The authors have exercised reasonable skill, care, and diligence to assess the information acquired during the preparation of this report, but make no guarantees or warranties as to the accuracy or completeness of this information. The information contained in this report is based upon, and limited by, the circumstances and conditions acknowledged herein, and upon information available at the time of its preparation. The information provided by others is believed to be accurate, but cannot be guaranteed. The contents do not necessarily reflect the official views or policies of Auburn University. This report does not constitute a standard, specification, or regulation. Comments contained in this paper related to specific testing equipment and materials should not be considered an endorsement of any commercial product or service; no such endorsement is intended or implied.

NOT INTENDED FOR CONSTRUCTION, BIDDING, OR PERMIT PURPOSES

ACKNOWLEDGEMENTS

We would like to express our appreciation to the Alabama Department of Transportation for providing additional personnel and equipment and assisting with this survey. This report is based on a study sponsored by the Alabama Department of Transportation. The authors gratefully acknowledge this support. The findings, opinions, and conclusions expressed in this paper are those of the authors and do not necessarily reflect the view of these individuals or the sponsor.

INTRODUCTION

Geophysical surveys were performed at two different locations in Talladega County, Alabama to investigate reported sinkhole activity. The first location is about 6 miles southwest of the city of Talladega on the northbound side of SR-21. The second site is about 2 miles southwest of the city of Talladega on the northbound side of SR-275. A map showing each location is shown in Figure 1. Site maps for locations 1 and 2 are shown in Figures 2 and 3 respectively. All surveys were performed on 10/10/2019.

Figure 1: Map of survey locations

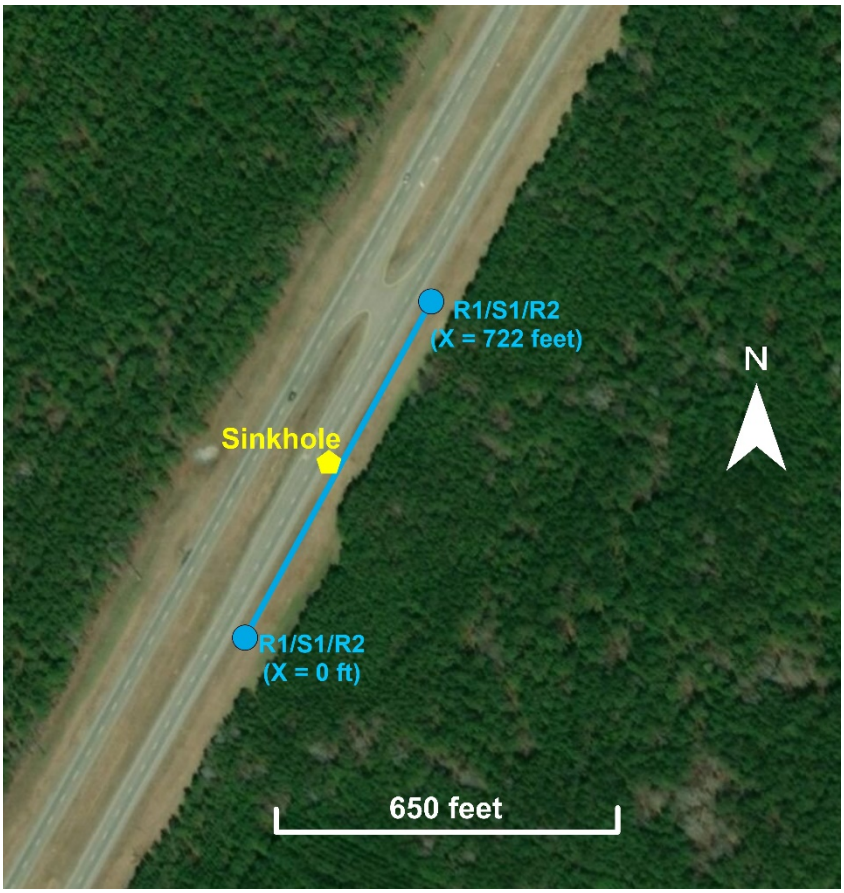

Figure 2: Survey lines at location 1

Figure 3: Survey lines at location 2

BACKGROUND

Previous Investigations

Previous investigations for this site were not available.

SITE DESCRIPTION

Location 1

Location 1 (Figure 2) is located on the northbound side of SR-21 about 6 miles southwest of the city of Talladega, AL. Subsidence of the roadway due to expected sinkhole activity has been reported and repaired. The sinkhole repair is about 13 feet wide and spans both lanes of traffic. A concrete box culvert runs beneath the roadway about 25 feet south of the sinkhole repair. The box culvert is about 4 feet tall and the bottom of the culvert was estimated to be at a depth of about 10 feet. The approximate GPS coordinate of the center of the sinkhole repair is 33.367220, -86.170224.

Location 2

Location 2 (Figure 3) is located on the northbound side of SR-275 about 2 miles southwest of the city of Talladega. Multiple sinkholes have been observed near the roadway as well as land subsidence. The approximate GPS coordinate of the center of the survey lines performed at this site is 33.41317, -86.13271

GEOLOGY

The surface geology at both sites consists of Knox Group undifferentiated in part. This unit consists of light-gray to light-brown locally sandy dolomite, dolomitic limestone, and limestone; and is characterized by abundant light-colored chert (Szabo et al. 1988). Over one-hundred sinkholes have been previously reported within 25 miles of each site in areas where the Knox Group exists at the surface. A few other geologic units containing carbonate rocks also exist within 5 miles of each site including the Rome formation, the Sylacauga Marble Group- Gantt's Quarry formation, Conasauga formation. Thrust faults are also abundant in the area

METHODOLOGY

GPS and Total Station

GPS and total station data were collected to identify the locations of important features and estimate topography along the geophysical survey lines. Important features such as the start and end of geophysical survey lines and landmarks were also recorded with a Garmin GPSMAP 64 handheld GPS system. Total station surveys were performed using a Topcon GTS-230W electronic total station. Total station data was primarily used to estimate topography along each geophysical survey line. The locations of landmarks and known borehole were also surveyed with the total station for comparison and verification purposes with the GPS data.

Electrical Resistivity Data Acquisition and Processing

Electrical resistivity techniques typically utilize four electrode arrays placed on the ground surface to provide an estimate of subsurface resistivity distribution (Loke 2004). Known amperage is injected through two current electrodes and the resulting potential difference is measured between different pairs of potential electrodes. An 'apparent' resistivity distribution is then calculated using the known injected current, the potential voltage difference and a geometric factor which is related to the geometry of the selected array. This 'apparent' resistivity is the value of resistivity that would be measured for the given electrode geometry in a half space of homogenous resistivity. An inversion procedure is then required to estimate the true subsurface resistivity distribution from the measured 'apparent' resistivity values. More details on resistivity theory are outlined in Loke (2004).

The electrical resistivity survey at this site was performed with an 8-channel SuperSting system from AGI. All surveys utilize 56 total electrodes and dipole-dipole arrays. A summary of the electrode spacing and depth of investigation for each survey are summarized in Table 1 below. Survey lines R1 and R2 were centered at the approximate center of the sinkhole repair at location 1 but 20 feet [6.1 m] off the edge of the pavement. The area of observed sinkholes at location 2 runs from about X = 207 feet [63m] to X = 443 feet [135m] along the length of survey line R3.

Inversion of the measured resistivity data was performed using the commercially published software EarthImager 2D to estimate 2D pseudo-sections of subsurface resistivity distribution. The terrain along survey line R3 was incorporated into the inversions as estimated from the total station surveys. No significant elevation changes were measured along survey lines R1 and R2 so terrain was not included in the inversion of these lines. The settings used in EarthImager 2D are summarized in tables A-1 through to A-4.

Table 1: Summary of resistivity surveys

Suvey Line	Location	Electrode Spacing (ft) [m]	Total Line Length (ft) [m]	Depth of Investigation (ft) [m]
R1	1	6.6 [2]	361 [110]	85.6 [26.1]
R2	1	13.1 [4]	722 [220]	155.8 [47.5]
R3	2	9.8 [3]	541 [165]	116.8 [35.6]

*All suveys utilize 56 total electrodes

Seismic Data Acquisition and Processing

Seismic data was collected on October 10, 2019. The seismic data was acquired using a set of 48 4.5-Hertz geophones connected to two Geometrics Geode seismograms. A 0.5 millisecond sample interval and a delay of -0.1 seconds was used for all recordings. A 2.0 second record length was for all the seismic lines. No acquisition filters were used. A 20 pound (90 Newton) sledgehammer was used as a source for line S1 and a 10 pound (45 Newton) sledgehammer was used as a source for line S3. A geophone spacing of 6.6 feet (2 meter) was used for both lines.

The seismic data was processed using the multichannel analysis of surface waves (MASW) technique. Note that only a subset of the collected seismic data was used for this processing technique. Various signal processing techniques can be used to transform the field records to show amplitude as a function of frequency and phase velocity. When viewed this way, a curve can be picked that relates the frequency of the surface waves to the velocity at which they travel. This curve is called the *dispersion curve*. Once the dispersion curve is picked, an inversion procedure is used to determine a one dimensional velocity model that fits the picked dispersion curve, typically in a least squares sense. The open source software Geopsy (Wathelet 2005) was used to create the velocity-frequency images, pick the dispersion curves, and perform the inversions. Note that as with all geophysical inversions, the results from MASW are non-unique. The profiles presented here are the “best fit” profiles from the inversion. It is possible that other profiles may fit the data equally well or better than the ones presented below.

A simplified seismic refraction analysis was also performed at location 2. With this method, the first waveform arrivals (p-waves) are picked on a seismic record. The velocity of these first arrivals can be determined using the arrival time and the distances between the receivers. By assuming a simplified structure of two constant-velocity layers, the equation below can be used to calculate the depth of the upper layer.

$$h_1 = \frac{x_{co}}{2}\left[\frac{V_2 - V_1}{V_2 + V_1}\right]^{1/2}$$

Where x_{co} is the cross-over distance, V_1 is the velocity of the upper layer, V_2 is the velocity of the lower layer, and h_1 is the thickness of the upper layer.

The seismic full waveform inversion (FWI) methodology was also used at location 1. This method is more experimental than the other methods used and has been implemented by the authors in Matlab. The method is summarized below.

The elastic wave equation and the subsurface velocity model govern the transmission of seismic waves through the subsurface. For the FWI procedure, the wave equation is solved numerically using a trial velocity model to generate a set of synthetic waveforms. The misfit between these synthetic seismograms and the seismograms recorded in the field is then calculated. A nonlinear optimization algorithm is used to adjust the velocity model in a way that minimizes the misfit between the observed and synthetic waveforms. This process is repeated iteratively until the misfit meets a predefined stopping criteria. Additional details may be found in Virieux and Operto (2009) and Modrak and Tromp (2016).

INTERPRETED RESULTS

Resistivity

The depth of investigation for survey R1 was not deep enough to detect rock and did not reveal any pertinent features so the results are not included in this section. The interpreted results from electrical resistivity survey R2 is shown below in Figure 4 along with the location of the sinkhole center and the concrete box culvert. The interpreted results from survey line R3 is shown in Figure 5 below along locations of observed sinkholes and land subsidence features adjacent to the survey line. Raw versions of the measured, calculated and inverted pseudo-sections are also shown in the appendix in Figures A-1 through A-3.

Surveys R1 and R2 appear to have been significantly affected by the presence of the culvert as evidenced by the shadowed zones extending away from the culvert in the measured apparent resistivity pseudosections (Figures A-1 and A-2). Because of this the electrode directly over the culvert were removed prior to inversion of survey R2. There appears to be an upper high resistivity layer as well as a deeper high resistivity layer in survey R2. The transition interface between these layers is indistinguishable due to the similar resistivity values. The deeper high resistivity zone is interpreted as rock, but further investigations are required to confirm the exact nature of the materials in both high resistivity zones. Due to the complex nature of having two materials of similar resistivity, the interpreted rock surface from the seismic FWI was overlain on the inverted profile for line R2. The top of the high resistivity zone near the bottom of the R2 inverted profile is consistent with the depth to rock from the seismic FWI.

The results from survey R3 shows a transition to a higher resistivity layer (> 1000 ohm-m) at a depth of about 20 feet at the north end of the site. This transition is represented by the dotted line in Figure 4. The depth to this higher resistivity layer at the north end of the site is

consistent with the depth to the p-wave velocity transition seen in Figure 8. A dip in the rock can be seen beneath the southernmost sinkhole which is consistent with sinkhole related dissolution features.

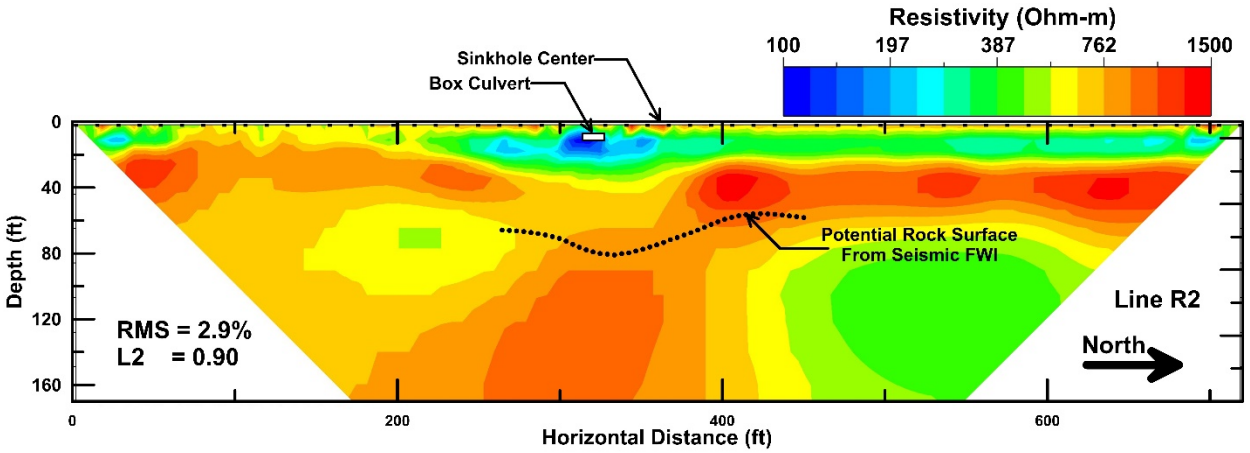

Figure 4: Resistivity results from survey line R2

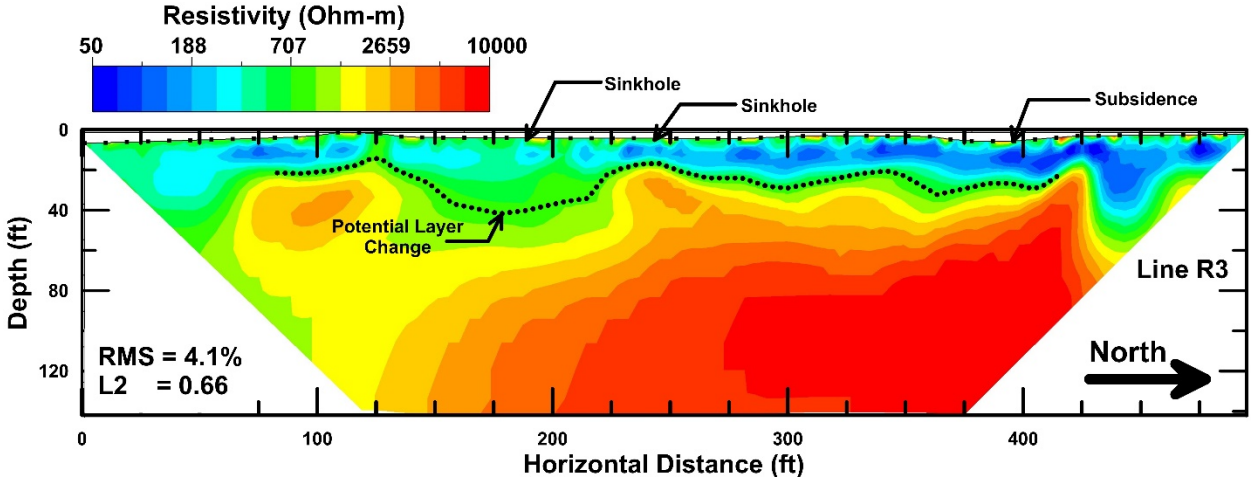

Figure 5: Resistivity results from survey line R3

Seismic

Site 1 – Line S1 MASW

The results from the MASW analysis from site 1 are shown in Figure 6. Note that the MASW method averages over the entire seismic line, so the properties and depths in Figure 6 do not correspond to one specific location. The results show that the overburden has shear wave velocities ranging from about 590 ft/s [180 m/s] to about 1030 ft/s [310 m/s]. There is a large increase in

velocity at a depth of about 66 feet [20.2 meters] that likely corresponds to a transition to rock, with a shear wave velocity of about 4000 ft/s [1225 m/s].

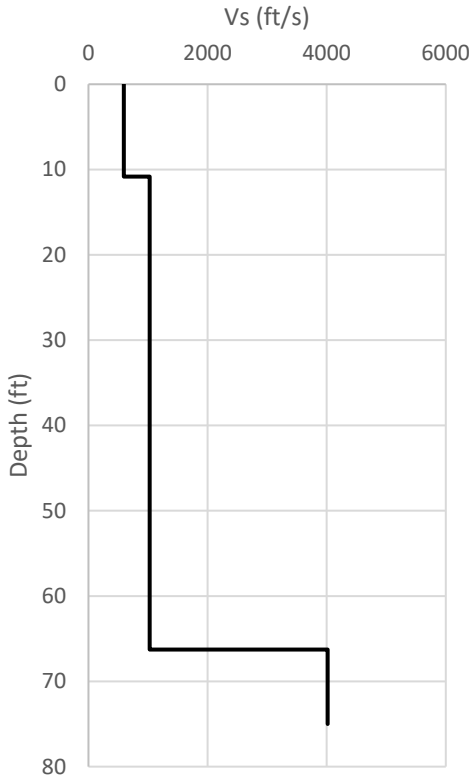

Figure 6: Best fit shear wave velocity profile from site 1 (Line S1)

Site 1 – Line S1 FWI

The full waveform inversion profile for line S1 is shown in Figure 7. The profile generally agrees with the MASW results, showing velocities less than 1000 ft/s [305 m/s] in the upper portion of the model, and velocities greater than 3000 ft/s [915 m/s] at depth. The profile shows stiffer material below about 60-70 feet [18-21 meters], indicated in Figure 7 by a velocity contour at 2300 ft/s [700 m/s] that is interpreted as the potential rock surface. This depth is in agreement with the electrical resistivity results. The profile also shows a dip in this stiffer material between 300 and 350 feet to depths greater than 75 feet [23 meters].

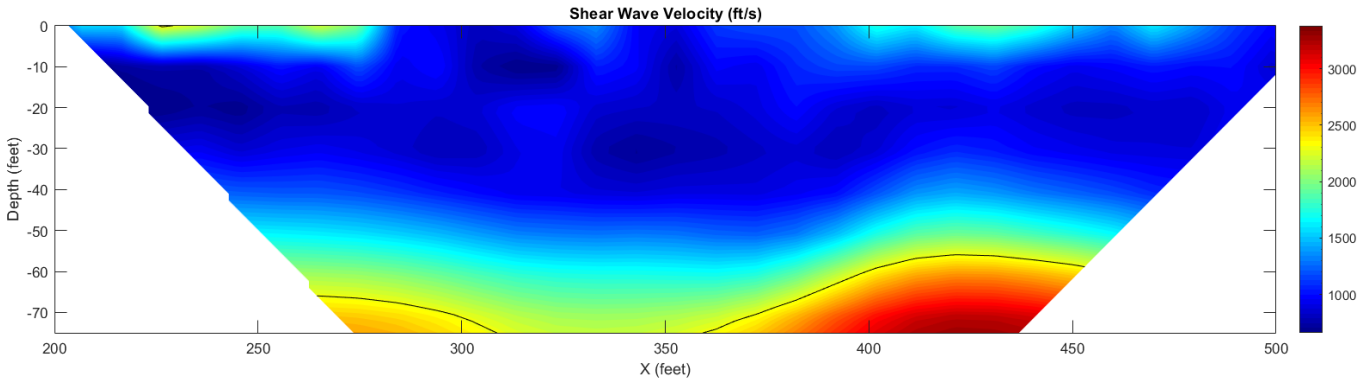

Figure 7: FWI shear wave velocity profile from site 1 (Line S1)

Site 2 – Line S3

At the second site, the seismic surface wave methods were relatively unsuccessful. There was significant contamination of data from traffic noise. Also, this site seems to have fairly shallow rock based on observations in the chimneys at the site. These conditions are not favorable for seismic surface wave testing, thus the results have relatively high uncertainty.

The best shear wave velocity model is shown in Figure 7. This model shows a transition to a stiffer material at a depth of about 8 feet [2.5 meters]. The lower layer has a shear wave velocity of about 2200 ft/s [675 m/s] which is within the range of typical values for rock or very stiff soil (ASCE 2017).

In addition to the surface wave analysis, a very simplified refraction analysis was performed to confirm the fact that rock was relatively shallow at this site. This analysis used the raw data from a single shot and assumed a two layer system. The first arrivals were estimated for the record and the velocities for the two layers were calculated as the reciprocal slope of a line fit through the first arrivals. The picks are shown in Figure B-5 in the appendix. The cross-over distance (the distance at which the slope changes) was also picked. The p-wave velocity profile is shown in Figure 7. Based on this simplified analysis, the upper layer had a p-wave velocity of about 2840 ft/s [864 m/s] and a thickness of about 18 ft [5.6 m], while the lower layer had a p-wave velocity of about 8140 ft/s [2480 m/s], again, within the range of p-wave velocities typical for rock (ASTM D5777).

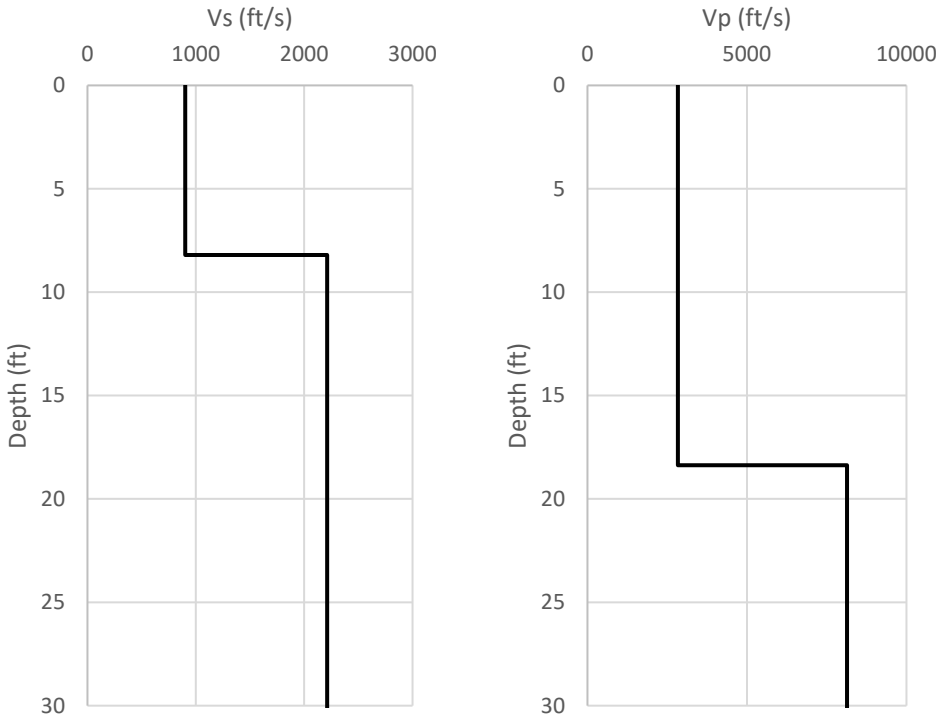

Figure 8: Shear wave velocity profile (left) and P-wave velocity profile (right)

REFERENCES

ASCE (2017). *Minimum Design Loads and Associated Criteria for Building and Other Structures* (ASCE/SEI 7-16). American Society of Civil Engineers, Reston, Virginia.

ASTM D5777 (2011) Standard Guide for Using the Seismic Refraction Method for Subsurface Investigation. American Society for Testing and Materials, West Conshohocken, PA.

Advanced Geosciences Incorporated (AGI). (2014). "Instruction Manual for EarthImager 2D Version 2.4.2 Resistivity and IP Inversion Software." Austin, TX

Loke, M. H. (2004). "Tutorial: 2D and 3D electrical imaging surveys. https://www.geotomosoft.com/downloads.php (accessed on Sept. 19, 2018)

Modrak, R. and Tromp, J. (2016). "Seismic waveform inversion best practices: regional, global, and exploration test cases," *Geophys. J. Int.* 206, 1864-1889. 10.1093/gji/ggw202

Ruffin-Bas, N. (1996). “Sinkholes in the marble and dolostone karst of Sylacauga, Alabama.” Thesis. University of Alabama.

Virieux, J. and Operto, S. (2009). “An overview of full-waveform inversion in exploration geophysics,” *Geophysics*, 74(6), WCC127-WCC152, 10.1190/1.3238367.

Wathelet, M. (2005). “Array recordings of ambient vibrations: surface-wave inversion.” Ph.D. thesis. Université de Liège, Liège, Wallonia, Belgium

Szabo, M.W., Osborne, E.W., Copeland, C.W. Jr., and Neathery, T.L., (1988). Geologic Map of Alabama, Geological Survey of Alabama Special Map 220, scale 1:250,000

APPENDIX

A. Resistivity

Table A - 1: Initial settings in EarthImager 2D

	Initial Settings	
Criteria for Data Removal	Min Voltage (mV)	0.2
	Min abs[V/I] (ohm)	0.0005
	Max Repeat Error (%)	3%
	Min App Res (Ohm*m)	1
	Max App Res (Ohm*m)	10000
	Max Recipricol Error (%)	5%
	Remove Neg Res (check box)	Yes
	Remove Spikes (check box)	No
	Keep All	No
	Skip Data	0
Inversion Method/ Y-axis	Inversion Method	Smooth Model
	Definition of Y-axis	Y=depth
	Orientation of Vertical Axis	Positive Upward
	Distance Scale Factor	1.0

Table A - 2: Forward modeling settings in EarthImager 2D

Forward Modeling	
Forward Model Method	Finite Element
Forward Equation Solver	Cholesky Decomp.
Type of Boundary Condition	Dirichlet
Number Mesh Divisions	2
Thickness Incremental Factor	1.1

Table A - 3: Resistivity inversion parameters in EarthImager 2D

	Resistivity Inversion	
Stop Critieria	Max Number of Iterations	8
	Max RMS Error (%)	4
	Error Reduction (%)	N/A
	L2 Norm (check box)	No
Misc.	Number CG Iterations	6
	Starting Iteration of Quasi-Newton	20
	Smoothness Factor	10
	Damping Factor	10
	Estimated Noise (%)	4.0%
	Use Recip. Error (check box)	No
	Suppress Noisy Data (check box)	Yes
	Resolution Factor	0.2
	Starting Model	Avg. App. Res.
	Min Resistivity (Ohm*m)	0.1
	Max Resistivity (Ohm*m)	10000
	Model Parameter Width	1
	Model Parameter Height	1
	Horizontal/ Vertical Roughness Ratio	0.5

Table A - 4: Terrain parameters in EarthImager 2D

Terrain	
Mesh Transformation Method	Damped Transformation
Boundary Topograpahy	Constant Slope

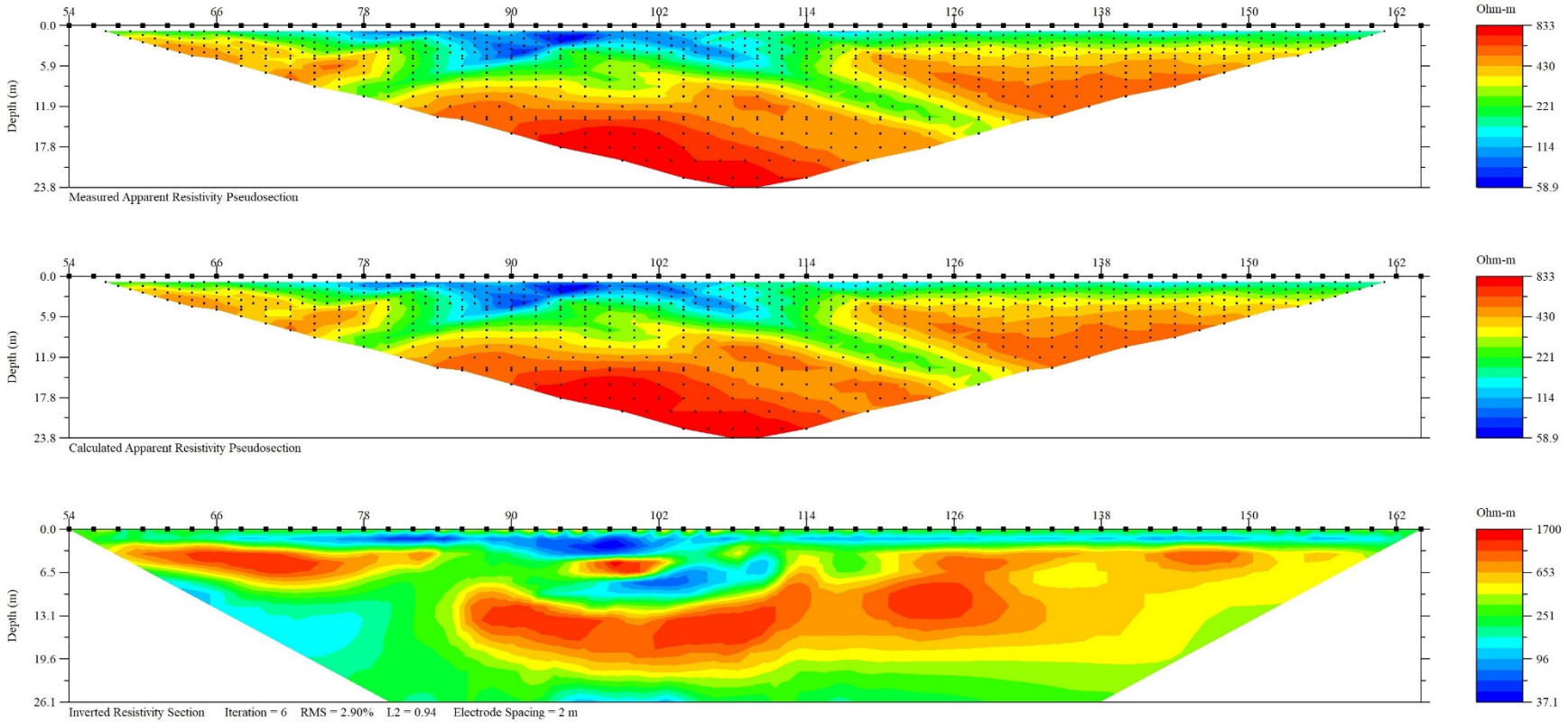

Figure A - 1: Measured resistivity pseudo-section (top); calculated resistivity pseudo-section (middle); inverted resistivity section (bottom) for survey line R1 (Note: distances are in meters)

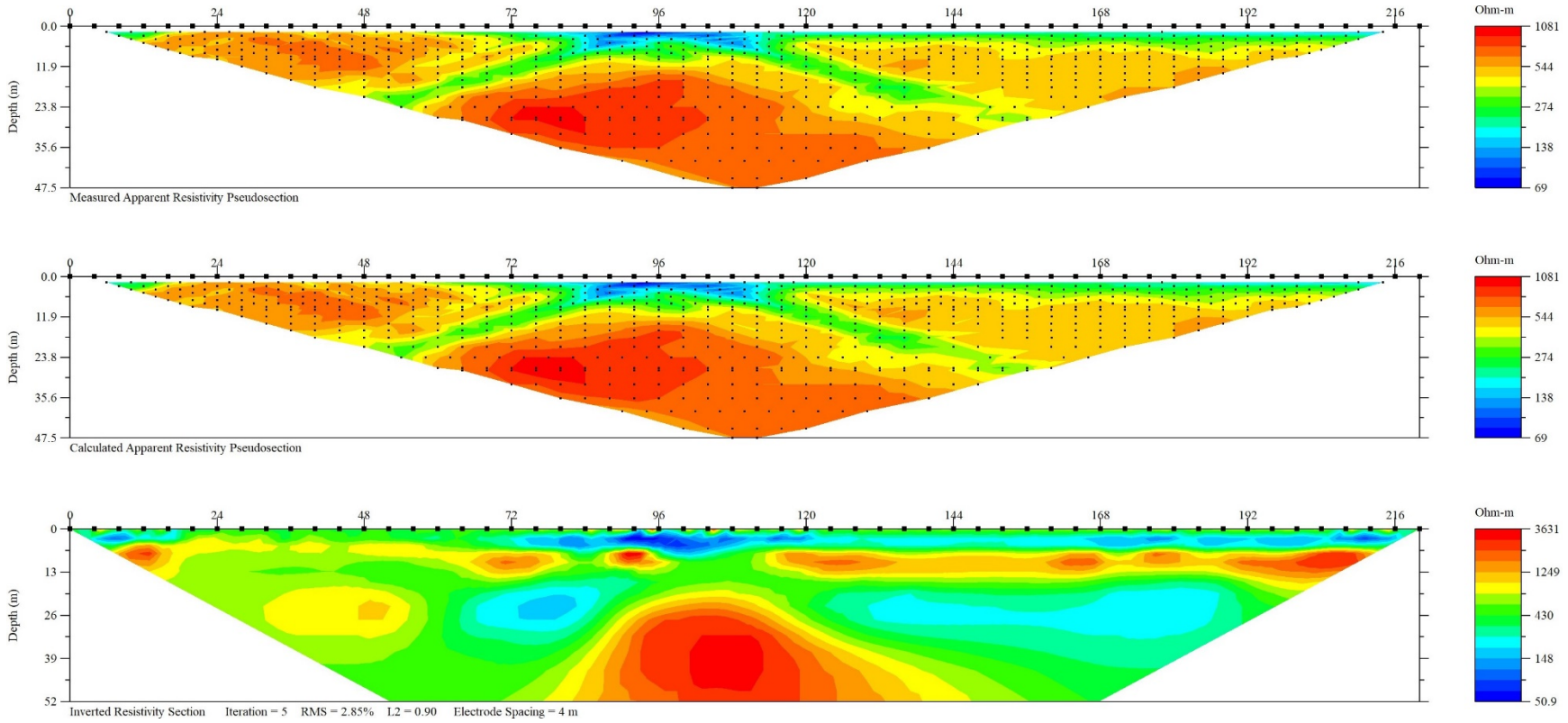

Figure A - 2: Measured resistivity pseudo-section (top); calculated resistivity pseudo-section (middle); inverted resistivity section (bottom) for survey line R2 (Note: distances are in meters)

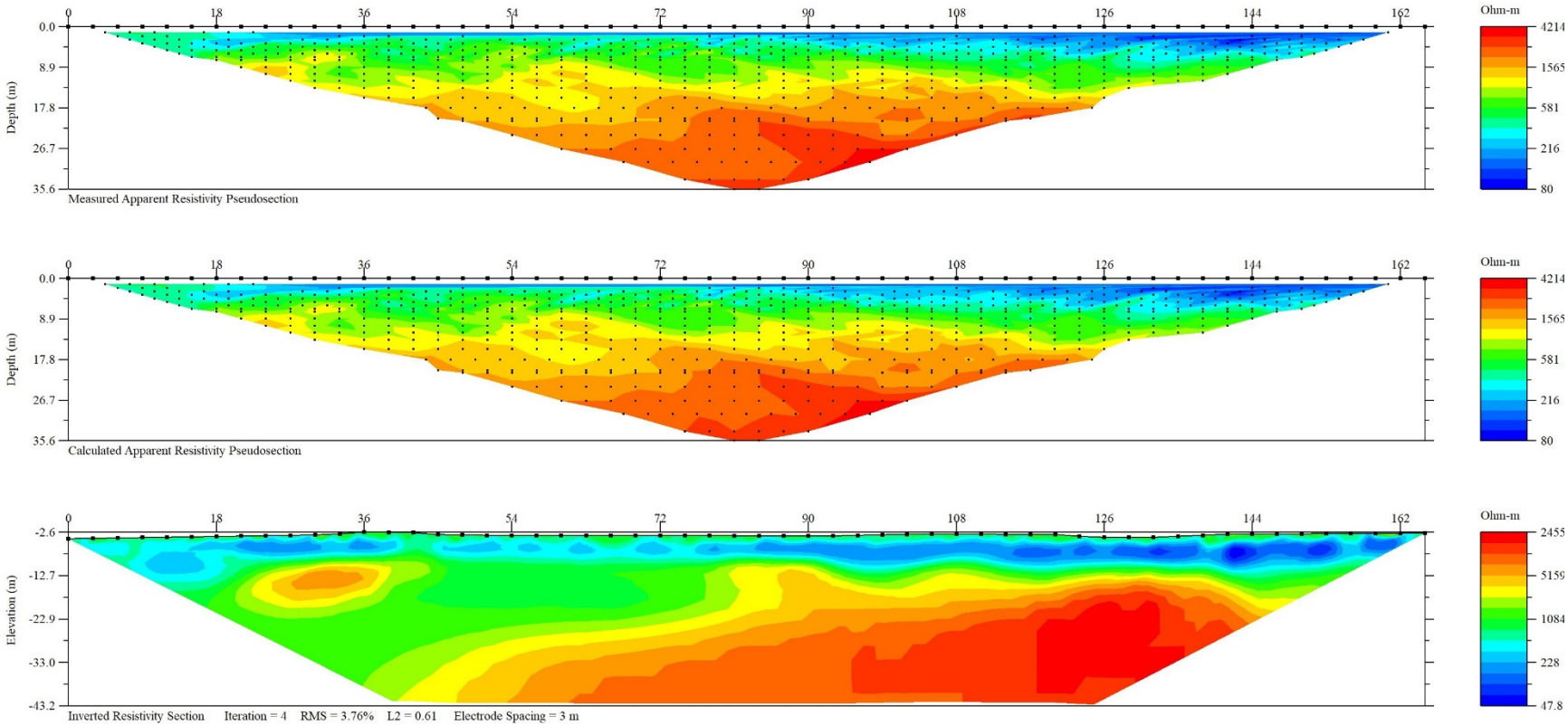

Figure A - 3: Measured resistivity pseudo-section (top); calculated resistivity pseudo-section (middle); inverted resistivity section (bottom) for survey line R3 (Note: distances are in meters)

B. Seismic

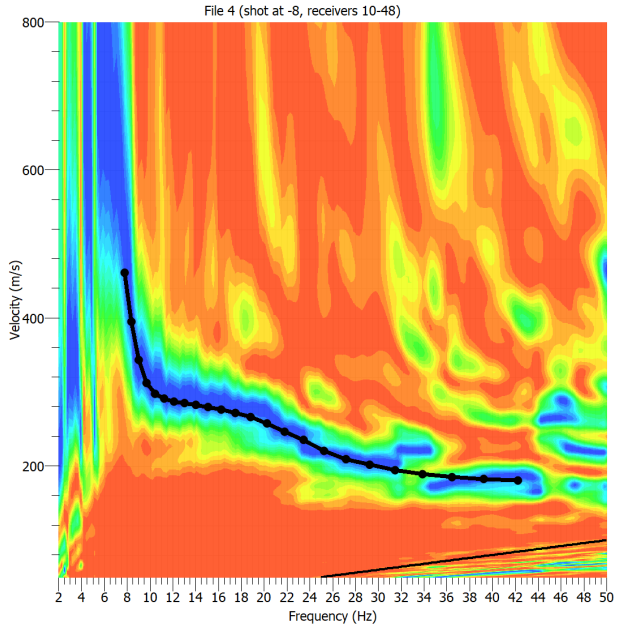

Figure B – 1: Dispersion curve picks for line S1

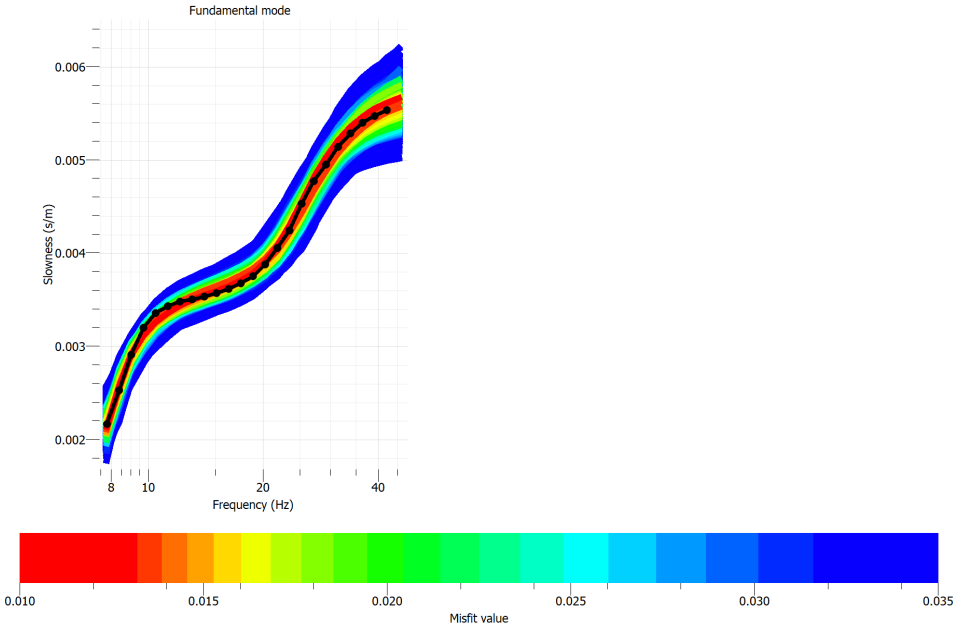

Figure B – 2: Dispersion curve fit for line S1

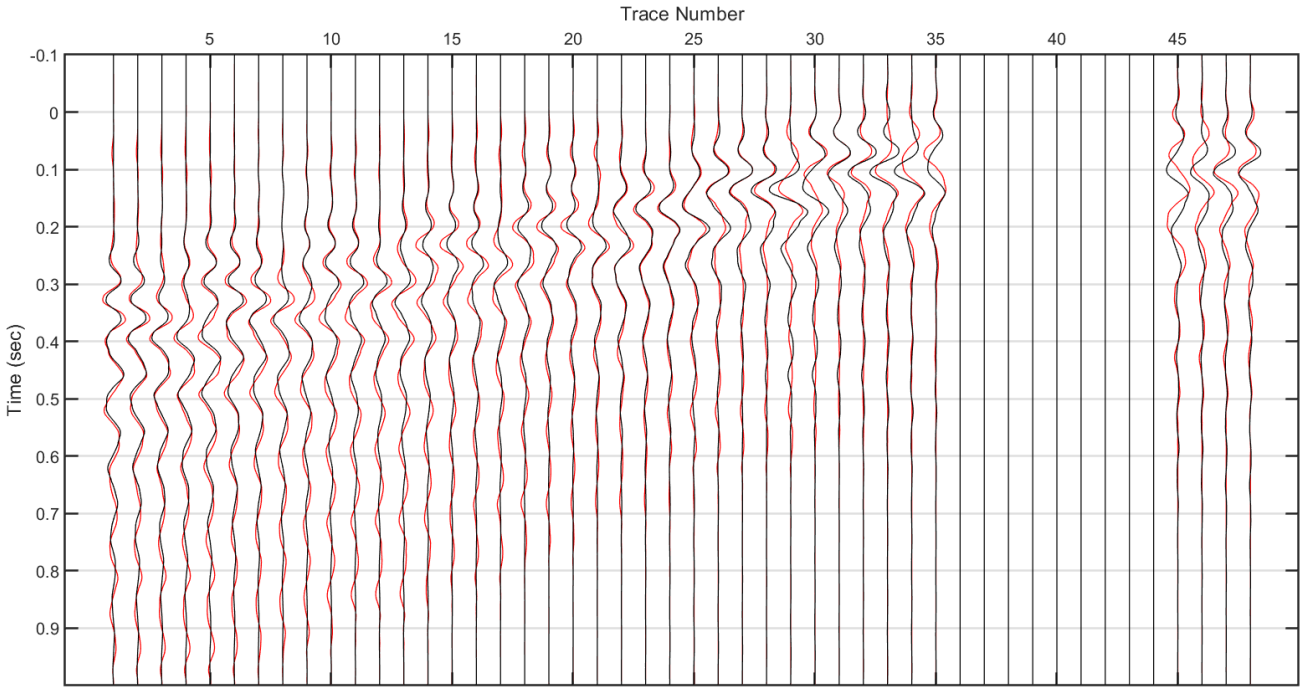

Figure B – 3: Waveform match for line S1

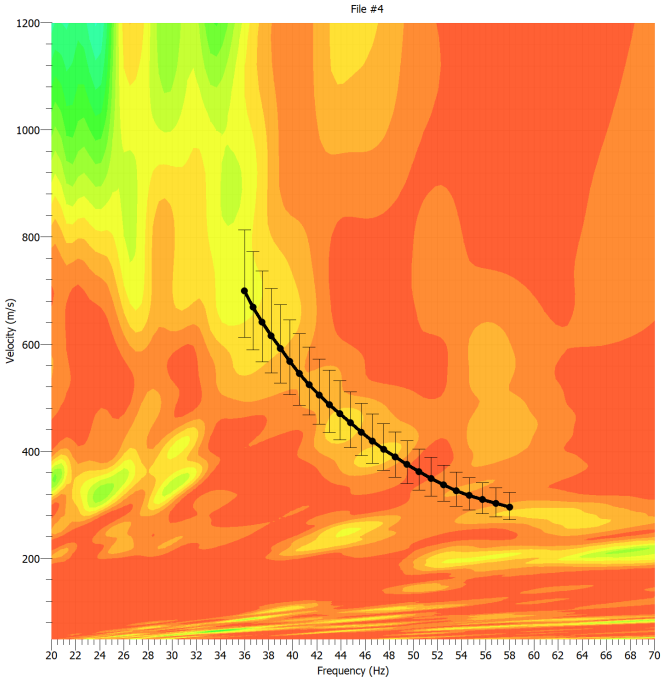

Figure B – 4: Dispersion curve picks for line S3

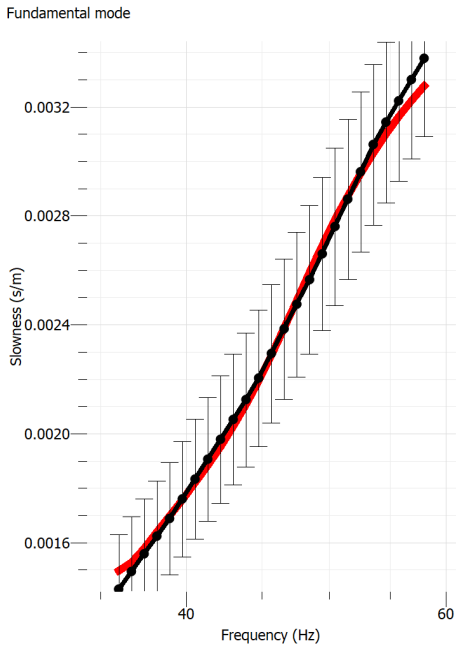

Figure B – 5: Dispersion curve fit for line S3

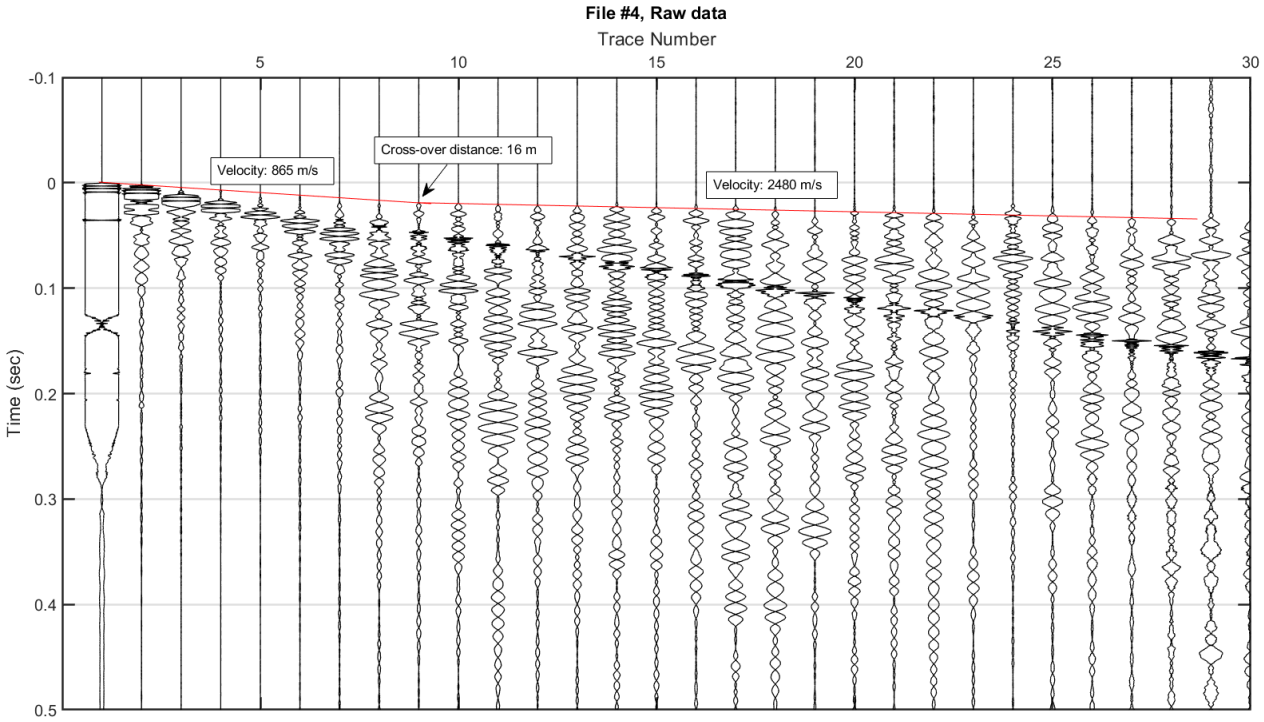

Figure B – 6: First arrival picks for line S3